MASTERARBEIT

Investigating complex carbon degradation in a beech forest soil and first insights into the application of single-cell methods to detect active microorganisms in soil systems

Strasser Florian, BSc

angestrebter akademischer Grad

Master of Science (MSc)

Wien, 2014

Studienkennzahl lt. Studienblatt:	A 033 830
Studienrichtung lt. Studienblatt:	Masterstudium Molekulare Mikrobiologie und Immunbiologie
Betreuerin / Betreuer:	Prof. Dr. Michael Wagner

1 Inhaltsverzeichnis

2 Abstract 4

3 Zusammenfassung 6

4 Acknowledgements 8

5 List of abbreviations 9

6 Introduction 10

6.1 The soil environment 10

6.2 Cellulose – a major C-source in soil 12

6.2.1 Structure of cellulose 13

6.2.2 Degradation of cellulose 13

6.3 Introduction in single-cell methods 17

6.3.1 Principles of Secondary Ion Mass Spectrometry (SIMS) and its application in microbial ecology 18

6.3.2 Principle of Raman microspectroscopy and its application in microbial ecology . 20

6.4 Aims of this study 21

7 Material and Methods 23

7.1 Soil sample collection 23

7.2 Determination of soil properties (pH and soil moisture) 23

7.3 Cellulose degradation time course experiment (soil microcosms) 23

7.3.1 Destructive sampling 24

7.3.2 CO_2 measurements 24

7.3.3 Enzyme assays 25

7.3.4 PLFA analysis 25

7.4 Set-up of diazotrophy soil microcosms 28

7.5 Single-cell analysis (Raman microspectroscopy and NanoSIMS) of soil microorganisms 28

7.5.1 Enrichments of soil microorganisms and soil microcosms set-up for Raman analysis 28

7.5.2 Cell detachment and concentration from soil samples 29

7.5.3 Analysis of soil microorganisms by Raman microspectroscopy 30

7.5.4 NanoSIMS analysis of soil microorganisms 31

7.5.5 Scanning electron microscopy (SEM) 33

7.5.6 Computational analysis 33

8 Results 34

8.1 Cellulose degradation in soil 34

8.1.1 Seasonal differences 34

8.1.2 Soil microbial community during cellulose degradation 38
8.2 Method development and testing for single-cell analysis of soil microorganisms 43
8.2.1 Applicability of different filter materials for NanoSIMS of microorganisms 43
8.2.2 Testing cell integrity after washing with buffers of different ionic strengths 44
8.2.3 Cell detachment and concentration enables single-cell analysis of soil microorganisms 47
8.2.4 Developed sample preparation pipeline for single cell analysis of soil microorganisms 48
8.2.5 Raman spectroscopy 51
9 Discussion 55
9.1 Cellulose degradation 55
9.2 Development and testing of sample preparation strategies for single-cell analysis of soil microorganisms 58
9.3 Conclusion and Outlook 63
10 References 65
11 Appendix 76
11.1 Supplementary figures 76
11.2 Recipes 79
11.2.1 10 x PBS: 79
11.2.2 Sodium-acetate- Buffer: 79
11.2.3 Citric acid buffer: 79
11.2.4 Vitamin Basal salt medium 79
12 Lebenslauf 81

2 Abstract

Mineral soils encompass the largest pool of carbon (C) on Earth. Source of a major part of this C is cellulose from plants. Major participants in recycling plant derived C are microorganisms. However, it is unclear if there is a differential response across different microbial groups. We hypothesized that by varying certain limiting edaphic background properties that can limit cellulose degradation (such as C and Nitrogen (N)) we would identify different groups of microorganisms that respond to the addition of cellulose. We used destructively sampled soil microcosms amended with ^{13}C uniformly labeled (UL) cellulose to identify cellulolytic microorganisms that respond to different types of background C and N in soil over a period of 25 days. Cellulose degradation was monitored using enzyme assays, CO_2 measurements and PLFA analysis. The C-primed microcosms exhibited the highest overall respiration activity as measured by evolved $^{12}CO_2$, whereas the N amended microcosms exhibited the highest activity of cellulose degradation, as measured by $^{13}CO_2$ evolution. Furthermore the addition of N significantly increased extracellular cellulolytic as well as hemi-cellulolytic enzyme activities. Using ^{13}C-PLFA analysis we quantitatively identified active microbial groups. N addition harbored the highest PLFA derived ^{13}C with a community shift towards fungi as compared to the starting soil. In contrast, simple C led to a shift towards bacteria, suggesting different nutrient limitations of these groups concerning cellulose degradation. Furthermore we compared cellulose degradation between summer and fall using extracellular enzyme assays and CO_2 measurements. Interestingly, respired $^{13}CO_2$ yields did not differ between the two seasons whereas enzyme activities across all additions were lower in fall.

Single-cell techniques such as high-resolution secondary ion mass spectroscopy (NanoSIMS) and Raman microspectroscopy are new and emerging techniques used to gain insights into activities of single microbial cells. To ascertain single-cell activities, these methods are often applied in combination with stable isotope tracer incubations. The application of these techniques however proves to be particularly challenging in terrestrial ecosystems due to the large background of organic and inorganic soil particles. In this thesis we successfully enhanced cell removal treatments in combination with density gradient to generate a cell fraction with reduced soil particle load and particles of small enough size to allow single-cell analysis by NanoSIMS or Raman microspectroscopy. For analysis cells have to be concentrated onto filters after density

centrifugation, thus different filter materials were investigated for their applicability in NanoSIMS analysis. As salt crystals interfere with both single-cell methods but especially NanoSIMS, washing with phosphate buffered saline (PBS) of different ionic strength was tested (1x PBS to pure ddH_2O water) hoping to identify a dilution that would permit NanoSIMS investigations but also preserve the cell morphology. In conclusion, cells washed with water exhibited the most integer morphology than cells washed with dilutions of PBS and also provided the cleanest sample. The optimized cell concentration protocol allows single-cell analysis by NanoSIMS or Raman microspectroscopy. As a proof-of-concept, we were able to successfully apply the cell extraction method to detect $^{15}N_2$-fixing and ^{13}C-cellulose-degrading microorganisms in soil microcosms by NanoSIMS. The ^{15}N-enrichment of diazotrophic microorganisms ranged from 2 to 27 atom % (C primed), and the ^{13}C-enrichment of cellulolytic cells from 11 to 36 atom % (C or N primed). The developed method was also suitable for single-cell Raman microspectroscopy. However, we uncovered that the incubation of soil samples with ^{13}C-carbon substrates not always generated the characteristic ^{13}C-phenylalanine peak in Raman spectra of active microbes. Further analysis revealed that environmental amino acids or oligopeptides served as a source of unlabeled phenylalanine, thereby rendering this method for detecting ^{13}C-enriched microorganisms in soil challenging.

3 Zusammenfassung

Terrestrische Ökosysteme beherbergen einen Großteil des auf der Erde vorkommenden Kohlenstoffs (C). Totes Pflanzenmaterial, das hauptsächlich aus Zellulose besteht, ist die Hauptquelle dieses Kohlenstoffs. Bakterien und Pilze sind die Hauptakteure im Abbau dieses Kohlenstoffreservoires. Wir stellten die Hypothese auf, dass durch die Zugabe von unterschiedlichen C- und Stickstoff (N) quellen unterschiedliche mikrobielle Gruppen aktiv Zellulose abbauen. Wir verwendeten destruktiv beprobte Mikrokosmen, die mit ^{13}C- markierter Zellulose und verschiedenen C- und N-Quellen versetzt wurden, um zellulolytische Aktivität zu messen und Zellulose abbauende mikrobielle Gruppen zu identifizieren. Während C-Zugaben generell die Atmungsaktivität (gemessen mittels $^{12}CO_2$) steigerten, zeigten $^{13}CO_2$ Messungen und Enzym-Assays, dass N-Zugaben gezielt den Zelluloseabbau förderten. Aktive Zellulose-abbauende mikrobielle Gruppen wurden durch ^{13}C-PLFA-Analyse identifiziert. Die höheren Abbauaktivitäten in den N-Zugaben waren auch durch erhöhte ^{13}C-PLFA Werte sichtbar. Die Zugabe von N führte zu einer Zunahme von Pilz-Markern im Gegensatz zur Zugabe von Glucose, welche zu einer höheren Abundanz der bakteriellen PLFA-Marker führte. Dies deutet darauf hin, dass der Zelluloseabbau durch diese mikrobiellen Gruppen unterschiedlich limitiert ist. In weiteren saisonalen Untersuchungen fanden wir heraus, dass die $^{13}CO_2$ Werte im Sommer und Herbst nicht signifikant unterschiedlich waren, dass allerdings Enzymaktivitäten im Herbst niedriger waren als im Sommer.

Um mikrobielle Aktivitäten feinauflösend untersuchen zu können ist die Analyse auf Einzelzell-Ebene unumgänglich. Hoch auflösende Sekundärionen Massenspektroskopie (NanoSIMS) und Raman Mikrospektroskopie sind neue Techniken mit denen es möglich ist einzelne mikrobielle Zellen zu untersuchen. In Kombination mit Stabilen-Isotopen-Tracern ist es möglich Aktivitäten einzelner Zellen zu messen. Aufgrund der Beschaffenheit von terrestrischen Ökosystemen wurden diese Techniken jedoch nur sehr begrenzt in diesen Ökosystemen eingesetzt, vor allem wegen dem hohen Hintergrund von organischen und anorganischen Bodenpartikeln. In dieser Arbeit konnten wir erfolgreich ein Zellextraktionsprotokoll in Verbindung mit Dichte-Zentrifugation anwenden und den Anteil von Bodenpartikel in unseren Proben stark reduzieren. Dies ermöglichte eine nachfolgende Analyse von Zellen mit NanoSIMS und Raman Mikrospektroskopie. Da nach der Dichte-Zentrifugation die Zellen auf Filtern konzentriert werden, wurden verschiedene Filtermaterialien auf ihre Verwendbarkeit für Messungen im NanoSIMS

untersucht. Salzkristalle können Raman- und NanoSIMS-Messungen beeinträchtigen-deswegen testeten wir unterschiedliche Konzentrationen einer Phosphat gebufferten Saline (PBS; 1x PBS bis ddH_2O) für die Aufreinigung von mikrobiellen Zellen. Ziel war es, eine Konzentration zu finden die NanoSIMS Messungen zulässt und die auf der anderen Seite die Zellintegrität aufgrund osmotischer Unterschiede nicht beschädigt. Überraschenderweise zeigten Zellen die mit Wasser gewaschen wurden die stabilste Morphologie.

In einer Machbarkeitsstudie demonstrierten wir, dass es möglich war, Mikroorganismen aus Bodenproben zu extrahieren und mittels NanoSIMS ihre ^{13}C-Cellulose-Abbau- und $^{15}N_2$-Fixierungsaktivität nachzuweisen. Die ^{15}N-Anreicherung in diazotrophen Zellen reichte von 2 bis 27 atom% (C-primed) und die ^{13}C-Anreicherung in Zellulose-abbauenden Zellen von 11 – 36 atom% (C- und N-primed). Das angewendete Zellextraktionsprotokoll konnte auch mit Raman Mikrospektroskopie verbunden werden. Es war jedoch nicht möglich, die Aufnahme von ^{13}C in Zellen desselben Mikrokosmus durch den charakteristischen ^{13}C-Phenylalanin-Peak im Zellspektrum nachzuweisen. Weitere Tests ergaben, dass Phenylalanin bevorzugt aus in der Umwelt vorhandenen Aminosäuren/Oligopeptide synthetisiert wird, anstatt es aus aufgenommenen C neu herzustellen. Dies erschwert die Anwendung von Raman Mikrospektroskopie zur Detektion von ^{13}C angereicherte Zellen aus Umweltproben mittels des charakteristischen ^{13}C-Phenylalanin-Peaks.

4 Acknowledgements

First of all I would like to thank my supervisors Dagmar Woebken and Stephanie Eichorst for letting me do a very versatile and interdisciplinary master thesis and for constant motivating support in the last year. I learned a lot from you.

I especially would like to thank Stephanie Eichorst for her patient supervision as well as for her scientific and humorous input throughout this thesis. Thank you for answering all of my questions, helping out and showing me the awesome world of soil-microbiology. I appreciate it and do not take it for granted.

Furthermore I would also like to thank my fellow Master students, namely Martin “Hümi” Huemer, Florian “Mr. Flo” Wascher aka Brain-Wascher, Stefan “Köste” Köstlbacher, Michaela “Bertl” Steinberger, Jasmin Schwarz and Michael “Mischa” Wozak for scientific and totally nonsense-discussions during this time in various coffee and beer brakes. And of course all the other DOMIES that were there that time.

I also highly appreciate the help of the TER-Team, namely Lucia Fuchslueger, Jörg Schnecker and Margarete Watzka for help with PLFA analysis and GC measurements.

I would also like to thank my friends in upper Austria and Vienna for necessary distraction and fun aside the lab.

Finally I would like to thank my family. Especially my parents for sharing their interest in nature with me and of course for constant moral and especially financial support to make the study of biology possible. Thank you!

This Master-thesis was part of a Marie Curie International Incoming Fellowship granted to Stephanie A. Eichorst (Proposal No.: 300807).

5 List of abbreviations

Abbreviation	Full name	Abbreviation	Full name
AA	Amino acids	N	Nitrogen
C	Carbon	NA	Nucleic acids
CFU	Colony forming units	NanoSIMS	High resolution secondary ion mass spectroscopy
CMC	Carboxy-methyl-cellulose	nmol	nanomol
Cs	Cesium	O	Oxygen
dw	Dry weight	(S)OM	(Soil) organic matter
EtOH	Ethanol	PBS	Phosphate buffered saline
(CARD-)FISH	(catalyzed reporter deposition-) fluorescence *in situ* hybrifization	PFA	Para-Formaldehyd
GC	Gas chromatography	Pg	Petagram
H	Hour(s)	Phe	Phenylalanin
IPCC	Intergovernmental Panel on Climate Change	PLFA	Phospho lipid fatty acid
IRMS	isotope-ratio-mass-spectroscopy	ROI	Region of interest
KLD	Klausen-Leopoldsdorf	UL	Uniformally labeled
M	molar	vol	volume

6 Introduction

6.1 The soil environment

Terrestrial ecosystems encompass 30% of the Earth's surface. They represent a major sink of carbon (C) and nitrogen (N) with estimates ranging from 1500 – 2400 petagram (Pg) C and 100 – 140 Pg N (Batjes 1996; IPCC 2013). As such these ecosystems and the processes within have global importance. The dominant participants in these nutrient cycles are microorganisms (Whitman *et al.* 1998; Lal 2004; IPPC 2013). However, although soils are a major foundation for society all over the world we only understand little about it.

Soil is a dynamic, three dimensional and complex habitat consisting of living and non living components. It is built up of mineral and organic matter that make up the solid proportion and water and air that fill up the pore space (Brady & Weil 1974). The mineral matter consists of sand, silt and clay particles whereas the organic matter encompasses nutrients, living (micro-) organisms as well as plant, animal and microbial decay of different stages (Brady & Weil 1974; Voroney 2007).Soil provides a very heterogeneous habitat for a diverse collection of microorganisms with estimates of 10^9- 10^{10} cells per gram of soil dry weight (dw) (Whitman *et al.* 1998). Diversity estimates vary from 2 000 to 8x 10^6 species g^{-1} dw soil (Schloss & Handelsman 2006; Roesch *et al.* 2007; Gans *et al.* 2005). However, this discrepancy across the estimates might be due to different tested soils, different sample sizes, different estimates and that there still is no clear definition of microbial species.

Soil heterogeneity can be observed at multiple levels, down to the micron scale. Mineral soils are separated into 5 different main layers whereas not all of them are abundant in every soil (Figure 1A). The O (organic matter) layer - if present - normally occurs above the mineral soil and consists of plant derived organic material in various decomposition states (Voroney 2007). The A layer is a surface layer consisting of mineral compounds mixed with humus derived from the O layer and shows thickness of up to 20 cm (Voroney 2007). The O and A layers are known to harbor the highest microbial activity (Agnelli *et al.* 2004). Below the A layer the subsoil or B horizon forms. It is characterized by the accumulation of organic and inorganic compounds such as soil organic matter (SOM), iron, aluminum, clay, silicates etc. that are washed in from the surface. Microbial activity can still be detected but decreases, as well as microbial abundance with depth (Taylor *et al.* 2002, Agnelli *et al.* 2004). The C- and R-horizons form the rock layers. The C-layer (parent rock) might consists of organic compounds that are washed in from above and weathered rock particles from the below lying R layer (bedrock), which forms the foundation of the complete soil profile.

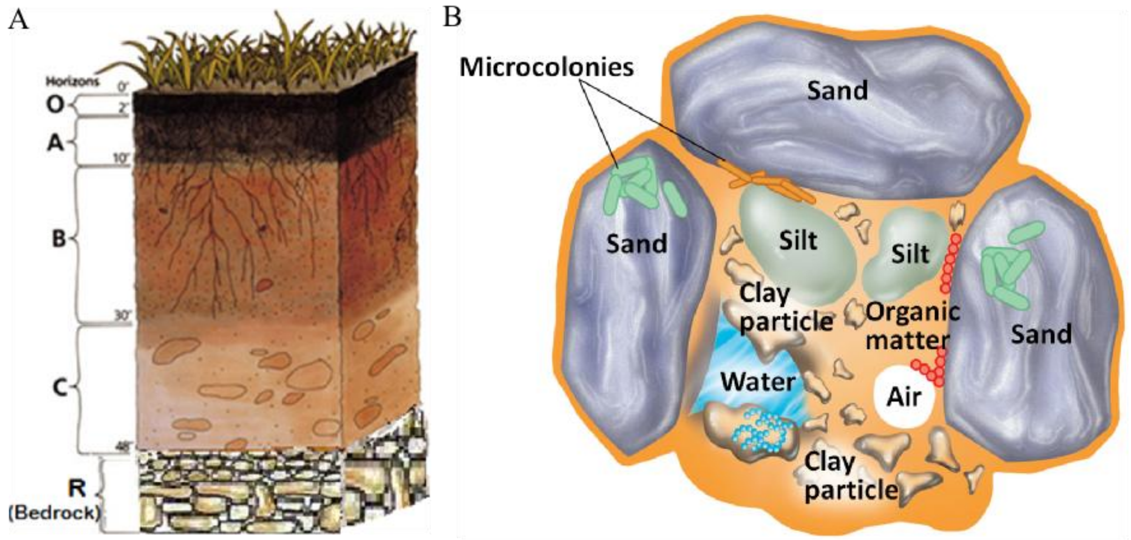

Figure 1: Soil heterogeneity on a bulk level (A) showing different distinct layers (wikipedia.org) and on the level of particles (B) showing different possible compartments (Brock of Microbiology).

Soil particles, as indicated in Figure 1B, consist of various biotic and abiotic compounds. Particles are associated with each other through binding agents such as humic substances, bacterial polysaccharides, plant roots and fungal hyphae, thus forming soil aggregates (Six *et al.* 2004). Soil environments sustain their heterogeneity at this aggregate level (Figure 1B). Due to different formation processes soil particles can be divided into silt sized aggregates (< 20 µm), which by the addition of microbial organic compounds can form microaggregates (20 – 250 µm), which in turn can form macroaggregates (> 250 µm) (the latter ones requiring hyphae for stability) (Six *et al.* 2004). Within an aggregate certain factors can vary, such as oxygen and nutrient concentrations, and RedOx-potential (Sexstone *et al.* 1985; Lehmann *et al.* 2007; Zausig *et al.* 1993), thus providing different microniches for microorganisms. Mummey and colleagues characterized the microbial community composition across micro- and macroaggregates and uncovered that certain bacteria can be more prevalently found on the surface of macroaggregates while others are more prevalent in the interior (Mummey *et al.* 2006). In another study aggregates that were clustered by their β-glucosidase activity exhibited different community composition depending on their degree of activity (Bailey *et al.* 2013) probably due to different access to nutrients.

6.2 Cellulose – a major C-source in soil

The source of terrestrial cellulose can be from microbial synthesis, yet the contribution from plant material is far more significant (Matthysse & Holmes 1981; Zogaj *et al.* 2001; Nobles *et al.* 2001). Amongst other polymers cellulose is the major component of plant cell walls. Approximately 30% - 50% of a plant's dry weight is composed of cellulose (Swift *et al.* 1979; Schmidt 2006). This makes cellulose one the most important sources of carbon in forest soils as it is introduced into this environment constantly. It is hard to quantify the amount of cellulose in soil, however, a recent study in an oak wood roughly estimated that about 15% of the litter derived cellulose reached the soil in the non-degraded form and was available for cellulolytic soil microorganisms (Snajdr *et al.* 2011).

Since the industrial revolution, atmospheric CO_2 levels have increased significantly. It is estimated that the atmospheric CO_2 yield increases annually by 4 Pg C (4x 10^{15} g C) (Lal 2004; IPCC 2013). It was shown that elevated CO_2 leads to enhanced photosynthetic activity and plant growth (Kubiske *et al.* 1997; Masle 2000; Zak *et al.* 2000). Thus, increasing atmospheric CO_2 levels could lead to an increase of the importance of cellulose as a carbon source in soils if plant primary production increases. So far it is not clear how the terrestrial microorganisms will react and whether additional C will more likely be respired or sequestered long term.

6.2.1 Structure of cellulose

Cellulose is a large homo-polymer built up of numerous β-D-Glucose molecules that are linked by a β-1,4-glycosidic bond. Even if the chemical composition seems to be simple, cellulose forms complex structures that are challenging to degrade, thus making it an ideal stabilizer for plant cell walls. The glucose chains assemble to each other by inter- and intrachainal hydrogen bonds (Figure 2A) leading to tight crystalline structures that are referred to as micelles. These micelles do not harbor a constant level of crystallinity - portions of them can contain a more amorphous structure, making cellulose accessible to cellulolytic enzymes (R.H. Marchessault 1957). Micelles in addition to hemicelluloses, lignin and other macromolecules assemble to higher structures, which build up the cell wall (Figure 2B).

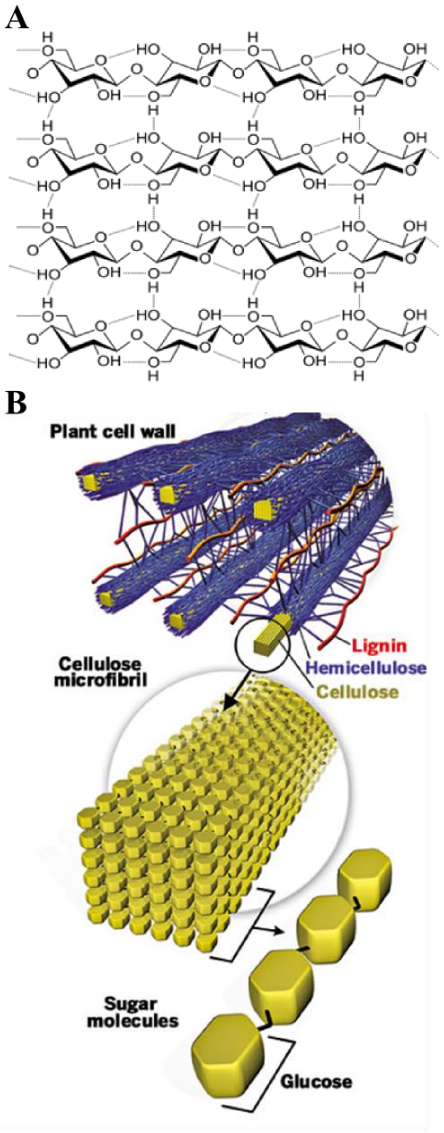

Figure 2: A) Structure of Cellulose. Glucose strands stabilized by hydrogen bonds. Taken from http://www.wikipedia.org

B) Structural hierarchy of cellulose in the cell wall. Taken from: http://www.lbl.gov/Publications/YOS/Fe

6.2.2 Degradation of cellulose

Microorganisms can degrade cellulose under both aerobic and anaerobic conditions. However, this study focuses on the aerobic degradation. The crystalline and insoluble structure of cellulose makes it a unique substrate to degrade. As cellulose is a long polymer, it cannot be readily taken up. As such, it must be degraded extracellularly into monomers prior to uptake. Cellulose can be degraded enzymatically and chemically. Chemical degradation which relies on the release of OH^- radicals is assigned to fungal microorganisms. It is seen as an initial step by breaking up the crystalline structure providing amorphous attachment sites for enzymes (Halliwell 1965; Baldrian & Valášková 2008).

The hydrolytic enzymes involved in the degradation of cellulose generally can be classified into three different groups: endoglucanases (EC 3.2.1.4), exoglucanases/ cellobiohydrolases (EC 3.2.1.91) and glucosidases (EC 3.3.1.21) (Beguin 1990; Wyman *et al.* 2005). These enzymes can be expressed by bacteria and fungi and oftentimes synergistically degrade cellulose stepwise to a unit that can be taken up -cellobiose or glucose (Wyman *et al.* 2005; Boer *et al.* 2005) (Figure 3).

Degradation is initialized by endo-β-1,4-glucanases acting at random amorphous sites in the cellulose molecule hydrolyzing the glycosidic bond providing open ends of the glucose-strands. Cellobiohydrolases are exo-β-1,4-glucanases, they hydrolyze cellulose from the ends releasing cellobiose or cellotriose. There are two types of cellobiohydrolases. Group 1 cellobiohydrolases act on the reducing end, whereas enzymes belonging to group 2 on the non-reducing end of the cellulose strand. Cellobiose can either be taken up or be further processed by β-glucosidases. Uptake of cellobiose can be performed by both, ABC-transporters and phosphotransferase systems (Schlösser & Schrempf 1996; Deutscher *et al.* 2006). In case of further extracellular processing glucose is being taken up by the microorganisms.

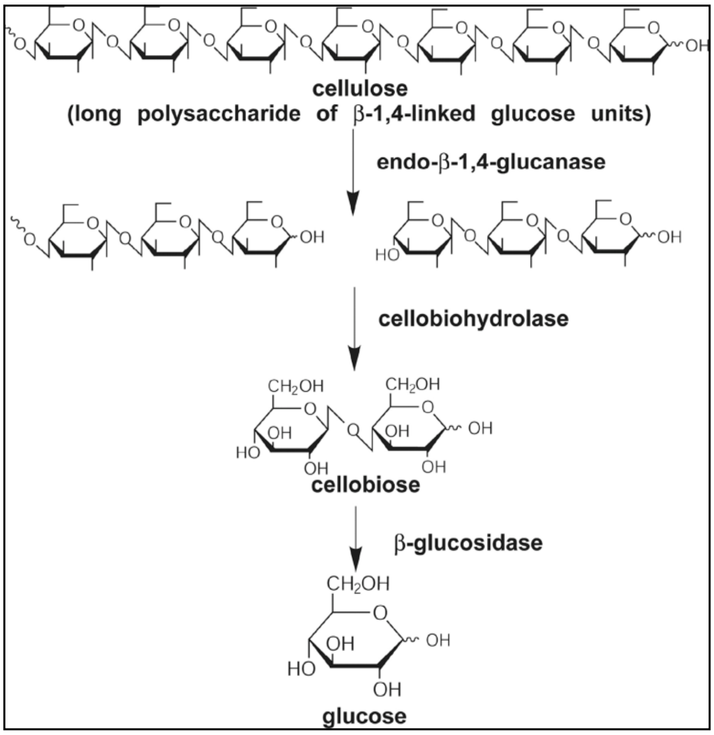

Figure 3: Schematic picture of the three major steps in cellulose degradation catalyzed by three different enzyme families. Taken from Xie et al. (2007).

Since cellulose in plant cell walls is embedded in a matrix including hemicelluloses, pectin and lignin normally a large number of additional enzymes are required to degrade plant material and make the cellulose accessible for degradation. Hemicellulases, such as xylosidases or arabinosidases, degrade the hemicellulosic portion of the cell wall. However, due to the heterogeneity of the hemicelluloses these enzymes also show a high variability concerning their substrate specificity (Wong *et al.* 1988; Bajpai 2009). In addition, also cellulases can degrade hemicelluloses. This cross-specificity most likely relies on posttranslational modifications like glycosilation and proteolysis (Wong *et al.* 1988). Microorganisms secrete extracellular enzymes to degrade this polymer into monomers for subsequent uptake. There are two basic strategies: (1) release and diffusion of the enzymes towards the substrate or (2) enzymes being attached to the outer surface of the cells. The latter was shown to be the major strategy of anaerobic bacteria by forming cellulosomes (Doi & Kosugi 2004). However, also aerobic bacteria show membrane bound structures related to cellulose degradation (Xie *et al.* 2007). In addition, higher cellulase-activities measured in cultures compared to cell-free supernatant support this hypothesis (Eichorst *et al.* 2013).

The majority of our knowledge on cellulose degradation has been restricted to organisms that we can grow under laboratory conditions (only 0.1-1%, Hugenholtz 2002), however, relying on these growth-based methods to understand cellulose degradation can be misleading. More recent molecular-based studies identified active cellulolytic bacteria and fungi across different soils, and the use of ^{13}C-labeled cellulose revealed bacteria as omnipresent cellulose degraders in terrestrial ecosystems (el Zahar Haichar *et al.* 2007; Štursová *et al.* 2012; Eichorst & Kuske 2012). Incorporation of ^{13}C into biomarkers that permit the identification of microorganisms (DNA, RNA, PLFAs and proteins) can be used to link function and identity of the active microorganisms. ^{13}C enriched PLFAs can be detected and identified by gas-chromatography-isotope-ratio-mass-spectroscopy (GC-IRMS) (Boschker *et al.* 1998), whereas enriched nucleic acids (NA) have to be separated from unlabeled NAs using density ultracentrifugation prior to community analysis (PCR and sequencing, or terminal restriction length polymorphism, microarrays, metagenomics etc.) (Radajewski et al. 2000; reviewed in Dumont & Murrell 2005). The big advantage of these approaches is that microorganisms can be incubated with labeled substrates in their natural matrix (soil, litter, sediments etc.) using microcosms instead of relying on cultivation of the organisms. By applying this type of approach, various cellulolytic communities were analyzed on the DNA, RNA or PLFA level (Bernard *et al.* 2007; Haichar *et al*. 2007; Bastias *et al.* 2009; Lee *et al.* 2011; Eichorst & Kuske 2012; Štursová *et al.* 2012; Koranda *et al.* 2013).

However, there are still unanswered questions concerning cellulose degradation. The importance of bacteria as true complex carbon degraders is still doubted in various ecosystems. Bacteria are referred to as “cheaters” or “mycoparasites” that do not actively degrade cellulose but grow on degradation products (cellobiose or glucose) released by fungal enzymes (Velicer 2003, Schneider *et al.* 2012; Štursová *et al.* 2012). Seasonal influence and the multiphasic character of cellulose degradation have previously been addressed but by far not been resolved. Based on the correlation of CO_2 evolution and the number of colony forming units (CFUs) at certain time points Hu and van Bruggen suggested that cellulose degradation in a 28 days time course was at the beginning driven by oligotrophic bacteria and shifted towards fungi during incubation (Hu & van Bruggen 1997). However CFUs rely on growth on solid medium encompassing the previously mentioned cultivation bias. In more recent studies Bernard and colleagues as well as Haichar and colleagues (Bernard *et al.* 2007; el Zahar Haichar *et al.* 2007) showed that the enriched bacterial community shows certain dynamics during cellulose degradation by applying distinctive Bacterial- Automated Ribosomal Intergenic Spacer Analysis (B-ARISA) fingerprints. These studies gave insights into dynamics but did not go into detail concerning the composition of the different cellulose degrading guilds over time.

Seasons also appear to have the potential to alter the cellulolytic communities in terrestrial ecosystems as the activities of various hydrolytic enzymes differ strongly across seasons (Andersson *et al.* 2004; Šnajdr *et al.* 2008, Kaiser *et al.* 2010; Baldrian *et al.* 2013; Voříšková *et al.* 2014). Background edaphic proportions like N-, C- and phosphate-contents or pH can alter the (cellulolytic) microbial community in terrestrial ecosystems. Soils with higher content of soil organic matter (SOM) or nitrate show higher mineralization rates (Eichorst & Kuske 2012), N addition was shown to increase β-glucosidase activities in three different soils (Waldrop *et al.* 2004). These effects are generally summarized as “priming effects”. Priming is defined as “strong short term changes in the turnover of soil organic matter caused by comparatively moderate treatments of the soil” by Kuzyakov and colleagues and relies on the activation or boost of a process (e.g. cellulose degradation) by a certain nutrient factor (C, N etc.) that was limiting (Kuzyakov *et al.* 2000). The mechanisms of priming are rather unclear; however, it might be due to the formation of new niches (Fontaine & Abbadie 2003; Kuzyakov *et al.* 2000).

In this study we address some of these open questions. We monitored cellulose degradation over a time course of 25 days using destructively sampled microcosms incubated with ^{13}C-UL-cellulose. Cellulose degradation was monitored by measuring $^{13}CO_2$, extracellular enzyme activities and ^{13}C-PLFAs. The influence of different edaphic background properties was addressed by the addition of simple C, complex C, organic and inorganic N (for details see Material and Methods). We also used the mentioned techniques to compare cellulose degradation between summer and fall microbial communities in microcosms over a time period of 25 days. The samples from the summer time course were used to investigate potential quantitative shifts in the microbial community across time and different treatments using the ^{13}C-SIP-PLFA approach.

6.3 Introduction in single-cell methods

One of the major aims in microbial ecology is to link the identity of microorganisms with their function, preferably in their natural habitat. There are many well-established methods to address this goal, however all with a given set of limitations. Various “meta-omics” approaches (using DNA, RNA or proteins) try to link certain functions with a population by tracing the presence or expression of genes (Handelsman *et al.* 1998; Moran 2009; Wilmes & Bond 2006). However, the presence of a gene, transcript or even of a protein does not provide full proof of a certain function as gene expression can be regulated at multiple levels up to the post-translational level. The combination of these techniques with the stable isotope approach explained before can provide evidence for a certain microbial activity to the functional level.

The use of stable isotopes (such as ^{13}C, ^{15}N or ^{18}O) in combination with molecular biology methods (like targeted sequencing of the rRNA gene) has a distinct advantage, as it allows linking a certain function with the identity of microorganisms. Stable isotope probing in combination with density gradients for NAs or mass spectroscopy for proteins, respectively, has been applied across various environments – by extracting and analyzing DNA, RNA or proteins (Taubert *et al.* 2012; Radajewski *et al.* 2003; Seifert *et al.* 2012). However, physical separation of enriched and non-enriched NAs requires a certain level of enrichment. For ^{13}C DNA-SIP, 10 – 20 atom % enrichment are stated to be the detection limit (Uhlík et al. 2009). Depending on the technique and the organisms ^{15}N has to be prevalent with 15 to 50 atom% for DNA-SIP (Cadisch *et al.* 2005; Buckley *et al.* 2007). This can lead to the negligence of certain groups that show enrichment levels below these thresholds. Furthermore, enrichment levels cannot be differentiated; thus the level of activity cannot be quantified and remains unknown. Therefore, it is not possible to gain information about what proportion of a certain group is carrying out a function and to which extent. Another potential problem with SIP studies is cross feeding, which is the incorporation of the heavy isotope into microorganisms that did not participate in the initial targeted process but feed on enriched metabolites or degradation products from other microorganisms.

In the last few years new methods were developed that can be used to investigate the function and identity of microorganisms on a single-cell level. High-resolution secondary ion mass spectroscopy (NanoSIMS) and Raman microspectroscopy are rather new techniques that can be used to detect heavy isotope incorporation into single cells. In combination with fluorescence *in situ* hybridization (FISH) (DeLong *et al.* 1989; Amann *et al.* 1990) these are potentially powerful tools to link identity and function of single cells. The application of these single-cell methods relies on an as clean and representative sample as possible. This means that cells need to be separated from soil particles sufficiently to reduce their influence during measurements. Furthermore, a certain cell density is required for these high-resolution techniques to allow analysis of many cells – depending on the method in parallel or sequentially. Our group has recently optimized a cell removal protocol for soil samples (S. A. Eichorst, unpublished data). It was one goal of this master thesis to test the applicability of this protocol in combination with single-cell methods on soil microorganisms.

6.3.1 Principles of Secondary Ion Mass Spectrometry (SIMS) and its application in microbial ecology

SIMS is a highly sensitive imaging mass spectroscopy method. It relies on a high-energy primary ion beam that bombards the sample surface and causes atoms or atom clusters to be ejected from the sample surface. A small fraction of these are ionized, focused into a secondary ion beam and analyzed by mass spectrometry, thereby revealing the chemical composition of the target area (Lechene *et al.* 2006; Boxer *et al.* 2009). Basically, there are two modes of how the sample-surface is treated with primary ions during measurements: dynamic SIMS and static SIMS, in this thesis however samples were measured with the first one (Boxer *et al.* 2009; Wagner 2009).

Dynamic SIMS uses a continuous ion beam of O^- or Cs^+ for the generation of positively or negatively, respectively, charged elemental and low molecular secondary ions, which are analyzed by a magnetic sector analyzer. It yields a high ionization and fragmentation efficiency leading to a high proportion of small ionized particles, and therefore expresses high sensitivity. Additionally, enhanced mass-resolving power of instruments like the Cameca NanoSIMS L50 permits now the separation of isobaric atomic species such as $^{12}C^{15}N$ and $^{13}C^{14}N$. Using this instrument seven different elements can be analyzed at the same time at a spatial resolution of up to 50 nanometers (Lechene *et al.* 2006; Boxer *et al.* 2009).

SIMS and NanoSIMS have already been applied to soil samples. Using TOF-SIMS ^{15}N and ^{13}C incorporation into soil microorganisms in an environmental sample was shown (Cliff *et al.* 2002). Herrman and colleagues added fixed ^{15}N-labeled *Pseudomonas fluorescens* cells to soil and could measure the enriched cells within the soil matrix by NanoSIMS (Herrmann *et al.* 2007). NanoSIMS measurements were also used to describe the formation of new soil particles from ^{13}C and ^{15}N labeled OM (Vogel *et al.* 2014). However, soil samples are challenging to prepare. For quantitative analysis of incorporated substrates or the combination with FISH techniques cells need to be separated from soil to reduce the influence of background elements and background fluorescence. The combination of FISH and SIMS has been applied to various environments as sediments, aquatic system and microbial mats (Dekas *et al.* 2009; D Woebken *et al.* 2012; Hannah Halm *et al.* 2009; Behrens *et al.* 2008; Musat *et al.* 2008; D. Woebken *et al.* 2014 in press) but so far not in soil.

Identifying the target microorganism for NanoSIMS analysis by FISH is essential to link identity with function. However, it introduces another investigation step that is not feasible with the NanoSIMS but instead needs an epifluorescence microscope. The use of halogen-labeled tyramides in CARD-FISH (Halogen *in situ* hybridization (HISH) or Element labeling (EL)-FISH) has been used to identify microorganisms through NanoSIMS measurements (Musat *et al.* 2008; Behrens *et al.* 2008; Halm *et al.* 2009). By using tyramides that are labeled with a halogen, the cells are enriched in these elements that can be detected by SIMS measurement. However, it seems that the applicability of this approach is rather limited due to background problems and instability of the halogen-labeled tyramides (D. Woebken, personal communication). Therefore, in this master thesis we developed a sample preparation strategy for soil samples that can be utilized in the CARD-FISH-NanoSIMS approach (Dekas & Orphan 2011; Dagmar Woebken *et al.* 2012). Especially in environmental samples that contain a diverse microbial community it is important to identify cells of interest before NanoSIMS and mark them using a Laser micro dissection (LMD) microscope. Obtaining additional visual information of the areas of interest, e.g. for cleanness, can be essential to avoid analyzing areas that are masked by soil particles that have not been removed successfully. The use of a scanning electron microscope is particularly valuable in this regard.

6.3.2 Principle of Raman microspectroscopy and its application in microbial ecology

Raman spectroscopy relies on the principle described by Raman & Krishnan (1928). Briefly, photons that illuminate molecules can be absorbed, transmitted or scattered. When photons are scattered, they are excited to a virtual energy level and can either harbor the same energy and wavelength as the incident photon when they return to their vibrational ground state (elastic Rayleigh scattering), or in a few cases (10^{-6} – 10^{-8}) the emitted photon has a lower or higher energy than the incident photon. In the first case the molecule’s vibrational state has an increased energy level (stokes scattering) leading to a photon with less energy and higher wavelength. In the second, less common case (anti-stokes scattering) the molecules new vibrational state has a lower energy level, leading to an increased energy and smaller wavelength of the photon. As only a small proportion of the photons show the anti-Stokes shift it is not commonly used in Raman spectroscopy (Wagner 2009; Eichorst & Woebken 2014).

Raman spectroscopy works with a monochromatic light source; therefore scattered photons with different energy, respectively wavelengths, can be detected and differentiated from the emitted light. Depending on the molecule (and its bonds) responsible for scattering, scattered photons have a certain distinct wavelength. A Raman spectrum consists of the wave length depending Raman wave number [cm^{-1}] and referring intensities (arbitrary unit) of the photons.

The Raman wave number is calculated with following formula:

$$\text{Raman wave number } [cm^{-1}] = (\lambda_0^{-1} - \lambda^{-1}) * 10^7$$

Whereas λ_0 is the wavelength of the monochromatic light and λ is the wavelength of the scattered photon (Wagner 2009).

Major advantages of Raman spectroscopy applied in microbiology are the combination with microscopy (Puppels *et al.* 1990) and its compatibility with FISH through combined epifluorescence and Raman imaging (Huang *et al.* 2007). The possibility of non-destructive measurements of single cells (Schuster *et al.* 2000) allows various downstream applications. Via optical tweezers cells can be sorted and cultivated or used for single-cell genomics (Huang, Ward, *et al.* 2009). Recent emphasis in Raman research lies on the detection of incorporated heavy isotopes. The prevalent phenylalanine-peak (Phe) for example shifts from 1004 cm^{-1} to 964 cm^{-1} due to ^{13}C incorporation into the phenylalanine-ring-structure (Huang *et al.* 2004). Even if other peaks shift as well, phenylalanine is present in every cell and shows an intense and easily detectable peak making it an ideal marker for ^{13}C incorporation.

A further heavy isotope which's application in Raman spectroscopy is being tested is deuterium (^{2}H, D). Incorporated deuterium can be detected with Raman spectroscopy due to its bond to carbon. The generated peak appears in a so-called silent region of a cell's Raman spectrum where no other chemical species interferes. Various deuterium labeled compounds showed a peak in this region (Tonegawa *et al.* 2002; Bergner *et al.* 2011). Deuterium labeled amino acids could be detected in eukaryotic cells by a generated peak at 2137 cm^{-1} (van Manen *et al.* 2008; Wei *et al.* 2013), as well as deuteriated liposomes with a peak at 2103 cm^{-1} (Matthäus *et al.* 2009). This suggests that depending on the molecule the C-D peak is generated at a different wave number; however being detectable in the silent region of the cell spectrum making it easily detectable. Water is the primary hydrogen source for lipid synthesis (Valentine *et al.* 2004; Wegener *et al.* 2012), and it has been shown that D_2O is an applicable substrate to detect active cells due to their incorporation of deuterium into lipids and thus biomass, since only active cells will build up lipids (Berry *et al.*, submitted). Through the use of D_2O as a stable-isotope substrate no additional nutrients are added, as it is often the case when adding ^{13}C- or ^{15}N-labeled substrates. Furthermore, using ^{13}C- or ^{15}N-labeled substrates often investigates a very particular function, while the use of D_2O would be an ideal marker for general cell activity studies.

6.4 Aims of this study

As atmospheric CO_2 levels continue to rise, there is a net increase in plant primary production that can lead to increased C inputs into soil (Kubiske *et al.* 1997; Masle 2000; Zak *et al.* 2000; Lal 2004; IPCC 2013). So far it is unclear whether this additional C will be sequestered in biomass and SOM or respired and subsequently released as CO_2. Due to the prevalence of C in soil it is important to better understand the microorganisms that cycle this C in terrestrial ecosystems. A large variety of microorganisms contributes to the cycling of C. Therefore it is hypothesized that the utilization of labile C, as well as complex C, encompasses a great deal of functional redundancy across members of the Bacteria and Fungi (Boer *et al.* 2005; Strickland & Rousk 2010). This functional redundancy suggests that the complex C degrading function can be maintained under varying environmental conditions due to differentially preferred niches across various species. Therefore we sought to exploit these niches of complex C degradation and hypothesized that by varying certain potentially limiting nutrient properties, such as C and N, we will discover different active cellulose-degrading guilds of bacteria and fungi and thereby elucidate their ecological niches. To test our hypothesis, we investigated cellulose degradation at the process level and assessed the effect of C and N priming on cellulose degradation by measuring total microbial respiration, extracellular enzyme potential and ^{13}C-PLFA to qualitatively and quantitatively document changes in the bacterial and fungal communities over time and supplemented nutrients.

The second major aim of this thesis was to establish and test a soil sample preparation strategy that allows single-cell investigations on soil samples. The combination of SIP with NanoSIMS and Raman microspectroscopy makes it possible to investigate the activity of single cells, thereby providing detailed information about the activity-distribution in a targeted population. This allows us to form a more profound picture of certain taxa that are e.g. involved in the degradation of complex C. We used a recently developed cell removal protocol to extract cells from soil and tested its compatibility with NanoSIMS and Raman microspectroscopy measurements. Additionally, we tested the practicability of the phenylalanine peak in a Raman spectrum as a ^{13}C-incorporation marker to identify ^{13}C-enriched cells from ^{13}C-cellulose amended soil microcosms. We further tested the applicability of D_2O as an activity marker measured by Raman microspectroscopy.

7 Material and Methods

Composition of used buffers and media can be found in 11.2

7.1 Soil sample collection

Soil samples were obtained from a beech forest soil in Klausen-Leopoldsdorf (48º7’1.1994”N; 16º3’0” W, in Spring, Summer and Fall 2013; for cellulose incubation, $^{15}N_2$ experiments, amino acids uptake experiment and D_2O incubations) and a grassland soil in Neustift (47°07′45″N, 11°18′20″E, for $^{15}N_2$ incubations). In case of a litter layer, it was removed prior to sampling. Depending on the amount of soil needed, at least three cores (5 cm depth, 8 cm diameter) were taken per site from three different sites. Soil was kept at 4°C until further processing. For microcosm experiments soil was 2 mm sieved-roots, plant material and stones were removed prior to that. A proportion of the soil was fixed with 4% (vol/vol) paraformaldehyde (PFA) for 16 hours (h) at 4°C. Fixed samples were washed three times in 1 x phosphate buffered saline (PBS, pH=7.6) and stored in PBS/ethanol (EtOH) (40/60, vol/vol) at -20°C. An aliquot of the soil was also archived at -80 °C.

7.2 Determination of soil properties (pH and soil moisture)

Soil pH was determined following the protocol of McLean (1982). In triplicates, 15 g of fresh soil were mixed with 30 ml deionized water and stirred for 30 minutes. Afterwards pH was measured. Soil moisture was determined by drying 10 g of fresh soil in triplicates for 48 h at 60 °C and calculated using following formula:

$$soil\ moisture(\%) = \frac{wet\ weight - dry\ weight}{dry\ weight} * 100$$

7.3 Cellulose degradation time course experiment (soil microcosms)

The soil of the three different replicate sites was mixed and sieved using a 2 mm sieve., Triplicate soil microcosms were established for 6 destructively sampled time points (day 3, day 6, day 9, day 12, day 15, and day 25) across 5 different treatments. Microcosms consisted of approximately 6 grams of soil in a 120 ml serum bottle (Ochs, Bovenden/Lenglern, Germany) and were supplemented with 0.012 grams of ^{13}C-UL-maize cellulose (99% atom; IsoLife, Wageningen, Netherlands). The 5 treatments were:

(1) no additions besides the labeled cellulose ("unamended"); (2) glucose amendment (20 mg); (3) beech leaf xylan (10 mg) and carboxymethyl-cellulose (10 mg) amendment; (4) casamino acids (10 mg); and (5) ammonium chloride (2 mg) and sodium nitrite (3 mg). ^{13}C-UL-maize cellulose and amendments were mixed into microcosm soil using a sterile spatula. As controls microcosms were prepared having the same amendments without ^{13}C-UL-maize cellulose. Microcosms were sealed with butyl rubber stoppers, incubated at 24°C in the dark and destructively sampled at the above-mentioned time points. To assure aerobic conditions, microcosms were vented with room air in intervals of three days until the day of destructive sampling. Chemicals were purchased from Sigma Aldrich unless otherwise noted.

7.3.1 Destructive sampling

The amount of destructive sampling time points varied with season. Table 1 gives an overview of the time points at which microcosms of different seasons were sampled. At each time point one set of triplicates of each treatment was destructively sampled. For enzyme assays 0.5 g were stored at 4 °C, for nucleic acid and PLFA extractions 4.5 g of soil were stored at -80°C. For downstream FISH-, NanoSIMS- or Raman-applications half a gram was fixed with 1 ml 4 % PFA in 1x PBS over night, washed three times in 1 ml 1x PBS and stored in 1 ml EtOH:PBS 60:40 (vol/vol) at -20 °C. Another 0.5 g were ethanol fixed by storage in 1 ml of EtOH:PBS 60:40 at -20°C.

Table 1: Overview of the destructive sampling time points in different seasons in 2013. X indicates that samples were taken that sampling-day.

Season	Day 3	Day 6	Day 9	Day 12	Day 15	Day 25
Spring			X		X	
Summer	X	X	X	X	X	X
Fall	X		X		X	X

7.3.2 CO_2 measurements

Headspace samples were taken from the longest incubating microcosms (of time point "25 days") every three days to follow cellulose degradation. The microcosms were shaken prior to sampling. Depending on incubation-length and treatment 0.5 or 1 ml of headspace samples were taken using a fresh sterile needle for each set of triplicates. The headspace was transferred into a clean 12 ml IVA-flask (IVA Analysentechnik e.K., Meerbusch, Germany) that was flushed and filled with N_2. Prior to venting of the microcosms, three 1 ml samples of lab air were taken to determine isotopic composition for correction during analysis. Samples were stored at 24°C in the dark until measurements. Gas chromatography was carried out in the Stable Isotope Laboratory at the University of Vienna for Environmental Research (SILVER, http://131.130.57.239/silver/index6p.html).

CO_2 values were normalized to soil dry weight. $^{13}CO_2$ levels were corrected for natural ^{13}C-abundance of lab air that was used for venting.

7.3.3 Enzyme assays

Enzyme assays were performed within 48 hours of sampling according to Marx *et al. (2001)* and Saiya-Cork *et al.* (2002) with modifications. Briefly, enzyme assays were performed by adding 0.1 gram of soil to 10 mL of 100 mM sodium acetate buffer (pH=5.5) and homogenized by vortexing for 10 minutes. 200 µl aliquots were dispensed into a black 96-well microplate (Greiner, Kremsmuenster, Austria) in triplicates for each tested substrate. The tested substrates were 4-methylumbelliferyl-β-D-glucopyranoside (glucosidase activity), 4-methylumbelliferyl-β-D-xylopyranoside (xylosidase activity), 4-methylumbelliferyl-β-D-cellobioside (exoglucanase activity), and 4-methylumbelliferyl-β-D-arabinopyranoside (arabinosidase activity). For each tested substrate, 50 µl of a 200 µM stock solution were added to each sample. The plates were sealed with parafilm and incubated at 24°C in the dark for approximately 4 to 5 hours. The reactions were stopped by adding 10 µl of 1 M Sodium hydroxide (NaOH). Negative controls consisted of 200 µl of pooled soil slurries and 50 µl of Na-acetate buffer. Fluorescent units were measured with an Infinite M200 Fluorimeter (Werfen, Austria) with an excitation of 365 nm, emission of 450 nm, emission slit of 9 nm and an average time of 20 µs. Activity rates were obtained by using standard curves with defined concentrations of MUB and normalized for incubation time and dry weight of soil.

7.3.4 PLFA analysis

The method relies on Frostegård *et al.* (1991) and includes modifications described in Kaiser *et al.* (2010). Glassware was muffled at 500°C prior to usage. Approximately two grams (wet weight) of frozen soil were weighed into 40 ml glass vials (Supelco, Bellefonte, Pennsylvania, USA) and freeze dried for two days using a Christ

ALPHA 1-4 LSC freeze-dryer (Christ, Osterode am Harz, Germany). Chemicals were purchased from Sigma Aldrich if not noted otherwise.

7.3.4.1 Extraction

The soil samples were mixed with 1.5 ml of 0.15 M citrate buffer (pH= 4.0), 1.9 ml chloroform, 3.8 ml methanol and 2.0 ml of a chloroform: methanol: citrate buffer mix (1:2:0.8, v/v/v) (CMB mix), vortexed for 30 seconds and incubated at 24°C over night. Samples were centrifuged at 15, 000 g for 10 minutes using a Beckman Avanti 30 (Beckman Coulter, Krefeld, Germany). Supernatants were transferred into new 40 ml vials whereas soil was re-extracted with 2.6 ml of the CMB mix for 60 minutes, after further centrifugation the supernatants were combined. For phase separation 3.2 ml chloroform and 3.2 ml citrate buffer were added, vortexed for 1 minute and incubated over night at room temperature. The organic phase was transferred into 10 ml glass vials (Supelco) and dried under a constant stream of N_2 using a RapidVap (Labconco, Kansas City, Missouri, USA) and stored at -20°C until further processing.

7.3.4.2 Fractionation

Silica columns (Supelco) were put into the valves of the Visiprep SPE vacuum manifold vacuum blocks (Sigma Aldrich) and connected with 20 ml syringes. The columns were conditioned by letting 10 ml of chloroform flow through. Chloroform was added until the columns were clear. No chloroform was left above the upper frit before continuing. Samples were taken up in 0.5 ml chloroform and transferred onto the columns. This was repeated before the sample was passed through until nothing was left above the upper frit. Neutral lipids were eluted by addition of 5 ml chloroform followed by washing with 20 ml of acetone. The lipids were then eluted with 5 ml methanol, collected in new vials and dried under a constant stream of N_2 as described before.

7.3.4.3 Derivatization

Twenty mg of the internal standard Methyl-nonadeceanoate were dissolved in a methanol:toluene mix (1:1, v/v). For application this stock solution was diluted 1:100 in the mentioned solvent. The samples were taken up in 1 ml methanol/toluene, 1 ml 0.2 M methanolic KOH and 100 µl of the diluted standard. The samples were incubated at 37 °C for 15 minutes. Afterwards 2 ml of hexane (Roth, Karlsruhe, Germany): chloroform (4:1, v/v), 2 ml MilliQ water and 0.3 ml of glacial acetic acid (Merck, Darmstadt, Germany) were added and samples were vortexed for 1 minute. The samples were then centrifuged at 552 g for 5 minutes in a Beckman Avanti 30 using a F0630 rotor. The upper, organic phase was transferred into new 10 ml glass vials whereas the previous step was repeated using 2 ml of the hexane/chloroform mix. After pooling the appropriate supernatants they were dried with N_2, as described before and stored at –20 °C.

7.3.4.4 Gas chromatography

Samples were dissolved in 100 µl iso-octane. GC- measurements were performed as described by Fuchslueger and colleagues with modifications (Fuchslueger *et al.* 2014). Briefly, we used a Trace GC Ultra connected with a GC-IsoLink to a Delta V Advantage Mass spectrometer (Thermo Fisher Scientific, Waltham, USA). Samples were injected splitlessly at a temperature of 300°C and separated using helium as a carrier gas on a DB23 column (60 m x 0.25 mm x 0.25 µm, Agilent, Vienna, Austria) with 1.5 ml min^{-1}. GC programme: 1.5 minutes at 70°C with 30°C min^{-1}, 1 min 150°C, 4°C min^{-1} to 230°C, 15 minutes at 230°C. For peak identification bacterial and fungal acid methyl esters (BAME, FAME) (Supelco, 10 mg/ml methyl-caproate) were used as standards in three different dilutions: 1:5, 1:10 and 1:20 in iso-octane. Samples were quantified using the internal standard Methyl-nonadeceanoate.

7.3.4.5 Analysis

PLFAs i15:0, a15:0, 15:0, i16:0, a16:0, 16:1(9), 16:1(11), i17:0, a17:0, 17:0, cy17:0, 17:1(11), 18:1(11), 18:1(13) and 10Me(18:0) represent bacterial biomass, whereas 18:1(9),18:2(9,12), 18:3(9,12,15) fungal. PLFAs i14:0, 14:0, 16:0, 16:1(5), 16:1(7), 17:1(11), 18:0, 19:1(11), 20:0 represent general non assignable microbial biomass.

For each PLFA ^{13}C excess was calculated using:

$$13C\ excess = \frac{(\mathrm{atom\%\ (sample)} - \mathrm{atom\%(natural\ abundance)}) * \mathrm{nmol\ carbon}}{100}$$

Atom% (sample) is the percentage of ^{13}C in the respective PLFA, whereas atom% (natural abundance) is the natural proportion of ^{13}C in the respective PLFAs of the untreated soil. Nmol C depicts the amount of C that was assignable to a certain PLFA. ^{13}C values were corrected for methyl-group addition during derivatization and natural abundance. To calculate biomass the sum of total or ^{13}C PLFA-derived C was used.

7.4 Set-up of diazotrophy soil microcosms

Two grams of 2 mm sieved soil from the sampling sites at Klausen-Leopoldsdorf or Neustift were transferred into 40 ml serum bottles with 10 µl of 0.5 M glucose solution. Samples were evacuated and filled with 80% $^{15}N_2$ gas (EurIsotope, Saint-Aubin Cedex, France) and 20% O_2 (Linde, Munich, Germany). Controls were incubated in normal lab air. Destructive sampling was performed after incubation of 21 days. From each microcosm 1 g of soil was stored for DNA/RNA extraction at -80°C and 0.5 g for IRMS analysis at -20°C. For NanoSIMS measurements 0.5 g were fixed in 4% PFA (v/v, in 1 x PBS) as described above and stored at -20°C.

7.5 Single-cell analysis (Raman microspectroscopy and NanoSIMS) of soil microorganisms

7.5.1 Enrichments of soil microorganisms and soil microcosms set-up for Raman analysis

Enrichments of soil microorganisms, as well as soil microcosms for amino acid uptake tests and D_2O-incubations were done with soil from Klausen-Leopoldsdorf sampled in November 2013 (soil was sieved as described before).

7.5.1.1 Soil microcosms with D_2O

For these microcosms, soil was dried to a moisture of about 25% for 50 minutes at 37°C. Two g of soil were put into serum bottles and rewetted with H_2O (control) or D_2O to an end moisture of 50%. Microcosms were incubated for 11 days and were rewetted with either H_2O or H_2O/D_2O (1:1, v/v) after 6 days of incubation. Samples were fixed with PFA as described above.

7.5.1.2 Enrichments of soil microorganisms

To remove cells from soil, approximately 30 gram of soil were incubated in 100 ml 1x PBS and 35 mg polyvinylpyrrolidone for 30 minutes at 20 °C. The subsequent concentration of cells by Nycodenz gradient centrifugation is explained under 7.5.2. The upper layers of approximately 36 individual Nycodenz extractions were pooled and ca. 4 ml were filtered per polycarbonate filter (0.2 µm, 25 mm diameter, Millipore, Billerica, Massachusetts, USA) for a total of 34 filters. These filters served as inoculums in the following experiments.

7.5.1.2.1 Soil-incubations for testing the applicability of the ^{13}C-phenylalanine peak as a ^{13}C-incorporation marker in Raman microspectroscopy

Extracted cells were incubated in two different sets of medium. The basic medium consisted of vitamins, inorganic salts and trace elements and had a pH of 6.5 (VSB-6.5); as described by Stevenson – recipe can be found in 11.2.4 (Stevenson *et al.* 2004). One set had a constant concentration of ^{12}C glucose (10 mM, Roth) and varying concentrations of ^{13}C-labeled algal amino acid mix (1 g/l, 0.1 g/l, 0.0001 g/l and 0 g/l, Cambridge Isotope Laboratories, Tewksbury, MA, USA), the other set had a constant concentration of 10 mM of ^{13}C-labeled glucose (Eurisotop) and varying concentrations of ^{12}C algal amino acids (same concentrations as above, Cambridge Isotope Laboratories). Amino acid mixtures (^{12}C and ^{13}C) consisted of the following components (16 amino acids with approximate percentages): L-Alanine (7%), L-Arginine (7%), L-Aspartic acid (10%), L-Glutamic acid (10%), Glycine (6%), L-Histidine (2%), L-Isoleucine (4%), L-Leucine (10%), L-Lysine (14%), L-Methionine (1%), L-Phenylalanine (4%), L-Proline (7%), L-Serine (4%), L-Threonine (5%), L-Tyrosine(4%) and L-Valine (5%). A stock solution of 5 g/l was prepared in water and filter-sterilized (0.2 µm). Medium was filter-sterilized, and 10 ml of the medium were inoculated with the cells on filters (prepared under 7.5.1.2.) in a 120 ml serum bottle (Ochs). Bottles were incubated in the dark for 48 h on an orbital shaker with 170 rpm (Eppendorf- New Brunswick, Enfield, CT). Cells were fixed in 1% PFA (v/v, in 1 x PBS) for one hour at 20 °C, washed 3 times in 1x PBS and stored in PBS/EtOH (40/60, vol/vol) at -20°C.

7.5.1.2.2 Incubations with the general activity marker D_2O

VSB-6.5 medium was prepared with 10 mM ^{12}C glucose and 1 g/l ^{12}C amino acids in a H_2O/D_2O (50:50, vol/vol) mix. Cells on filters (prepared under 7.5.1.2) were used to inoculate 10 ml medium in 120 ml serum bottles (Ochs). Cells were fixed after 48 h incubation as described before.

7.5.2 Cell detachment and concentration from soil samples

PFA-fixed soil samples (0.5 g, stored in 1 ml EtOH:PBS), were pelleted and resuspended in 10 ml of 1 x PBS containing Polyoxyethylene-(20)-sorbitan-monolauraten (TWEEN 20) (Sigma Aldrich, 0.5% vol/vol), 3 mM sodiumpyrophosphate and 36 mM polyvinylpyrrolidone (PVP). The slurry was incubated in a 100 ml Erlenmeyer flask at

24°C for 30 minutes while stirring to detach cells from soil particles. Cells were separated from soil particles by gradient centrifugation with Nycodenz (Axis Shield; Dundee, Scotland). Three and a half ml of the soil slurry were mixed with 3.5 ml of a 1.42 g/ml Nycodenz solution (in 1x PBS). Cells were separated by centrifugation at 13 000 rpm and 4°C in a SWT14i rotor (Optima L-100XP ultracentrifuge; Beckman Coulter; Pasadena California). The supernatant was collected and processed within 2 hours.

7.5.3 Analysis of soil microorganisms by Raman microspectroscopy

To optimize Raman sample preparation and detect ^{13}C incorporation spring microcosms amended with (1) ^{13}C-cellulose + CMC/Xylan; and (2) ^{13}C-cellulose + inorganic nitrogen, incubated for 15 days, were measured. Furthermore, microcosms and soil-enrichments, labeled with deuterium were analyzed by Raman microspectroscopy (7.5.1).

7.5.3.1 Sample preparation

7.5.3.2 Soil microcosm experiments

Cells collected in the Nycodenz upper fraction (see 7.5.2) were concentrated by filtering ca. 4 ml of the fraction onto a 0.2 µm polycarbonate filter (Millipore). Cells were washed with 10 ml 1x PBS to remove the remaining Nycodenz. Each filter was transferred into a 1.5 ml tube containing 1ml of 1 x PBS. Tubes were vortexed for 10 minutes at highest power to remove the cells from the filter. The filter was removed and the cells pelleted by centrifugation at 4°C with 13 000 rpm. The cells were resuspended in 30 µl PBS:EtOH 40:60 and stored at -20°C.

7.5.3.2.1 Enrichments of soil microorganisms

100 µl of the fixed culture were mixed with 900 µl PBS and sonicated in a sonication bath (Bandelin Sonorex RK51, Bandelin electronic, Berlin, Germany) for 1 minute at maximum intensity. Afterwards, cells were pelleted and resuspended in 200 µl PBS:EtOH 40:60.

7.5.3.3 Raman microspectroscopy measurements

Approximately 2 µl of the samples were spotted onto an aluminium covered slide (Al136, EMF Corporation, Ithaca, New York, USA) and dried at 46°C for 10 minutes. Slides were dipped once in ddH_2O to remove salt crystals. Measurements were performed on a LabRAM HR800 confocal Raman microscope (Horiba Jobin-Yvonm Kyoto, Japan).

To determine ^{13}C incorporation, spectra from cells were obtained using a 532 nm laser and the 600 gr/mm grating with a spectral resolution of 3.3 cm^{-1}. D_2O-incubated samples were measured using the 800 gr/mm grating, as lower spectral resolution of 6.7 cm^{-1} is still applicable for obtaining the broad peak originating from the D-C bond in lipids. Spectra were obtained between 300 cm^{-1} and 3200 cm^{-1}.

7.5.4 NanoSIMS analysis of soil microorganisms

7.5.4.1 Testing filter materials for NanoSIMS applications

Polycarbonate is a standard material for filter in microbial ecology. However, as this material is complicated to handle, we inspected potential alternative filters in regards of their planarity and topology, using SEM. The potential alternative filter material was chosen in regards of stability, conductivity and planarity and is listed in Table 2. Additionally we analyzed a further polycarbonate filter from another provider. Filter sections were prepared and analyzed as described in 7.5.5.

Table 2: Filter material used for SEM-analysis

Name	**Material**	**Company**	**ID-number**	**Pore size**	**Pre-treatment**
Nucleopore Track-Etch	Polycarbonate	Whatman	110606	0.2 µm	Gold sputterd
GTTP	Polycarbonate	Millipore	GTTP02500	0.2 µm	Gold sputterd
Anodisc	Aluminum oxide (Al_2O_3)	Whatman	28420418	0.2 µm	Gold sputterd
GNWP	Nylon	Millipore	GNWPO2500	0.2 µm	Gold sputterd
AG45	Silver (Ag)	Millipore	AG4502500	0.45 µm	No sputtering
-	Cellulose-nitrate	Sartorius	11407	0.2 µm	Gold sputterd

7.5.4.2 Testing the influence of buffer strengths on bacterial cell integrity

Bacillus subtilis and *Escherichia coli* as representatives for Gram-positive and Gram-negative bacteria, respectively, were grown in 10 ml of R2B-medium over night at 37°C. One half of each culture was ethanol fixed by storing it in EtOH:PBS 40:60. The other half was fixed over night at 4°C using 2% PFA (v/v, in 1 x PBS). PFA-fixed cultures were washed 3 times with 1 x PBS to remove residual PFA. An aliquot of the cell solutions (1.5 to 40 µl) were filtered onto 0.2 µm polycarbonate filters (Millipore) to obtain a cell density of ca. 1,000 cells per viewing grid (0.015 mm^2). To test the reaction of fixed cells to different ionic strengths, aliquots of the cells were mixed with 10 ml of (1) ddH_2O; (2) 0.01 x PBS; 3) 0.1 x PBS; 4) 0.5 x PBS; and 5) 1 x PBS, vortexed, filtered and washed with 30 ml of the respective buffer solution and air-dried.

7.5.4.3 Sample cleanness after cell removal and density-centrifugation

Half a gram of the control soil samples from the CMC/Xylan treatment from spring (see 7.3) after 15 days of incubation were resuspended in 10 ml 1x PBS. One half went through the cell extraction protocol (see 7.5.2) the other half remained untreated. To analyze the same “soil-equivalent”, the same volumes of the Nycodenz-cell fraction and the untreated soil slurry were filtered. As performed in other protocols (Eickhorst & Tippkötter 2008), also a dilution (1:100) of the untreated soil slurries were filtered.

The filters were analysed by SEM (as described in 7.5.5) and Laser scanning microscopy (LSM). For LSM filter sections were stained with 4´,6-Diamidin-2-phenylindol (DAPI) and mounted with Citifluor (Agar Scientific, Essex, UK). DAPI stained samples were analysed using a Leica TCS SP8 (Leica, Wetzlar, Germany).

7.5.4.4 Soil sample preparation for NanoSIMS measurements

Polycarbonate filters (0.2 µm, Millipore) were gold-palladium sputtered prior to filtration using an EM ITECH K550X sputter coater (Quorum Technologies, Guelph, Canada). Cell-extracts from ^{13}C-cellulose microcosm experiments (inorganic N and CMC/Xylan amended soil microcosms from spring 2013, see 7.3) and from the $^{15}N_2$ incubation experiment (see 7.4), including the respective controls, were filtered onto gold-palladium sputtered filters to obtain a cell density of 1000 cells per viewing-grid (0.015 mm^2). Filters were washed with 30 ml of 1x PBS and with 30 ml of sterile water afterwards. For measurements filters were glued onto 5 x 5 mm silicon wafer pieces (Active Business Company, Germany) and mounted onto the sample holder.

7.5.4.5 NanoSIMS measurements

NanoSIMS measurements were performed at the Large-Instrument Facility for Advanced Isotope Research at the University of Vienna using a NanoSIMS 50L (Cameca, France) as previously described (Woebken *et al*, 2014). Briefly, target areas were pre-sputtered prior to measurements. Data were obtained using a primary Cs^+ ion beam of ~100 nm diameter. For ^{13}C abundance, $^{13}C^-$ and $^{12}C^-$ secondary ions were detected, whereas ^{15}N abundance was calculated from $^{12}C^{14}N^-$ and $^{12}C^{15}N^-$ secondary ions. Pictures were obtained as multistacks consisting of 8 to 10 layers. Data were processed using custom software (WinImage, Cameca, France), and corrected for detector dead-time and image shift from layer to layer. Regions of interest (ROIs), referring to individual cells, were manually defined based on the CN^- secondary ion maps and cross-checked by the topographical/morphological appearance in secondary electron images. The isotopic composition for each ROI was determined by averaging over the individual images of the multilayer stack. Isotopic compositions are expressed as the abundance of the tracer relative the total tracer element (e.g., $a_N = {}^{15}N/({}^{14}N+{}^{15}N)$ and $a_C = {}^{13}C/({}^{12}C+{}^{13}C)$) in atom %.

7.5.5 Scanning electron microscopy (SEM)

Sections of filters (filter material from 7.5.4.1, buffer tests and soil samples as part of the sample preparation pipeline for NanoSIMS analysis) were mounted on SEM Pin Stubs (12 mm diameter, Philips, Amsterdam, Netherlands) and gold sputtered using an Agar 108 sputter coater (Agar scientific, Essex, UK). Pictures were obtained on a Philips FEI XL 30 environmental scanning electron microscope using an acceleration voltage of 12 kilo volt (kV) at the Core Facility for Cell Imaging and Ultrastructure Research (CIUS) of the University of Vienna (http://cius.univie.ac.at/).

7.5.6 Computational analysis

β-Diversity across the bacterial, fungal and general PLFAs was estimated using the Bray-Curtis diversity index using the R software and packages “vegan” and “MASS” (Oksanen *et al.* 2013; Venables & Ripley 2002; R Development Core Team 2008). Plots were made in R using the ggplot2 package (Hadley 2009). CO_2 concentrations, enzyme activities and PLFA-yields across different treatments and seasons were analyzed for significant differences (95% confidence) using one way student t tests in R (R Development Core Team 2008).

8 Results

8.1 Cellulose degradation in soil

8.1.1 Seasonal differences

8.1.1.1 Soil properties

The experimental site is an approximately 65 years old beech forest (Hordelymo-Fagetum) with Fagaceae (beeches) representing the main vegetation. The soil is classified as a Dystric cambisol over sandstone, with a loam-loamy clay texture. An overview of measured soil properties in three different seasons can be seen in Table 3. Moisture as well as pH values varied with season. The spring community in general showed higher extracellular enzyme activities as compared to communities of summer or fall, except for β-glucosidase where the summer community showed highest enzymatic activity. Generally, the fall community showed lowest enzymatic potential across all analyzed enzymes.

Table 3: Properties of Klausen-Leopoldsdorf beech forest soil in three different seasons including cellulolytic and hemicellulolytic potential of untreated soil. Enzyme activities are represented in nmol substrate h^{-1} g^{-1} dw soil +/- sd.

Season	pH	Moisture	Cellobiohydrolase	Glucosidase	Arabinosidase	Xylosidase
Spring	5.49	50 %	4.81 +/- 0.08	54.77 +/- 4.74	3.94 +/- 0.29	18.8 +/- 0.84
Summer	6.0	49.6 %	4.27 +/- 1.32	82.37 +/- 3.91	2.49 +/- 0.36	15.9 +/- 1.62
Fall	6.27	55.2 %	1.91 +/- 0.58	21.54 +/- 0.73	1.53 +/- 0.06	3.89 +/- 0.15

8.1.1.2 Activities of extracellular enzymes

Enzyme activities of cellobiohydrolases, glucosidases, arabinosidases and xylosidases of our microcosms were estimated at 6 (summer) and 4 (fall) time points during the incubation. The addition of various amendments affected the activity levels of various enzymes. Overall, the addition of inorganic N and to a less extent of organic N increased the activity of each enzyme across all time points and seasons. In most cases C priming did not change activity levels. However, activity-patterns over time did not seem to be altered by different amendments. Compared to summer, fall microcosms exhibited lower enzymatic potential at the beginning of the incubation. After 25 days, however, the differences were mainly insignificant. Although given a lower resolution in fall by only measuring 4 time points it seems that similar activity patterns appeared in summer and fall, however less distinct in fall.

Cellobiohydrolases in summer showed activity peaks at days 6 (inorganic N, organic N and glucose) and 9 (control and organic N) followed by a decrease until day 12. Activities increased again until day 15 (amendments) and day 25 (control) (Figure 4A). In fall, cellobiohydrolases had lower rates, especially at the beginning of the incubation (Figure 4B). However, after 25 days of incubation activity levels in summer and fall microcosms were not significantly different for the C amendments and inorganic N ($p > 0.1$ for all). The organic N amendment however increased cellobiohydrolase activity in the fall microcosms after 25 days significantly as compared to summer ($p < 0.05$).

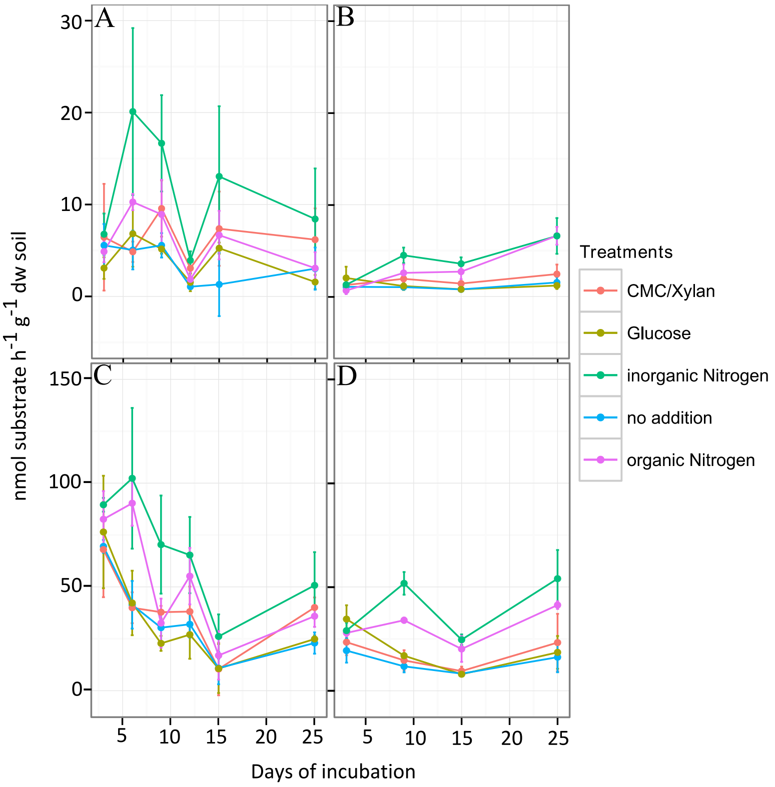

Figure 4: Enzymatic activities of cellobiohydrolases in summer (A) and fall (B), and of glucosidases in summer (C) and fall (D) over a time course of 25 days. Data points are means of triplicates +/- sd.

Glucosidase activities in summer decreased until day 15 (besides local peaks within the organic N and glucose treatments) and showed increased levels after 25 days of incubation. In fall, the enzymatic potential decreased until day 15 in control and C amended microcosms. Amendments with different N sources show an activity peak after 6 days before an increase at day 15. Increased levels after 25 days are also similar to values detected in summer ($p > 0.1$ for all) (Figure 4C, D).

Hemicellulolytic activities also were significantly activated by inorganic N amendments whereas other amendments had no general significant effect (Figure 5). Over the summer time course, arabinosidases showed peaks at day 6 (control) and 9 (inorganic N) before a decrease at day 15. In fall, also a local minimum is detectable after 15 days followed by an increase until day 25, showing similar levels as in summer. However, these differences were insignificant ($p > 0.1$ for all). Xylosidases in summer had highest activities at day 3 for the control and at day 12 for the amendments. All treatments showed lowest potential after 15 days of incubation, followed by an increase again until day 25. In fall, CMC/Xylan addition led to a minor peak at days 3 and 25, which can also be seen with the inorganic N amendment at higher levels. The control and glucose microcosms showed a low basal activity throughout the incubation, whereas activities in organic N amended microcosms increased constantly. Surprisingly, the xylosidase rates were higher after 25 days of incubation in fall than in summer, however none of the observed differences were significant ($p > 0.5$ for all).

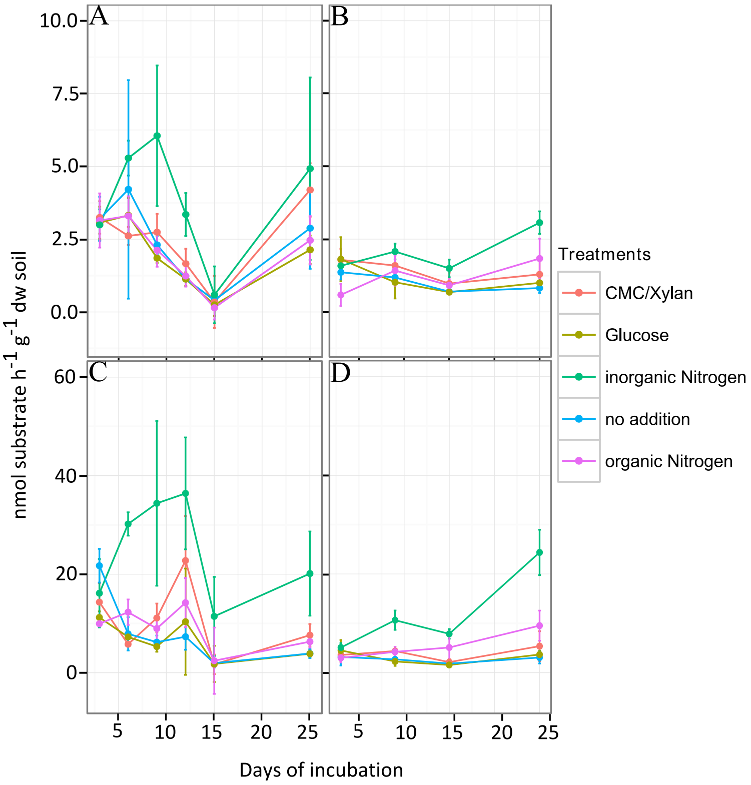

Figure 5: Enzymatic activities of hemicellulases: arabinosidases activities in summer A) and fall l B) and xylosidases in summer C) and fall D). Data points are means of triplicates +/- sd.

The addition of cellulose had different influences on the enzymatic activity-rates (Supplementary Figure 1, 2). In most cases it led to a slight increase of the enzymatic activities of our samples although some samples seem to show decreased levels at certain days. Largest influence was introduced by the combination of cellulose and inorganic N. Enzymatic activities were increased up to 7 fold in summer by adding ^{13}C labeled-cellulose (xylosidase, Day 9). A similar pattern could be detected in fall, however less intense. Highest increase in fall was 3.8 fold for xylosidase after 25 days (Supplementary Figure 2).

8.1.1.3 CO_2 –evolution

Cumulative $^{12+13}CO_2$ increased over the incubation period of 25 days in samples from summer and fall with and without ^{13}C-cellulose (Figure 6). We could detect two general trends across the two seasons: (1) N amendments increased ^{13}C-cellulose respiration (2) Glucose, CMC/Xylan and organic N additions increased general ^{12}C respiration activity (Figure 6), indicated by increased $^{12}CO_2$ levels as compared to the control. In summer and fall significantly more $^{13}CO_2$ was produced after 25 days in microcosms that were amended with inorganic N (both $p < 0.0001$) or organic N ($p < 0.0001$ and $p = 0.012$, respectively). According to CO_2 yields, complex and simple C additions decreased ^{13}C-cellulose mineralization rate not significantly ($p > 0.6$ and $p > 0.06$) as compared to the control. Fall microcosms showed slightly lower $^{13}CO_2$ production rates as compared to summer, especially those amended with additional C sources, however not significantly ($p>0.5$ for all). $^{12}CO_2$ production was significantly higher in microcosms that were amended with glucose, CMC/Xylan or casamino acids in both seasons (all $p < 0.05$). Addition of inorganic N surprisingly did not have any influence on ^{12}C mineralization in summer and fall ($p > 0.9$). Across the different treatments, fall $^{12}CO_2$ respiration rates did not differ from summer significantly ($p>0.2$ for all). Controls without labeled cellulose show enrichment at natural abundance of about 1.08 atom% (Supplementary Figure 3).

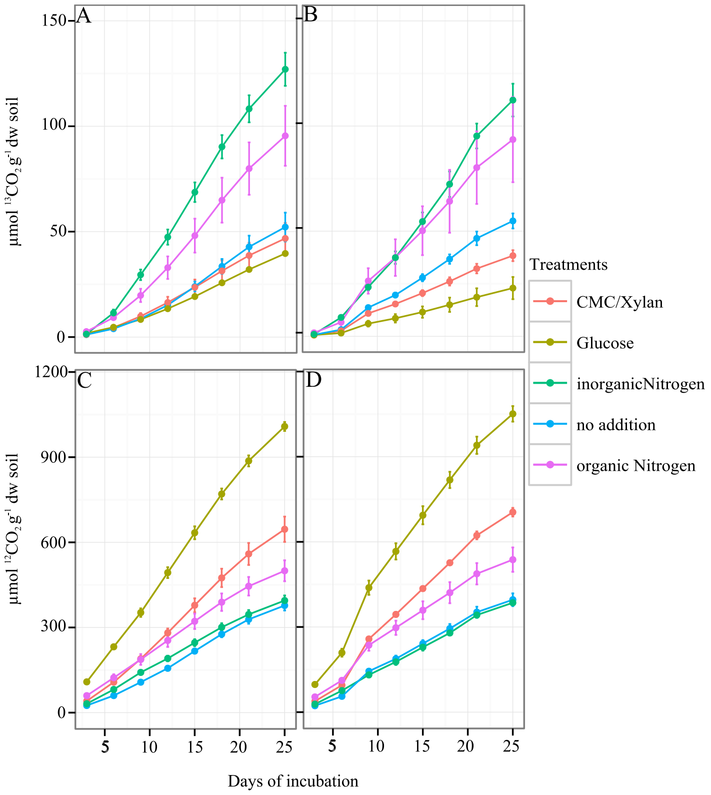

Figure 6: Cumulative $^{13}CO_2$ and $^{12}CO_2$ evolution of cellulose amended summer and fall microcosms over a time span of 25 days. A) Summer $^{13}CO_2$ evolution. B) Fall $^{13}CO_2$ evolution, C) Summer $^{12}CO_2$ evolution, D) Fall $^{12}CO_2$ evolution

The addition of ^{13}C-labeled cellulose slightly increased ^{12}C mineralization. In summer ^{12}C respiration was in average 1.1 times higher in the N amended microcosms, 1.2 times in the control, and 1.3 times in the C amended ones (Supplementary Figure 3). The trend was similar in fall (Supplementary Figure 4). Cellulose addition led to a 1.06 fold increase in N additions, 1.16 fold in the control and 1.25 fold in the C amended microcosms.

8.1.2 Soil microbial community during cellulose degradation

8.1.2.1 Microbial PLFA analysis

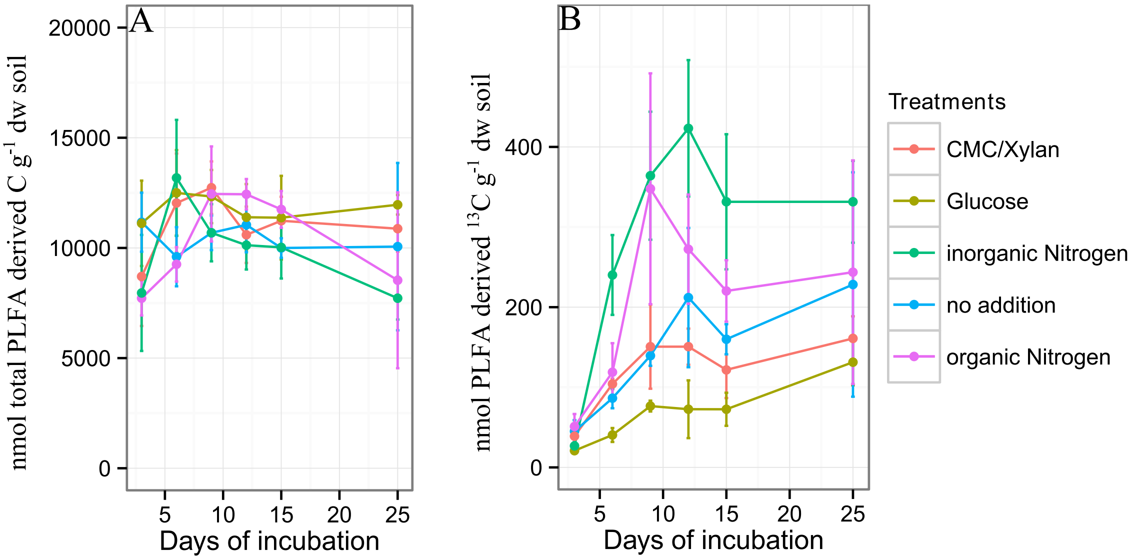

Figure 7: PLFA biomass dynamics of microcosms amended with ^{13}C-labeled cellulose and different C- and N-sources over a time period of 25 days. A) Nanomol of total PLFA derived C. B) Nanomol of PLFA-derived ^{13}C. Data points represent means of three replicates +/- standard deviation

Soil incubation in microcosms with different background properties led to a significant 2 to 3 fold increase of total PLFA-biomass within the first 3 to 6 days compared to natural soil (4750 nmol C g^{-1} dw soil) in all amendments, besides organic N (Figure 7, Table 4). Across the C-amendments, there was no significant difference in the amounts of PLFA derived C over the 25 days lasting time course. However, there are dynamics showing C-biomass-peaks at days 3 (control), 6 (inorganic N, Glucose) and 9 (organic N, CMC/Xylan). After a peak at day 6 (inorganic N), respectively day 9 (organic N), PLFA yields decreased constantly during the rest of the time course - significantly for inorganic N ($p = 0.015$). In contrast to $^{12}CO_2$ production, the amendments do not seem to have a major influence on the total PLFA-biomass.

Table 4: Overview of adjusted p-values of T-test on comparison of total PLFA-C-biomass between starting soil and soil incubated with various treatments for 3 and 6 days at 95% confidence level

Treatments	**Day 3**	**Day 6**
No addition	$p<0.0001$	0.046
Glucose	$p<0.0001$	0.001
CMC/Xylan	0.030	0.002
Organic Nitrogen	0.136	0.068
Inorganic Nitrogen	0.095	$p<0.0001$

The PLFA-derived ^{13}C yields revealed similar patterns compared to ^{13}C mineralization rates (Figure 7B). Inorganic N amendment led to highest yields of PLFA-derived ^{13}C atoms throughout the entire time course, followed by organic nitrogen, the control, and complex and simple C additions. Highest extractable ^{13}C-yields were detected after 9 (organic N, CMC/xylan, and glucose) and 12 days (inorganic N and control), followed by a decrease until day 15.

8.1.2.2 Community dynamics within the cellulose degrading guilds

Incubation of soil in microcosms led to a relative decrease of Gram-negative PLFA marker within the ^{13}C-enriched community across all treatments and days as compared to the starting soil (data not shown). Nitrogen addition (organic and inorganic) led to highest ^{13}C incorporation into fungal, bacterial and general PLFA markers as compared to other treatments (data not shown). The highest ^{13}C-enriched PLFA (18:2(9, 12)), a fungal marker, reached up to 20 atom %, whereas other fungal markers showed significantly lower enrichments. This aforementioned fungal marker had highest relative abundance in the inorganic N treatment (20 – 30%) and lowest in the glucose treatments, however not changing significantly over time (Figure 8B). The most abundant enriched general marker (16:00) was highly abundant across all treatments after 3 days of incubation but decreased quickly and had constant abundance levels below 20 % through the rest of the incubation (Figure 8A). In untreated starting soil this marker made up about 10% of the PLFA derived biomass.

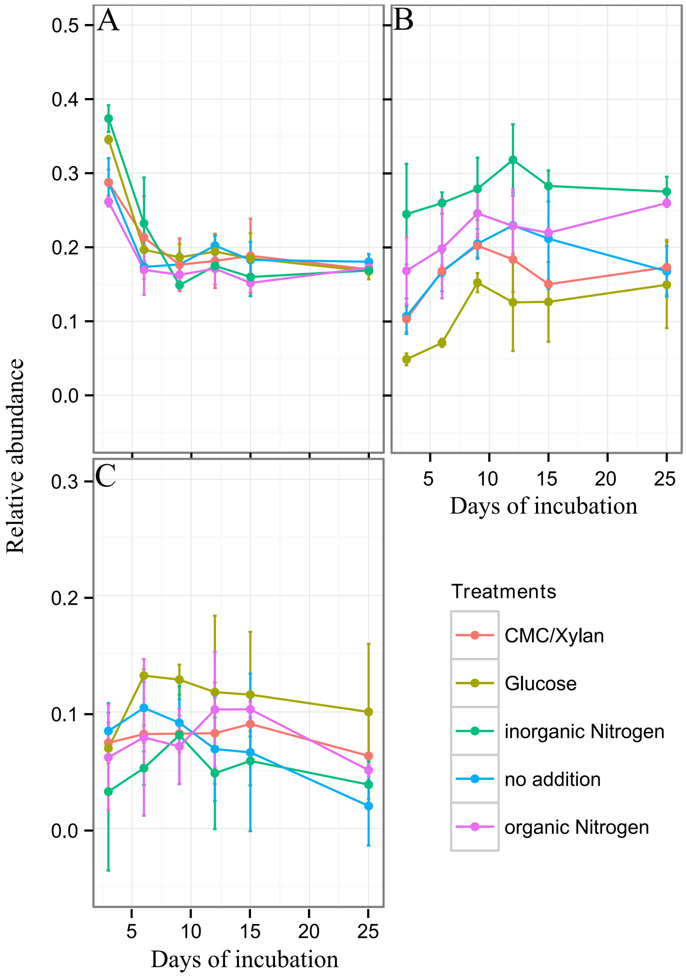

Figure 8: Time course of the most abundant general (A, 16:00), fungal (B, 18:2(9, 12)) and bacterial (C, i15:0) markers in the enriched fraction across different treatments.

PLFA i15:0 was the most abundant bacterial marker of the enriched fraction. Glucose addition increased the relative

abundance of bacteria as compared to other treatments (Figure 8C). Single bacterial markers general showed lower relative abundance; however, the sum revealed relative bacterial biomass of 20 -50% of all PLFA-derived ^{13}C (depending on the treatment).

The ratios of the sum of assignable bacterial marker and fungal marker derived ^{13}C were calculated to ascertain the prevalence of bacteria and fungi across the treatments and time (Figure 9). The addition of glucose caused a community shift towards bacteria as compared to the starting community through the entire time course, especially at days 3 and 12. In contrast, inorganic N decreased the bacteria to fungi ratio to about 1, revealing a shift towards fungi in these incubations, specifically at days 3 and 12. The ratio is significantly different between the two treatments at days 3, 6 and 12 ($p< 0.05$). The “No Addition” control-community shifted towards bacteria in the first part of the incubation and marginally towards fungi in the later period of the incubation, however not significantly. Neither of the other treatments -organic N and CMC/Xylan- showed significant changes in the bacteria to fungi ratios as compared to starting soil; however, after 25 days of incubation the organic N treatment also seemed to relatively increase in fungal biomass. The dissimilarities of the enriched communities across the treatments and over time were assessed using the Bray-Curtis dissimilarity index targeting the enriched markers. The results were visualized using multidimensional scaling plots (MDS, Figure 10).

The inorganic N treatments were distinct from all other treatments. Triplicates of inorganic N treatments formed distinct clusters across all sampling time points. Glucose amended communities formed specific clusters only at day 3. The influence of organic N on the ^{13}C-enriched communities was evident at day 15. The organic and inorganic N ^{13}C-enriched communities appeared to converge to a common cluster after 25 days of incubation. CMC/Xylan and control communities did not form distinct clusters over time, except for the control at day 9. MDS-visualization of Bray-Curtis dissimilarities for each treatment across different time points did not show any time depending clustering, except for all treatments at day 3 (data not shown). Agglomerative hierarchical clustering based on Bray-Curtis dissimilarity index further supports the long lasting influence of inorganic N on community structure defined by PLFA. Most of the inorganic N samples formed a distinct cluster, which also included some organic N samples (Figure 11). Across all treatments, the day 3 enriched communities formed a distinct cluster, with the

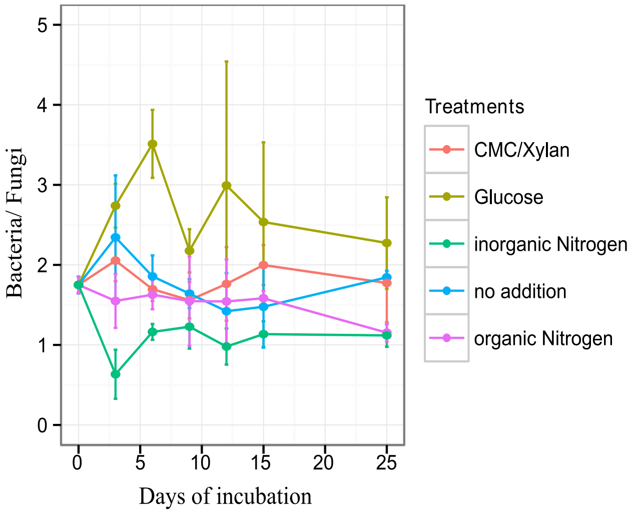

Figure 9: Ratio of bacterial and fungal ^{13}C enriched PLFA-biomass across different treatments and time points.

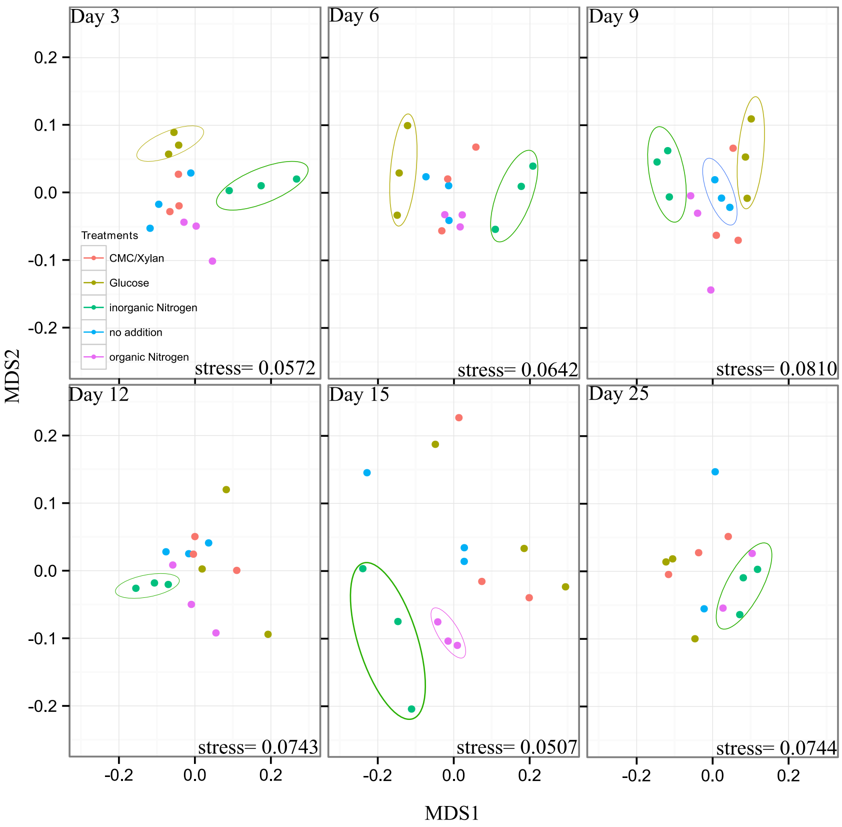

Figure 10: MDS plots of Bray-Curtis-dissimilarities of ^{13}C-PLFA composition across different treatments at different time points.

exception of samples amended with inorganic N. These samples form an own cluster distinct from the “Day3” and “inorganic Nitrogen”.

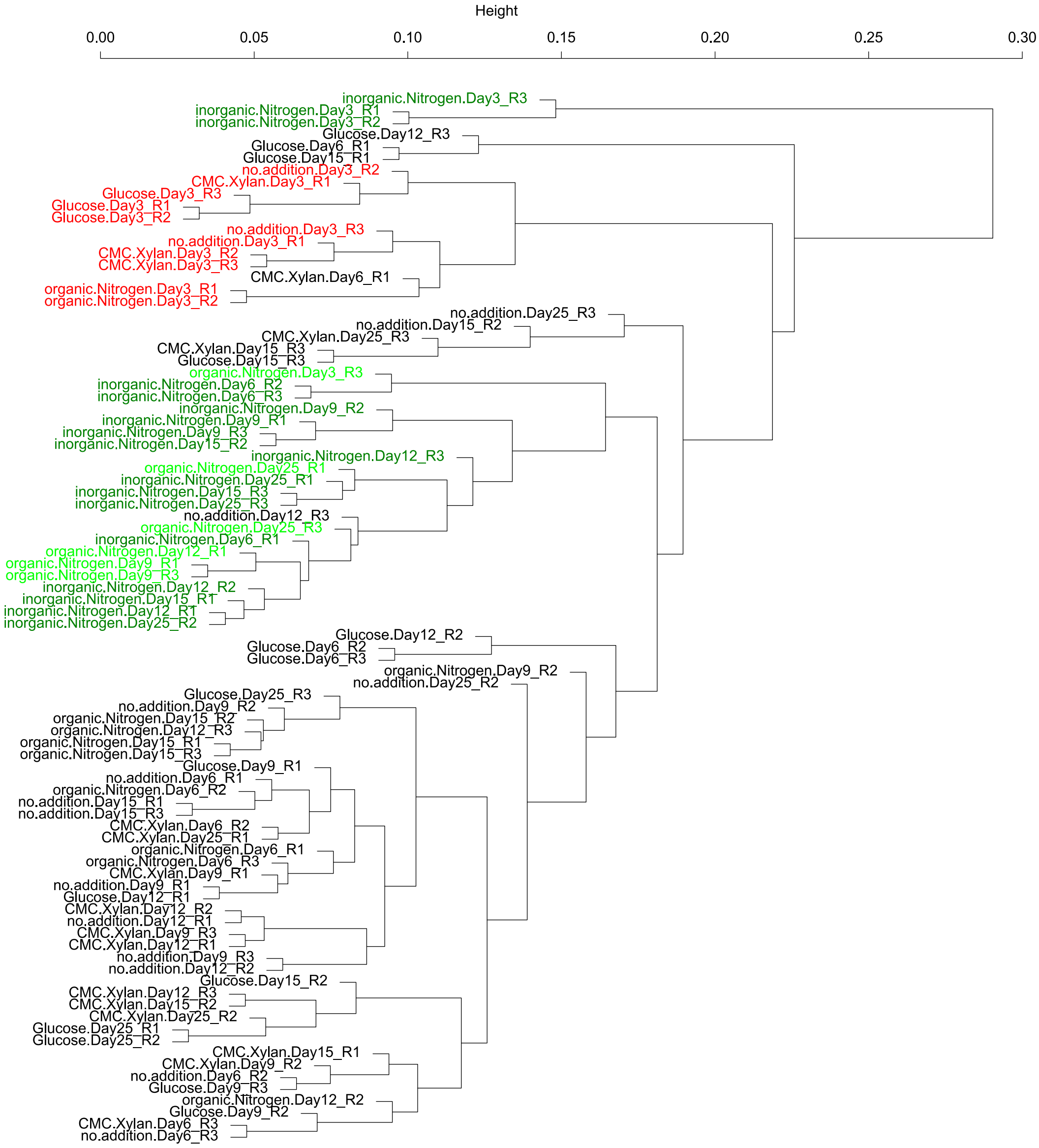

Figure 11: Hierarchical dendrogram of ^{13}C-PLFA patterns of all treatments across 6 time points. Nitrogen cluster is colored in dark green (inorganic N) and lime green (organic N). Day 3 cluster is indicated in red.

8.2 Method development and testing for single-cell analysis of soil microorganisms

8.2.1 Applicability of different filter materials for NanoSIMS of microorganisms

Al_2O_3- filters seemed to have the declared pore size (212.1 +/- 27 nm) and a rather planar surface, although some asperities distributed all over the filter were detectable (Figure 12 B). The polycarbonate-filters (Figure 12E and F) also seemed to have the declared pore size and a plane surface. Interestingly, the filters from two different producers exhibited differences concerning pore size and pore density. The filter from Millipore seems to have bigger pores (236 +/- 15 nm) that are more densely distributed than the pores on the Whatman-filter (173.7 +/ 13 nm). Furthermore, merged pores on the Millipore filters were observed. These pores reached up to 1 µm in diameter.

Oxidation was a problem with the Ag-filter, indicated by crystalline structures all over the filter annihilating the major advantage of this material: conductivity (Figure 12A). Cellulose-nitrate (Figure 12C) and nylon (Figure 12D) filters seemed to have larger pore size than declared, however, due to the three dimensional structure it was challenging to measure. Furthermore, they seemed to be topographically unfavorable for filtration of bacterial cells, as they would be masked by filter material. Additional problems arose with nylon. The filter was instable during scanning and its hygroscopic behavior led to a much longer evacuation time of the SEM-column.

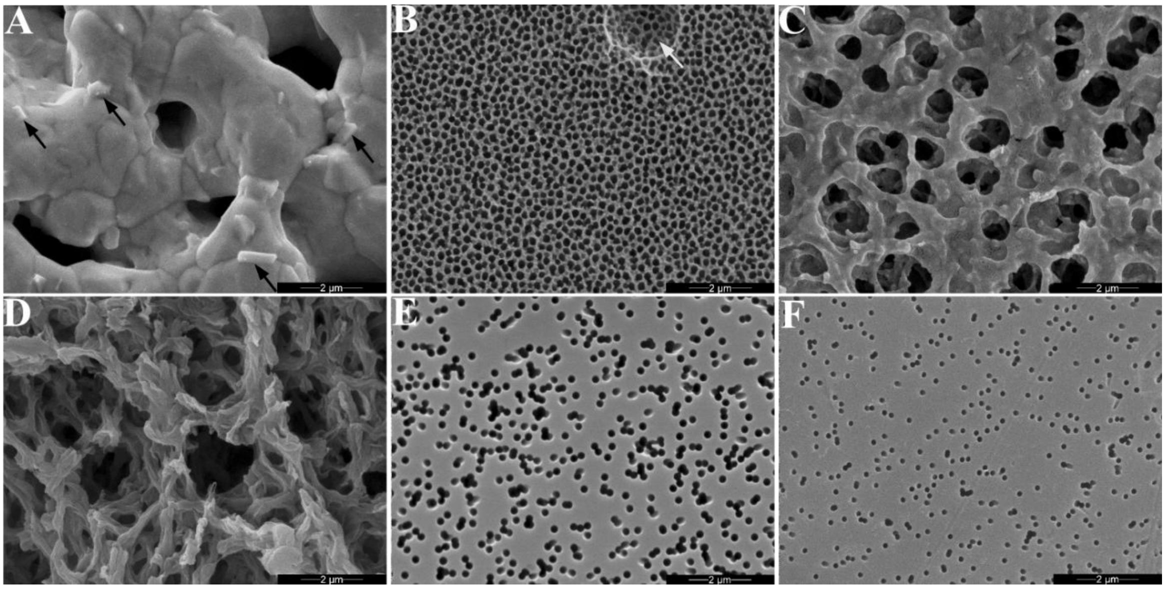

Figure 12: Different filters with the potential for application in NanoSIMS analysis of microorganisms. A) Ag-filter, black arrows indicate crystals that suggest oxidation of the filter; B) Al_2O_3-filter; white arrow shows a representative asperity that sometimes can be seen. C) Cellulose-nitrate filter; D) Nylon filter, E) Polycarbonate filter (Millipore), F) Polycarbonate filter (Whatman). Pictures were taken with a magnification of 20, 000x.

8.2.2 Testing cell integrity after washing with buffers of different ionic strengths

Bacillus subtilis (*B. subtilis*) and *Escherichia Coli* (*E. coli*) were chosen as model organisms for Gram-positive (ethanol-fixed) and Gram-negative (PFA-fixed) bacteria to see their response when washed with different buffer strengths after fixation (Figure 13). The experiment was repeated with *B. subtilis* being PFA-fixed and *E. coli* EtOH-fixed depicting overfixed and underfixed cells, respectively. However, in these tests only the extremes (ddH_2O and 1 x PBS) were used.

E. coli cells as well as *B. subtilis* were more likely to aggregate to each other when they were treated with buffer. Evenly distributed separated cells were more common in the sterile water treatment (Figure 13A, E). Surprisingly, the cells looked much healthier after ddH_2O treatment than after buffer treatment. Under hypoosmotic conditions the cells appeared to have a normal shape whereas under isoosmotic (1x PBS) they appeared collapsed (Figure 13A, E and D, H; respectively). Diluted buffers (0.01 x PBS and 0.5 x PBS) led to similar results even though with less intense effect on cell shape as compared to 1 x PBS (Figure 13B, F and C, G, respectively). With the highest concentrated buffer salts crystals can be seen (indicated by arrows in Figure 13D, H).

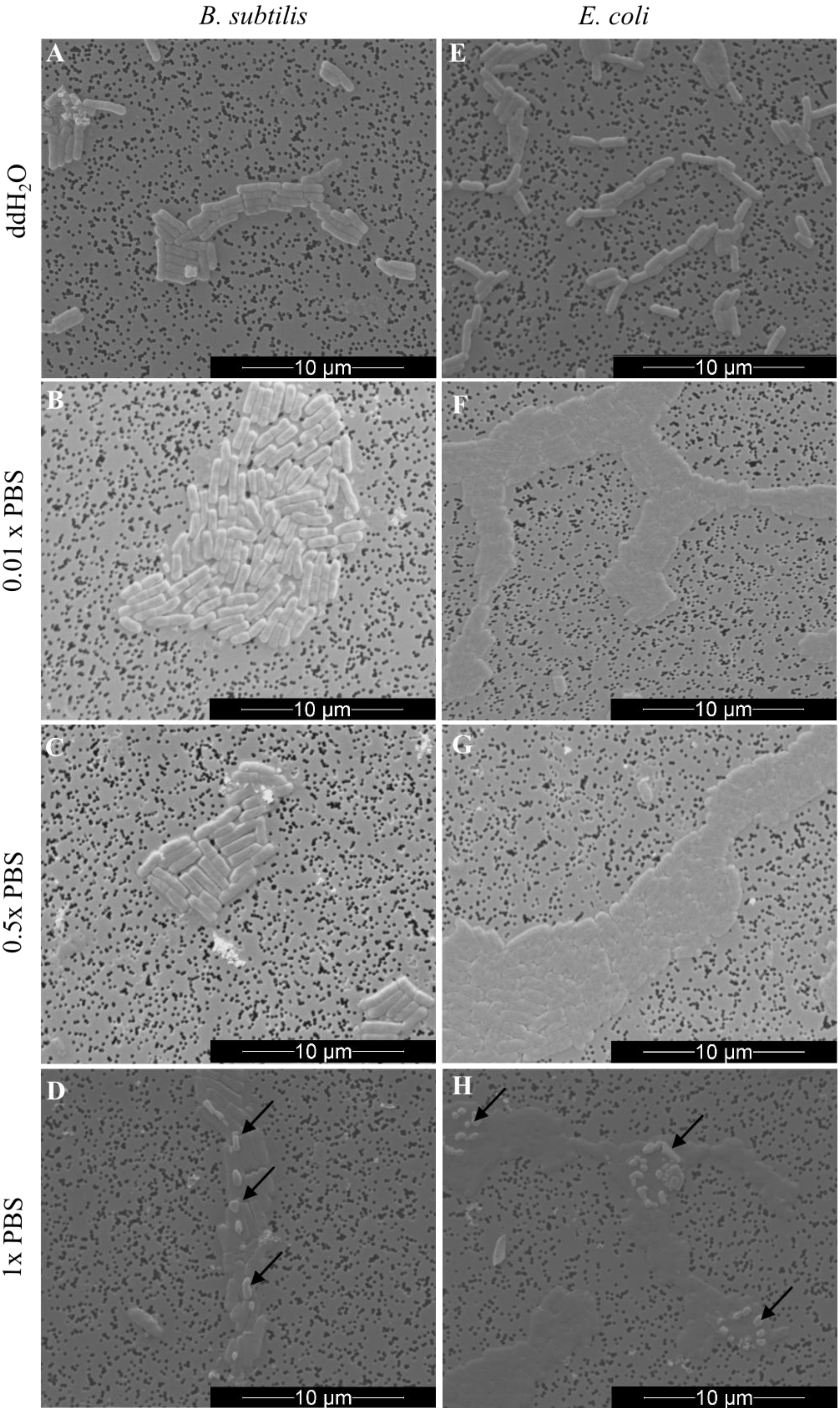
B. subtilis
E. coli
ddH2O
0.01 x PBS
0.5x PBS
1x PBS
A
B
C
D
E
F
G
H
10 µm

Figure 13: *B. subtilis* (EtOH-fixed) and *E. coli* (PFA-fixed) cells taken up in and washed with buffers of different concentrations and sterile water. Arrows in D) and H) point out potential salt crystals.

The effect of buffer-strength on “over fixed” Gram-positive cells was strongly reduced. PFA-fixed *B. subtilis* cells hardly differed in regards of their cell morphology compared between being washed with 1 x PBS and water (Figure 14A, B).

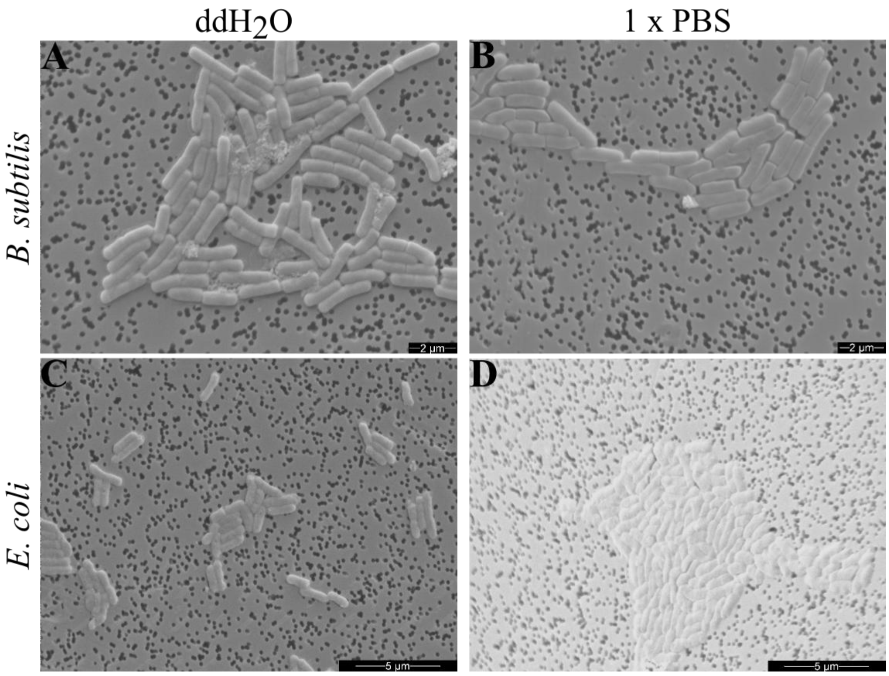

Figure 14: *B. subtilis* (PFA-fixed) and *E. coli* (EtOH-fixed) washed with either ddH$_2$O (A and C) or 1 x PBS (B and D).

In contrast, the fixation method did not seem to have any influence on the effect of buffer strength on Gram-negative cells. Ethanol-fixed *E. coli* showed the same irregular shape like PFA-fixed cells when being washed with 1 x PBS (Figure 14D). Ethanol-fixed *E. coli* cells that were washed with water also seem slightly distorted supporting the fact that Gram-negative bacteria require crosslinking fixatives as PFA (Figure 14C). Additional washing steps that were introduced by DAPI staining (10 minutes in DAPI in, 5 minutes in H$_2$O and 1 minute in ethanol) partially reversed the effect of morphology change introduced by washing with 1x PBS. Both PFA-fixed *E. coli* and EtOH-fixed *B. subtilis* appear to have normal cell morphologies after DAPI staining (Figure 15).

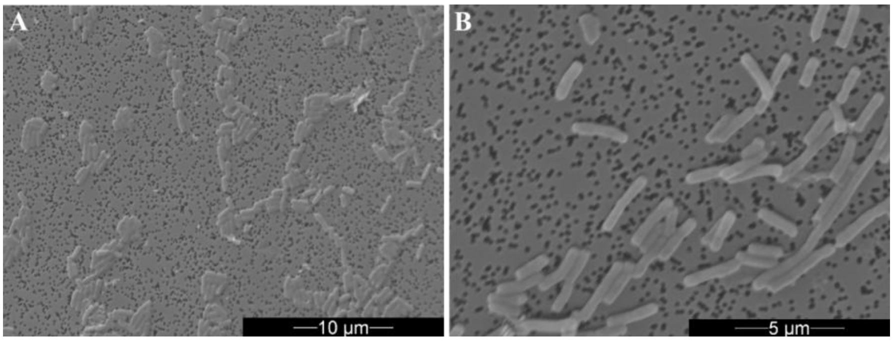

Figure 15: *B. subtilis* EtOH-fixed (A) and *E. coli* PFA-fixed (B) 1 x PBS washed and DAPI stained.

8.2.3 Cell detachment and concentration enables single-cell analysis of soil microorganisms

To proof that our Nycodenz density centrifugation sufficiently separates cells from soil particles, the cell fractions from two different soils (Klausen-Leopoldsdorf and Neustift) were filtered onto polycarbonate filters (GTTP, 0.2µm) and analyzed by SEM and LSM after DAPI staining. To investigate particle reduction, the same volumes of the untreated soil slurries were filtered and analyzed too. However, the soil slurries had to be diluted 1:100 to be mountable for the LSM analysis, since too much soil material was on top of the filters, which prevented coverslip deposition (Supplementary Figure 5). As shown in Figures 16 and 18, still many soil particles are present in the soil slurry after a 1:100 dilution, making it difficult to detect cells in SEM as well as in LSM-micrographs. However, as expected, dilution of the soil slurries leads to a high cell loss (Figures 16 and 18; panels B, D). Nycodenz separation, in contrast leads to high reduction of soil particles in our samples - especially of those of larger size (Figure 16 and 18, panel A). As indicated in Figure 17, we were able to extract single cells from one of our

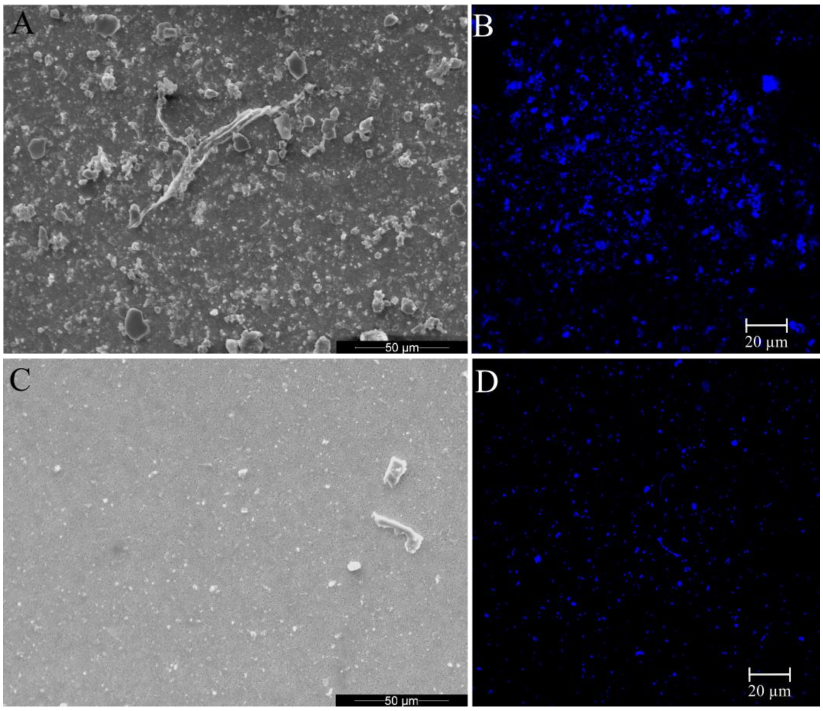

Figure 16: SEM and LSM-micrographs (the latter showing DAPI-stained cells) of samples from Klausen-Leopoldsdorf without (A, B) and with (C, D) the application of the cell removal protocol. Soil slurries were diluted 1:100.

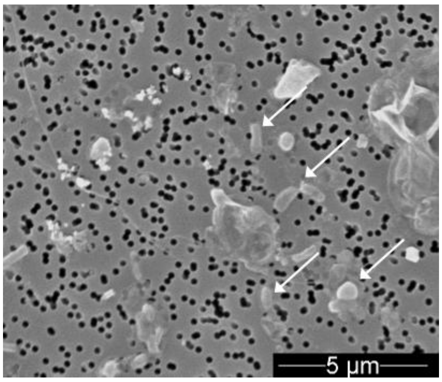

Figure 17: SEM micrographs of single cells extracted from one of our inorganic N amended microcosms, using our cell removal protocol. Cells are indicated by arrows.

microcosms (spring 2013, inorganic N control) that are not masked by particles, therefore being suitable for NanoSIMS measurements.

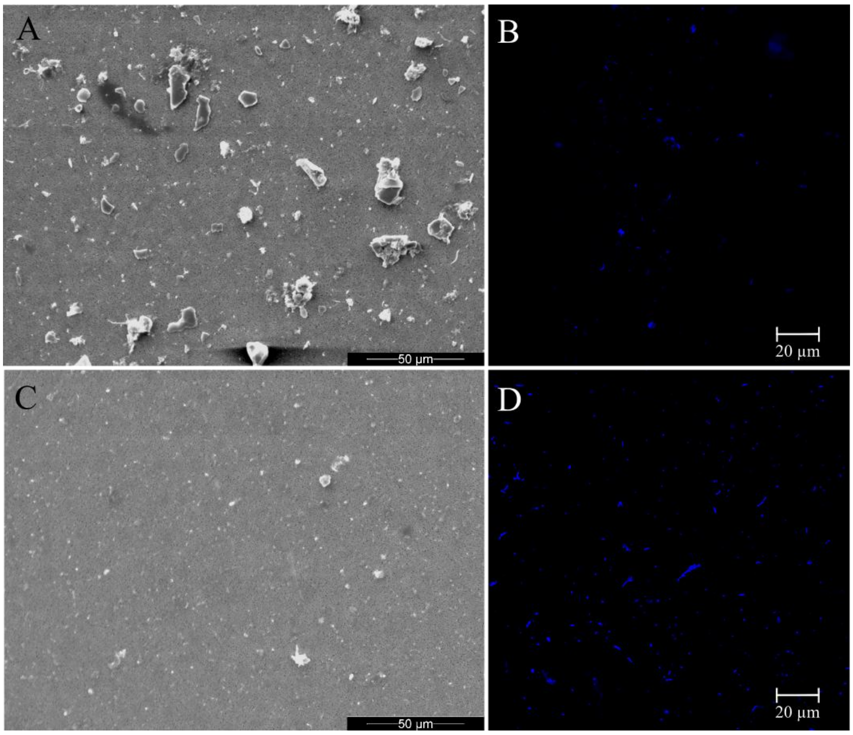

Figure 18: SEM and LSM-micrographs (the latter showing DAPI-stained cells) of samples from Neustift without (A, B) and with (C, D) the application of the cell removal protocol. Soil slurries were diluted 1:100.

8.2.4 Developed sample preparation pipeline for single cell analysis of soil microorganisms

We successfully detached cells from soil particles using a combination of chemical treatments and separated them by Nycodenz gradient centrifugation (7.5.2). As soil particles were sufficiently removed (Figure 16 and 18, panel C), samples should be suitable for analysis by NanoSIMS or Raman microspectroscopy. Therefore we developed a sample preparation pipeline for mentioned methods (Figure 19).

For NanoSIMS measurements, the cell fraction is filtered onto a gold-palladium sputtered polycarbonate filter to obtain a proposed cell density of about 1 000 cells per viewing grid (0.015 mm^2). To confirm filter cleanness and integrity we recommend evaluation with a stereoscope. In case of specific groups that should be investigated, microorganisms should be identified by (CARD-)FISH. Regions encompassing targeted cells can be marked by LMD-microscopy.

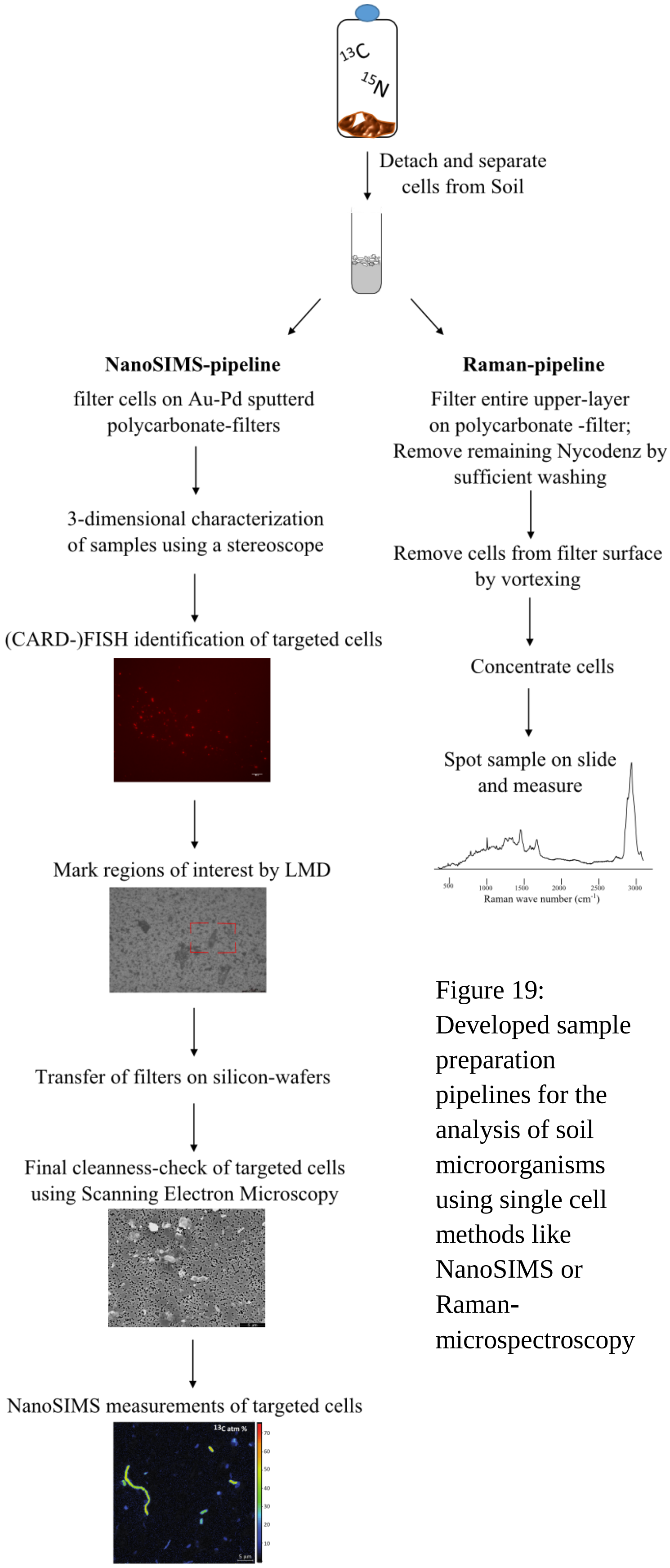
13C
15N
Detach and separate cells from Soil
NanoSIMS-pipeline
filter cells on Au-Pd sputterd polycarbonate-filters
3-dimensional characterization of samples using a stereoscope
(CARD-)FISH identification of targeted cells
Mark regions of interest by LMD
Transfer of filters on silicon-wafers
Final cleanness-check of targeted cells using Scanning Electron Microscopy
NanoSIMS measurements of targeted cells
13C atm %
70
60
50
40
30
20
10
5 µm
Raman-pipeline
Filter entire upper-layer on polycarbonate -filter; Remove remaining Nycodenz by sufficient washing
Remove cells from filter surface by vortexing
Concentrate cells
Spot sample on slide and measure
500
1000
1500
2000
2500
3000
Raman wave number (cm-1)

Figure 19: Developed sample preparation pipelines for the analysis of soil microorganisms using single cell methods like NanoSIMS or Raman-microspectroscopy

To provide a plane surface area of the filter we recommend mounting the filter on silicon-wafers using super glue. As a final check before NanoSIMS measurements the region of interest should be checked for covering soil particles using SEM, as fluorescent methods cannot provide sufficient information on impurities.

For Raman microspectroscopy the entire cell fraction is filtered onto a polycarbonate filter and washed sufficiently with 1x PBS to remove remaining Nycodenz, which could interfere with Raman measurements. The cells are removed from the filter by vortexing. The cells should be concentrated in 1x PBS (depending on the sample 20 - 40 µl should be ideal). To prevent possible cell aggregates, the sample can be slightly sonificated prior to cell-concentration.

8.2.4.1 Proof-of-principle for NanoSIMS analysis of cellulolytic and diazotrophic cells from soil microcosms

The developed sample preparation pipeline is compatible with NanoSIMS analysis: Larger soil particles were sufficiently removed to allow NanoSIMS analysis, and we were able to identify detached cells in our samples (Figure 17). We could successfully apply NanoSIMS measurements to detect microbial cellulose degradation and diazotrophy. Secondary electron micrographs depict that the measured cells were free from soil and substrate contaminations (Figure 20 and 21, panels B and D). We successfully documented ^{13}C incorporation into cells of our spring soil microcosms primed with inorganic N and complex C (Figure 20). We could measure enrichment levels between 11 and 55 atom% in both treatments at randomly chosen spots. We observed differential cell morphologies, indicating a potentially diverse population of microorganisms responding to this treatment. We were also able to apply our NanoSIMS pipeline on samples incubated with glucose and $^{15}N_2$ to confirm microbial diazotrophy across two different soils, a beech forest soil (Klausen-Leopoldsdorf) and an alpine meadow soil (Neustift) (Figure 21). Differences in the level of enrichment (2.4 – 41 atom %) between the two soils might not necessarily represent efficiency differences between the two communities as a random spot on the filter was chosen and identity of the microorganisms is unknown.

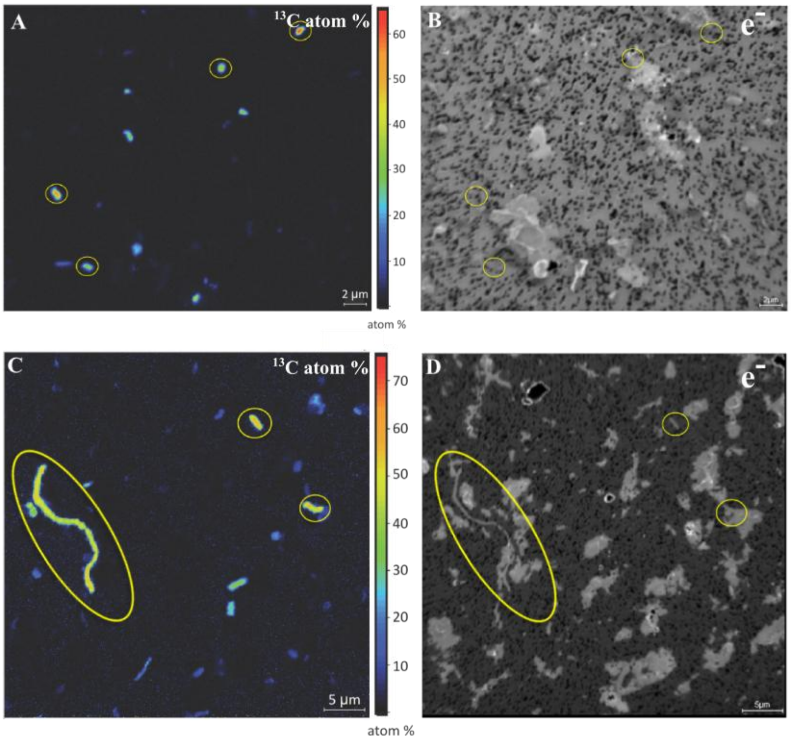

Figure 20: NanoSIMS measurements of ^{13}C-cellulose microcosms primed with inorganic N (A) and complex C (B) after incubation for 15 days. Legends indicate ^{13}C atom %. (B) and (D) indicate the respective secondary electron images.Yellow marks indicate analyzed cells.

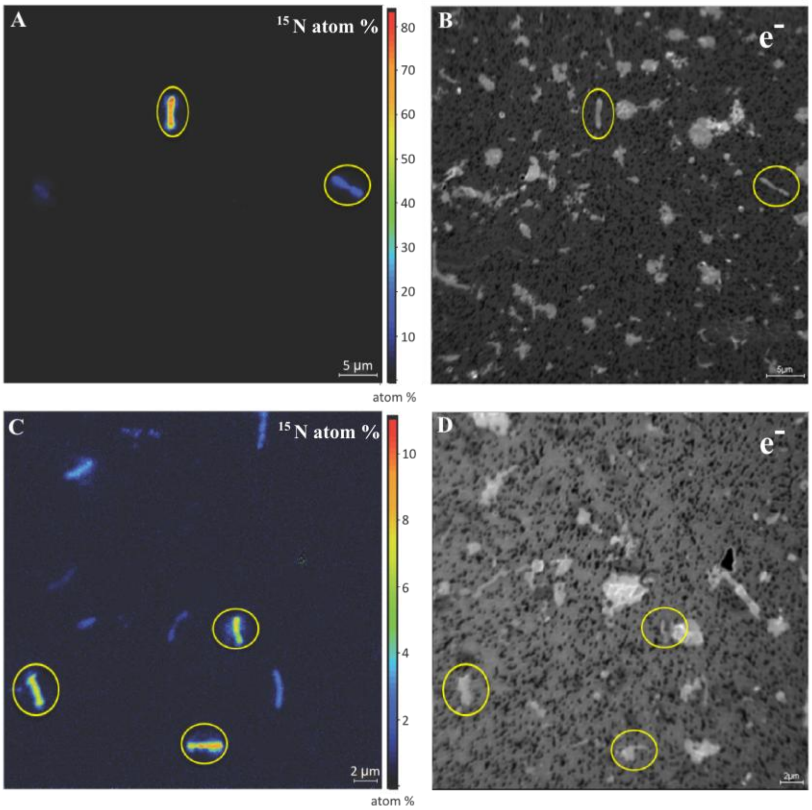

Figure 21: NanoSIMS measurements of samples from Klausen-Leopoldsdorf (A) and Neustift (C) incubated with $^{15}N_2$ and glucose for 21 days. Legends indicate ^{15}N atom %. (B) and (D) indicate the respective secondary electron images. Yellow marks indicate analyzed cells.

8.2.5 Raman spectroscopy

8.2.5.1 Proof-of-principle for Raman microspectroscopy of cells from soil microcosms

Using the developed cell-separation/concentration and sample preparation methods we could obtain a sufficiently clean sample to apply Raman microspectroscopy to cells from our soil microcosms. As indicated in Figure 22 we were able to measure spectra from single cells showing specific marker peaks like Phe (1004 cm^{-1}), glycogen (485 cm^{-1}) or the prevalent C-H bond derived lipid-peak (around 2 900 cm^{-1}). However, it was not possible to detect ^{13}C-incorporation within 100 cells from microcosms amended with ^{13}C-Cellulose and inorganic N or CMC/Xylan, based on the characteristic ^{13}C-Phe peak at 964 cm^{-1}. However, cells from the same treatment did show ^{13}C-enrichment of up to 55 atom % measured by NanoSIMS measurements (Figure 20).

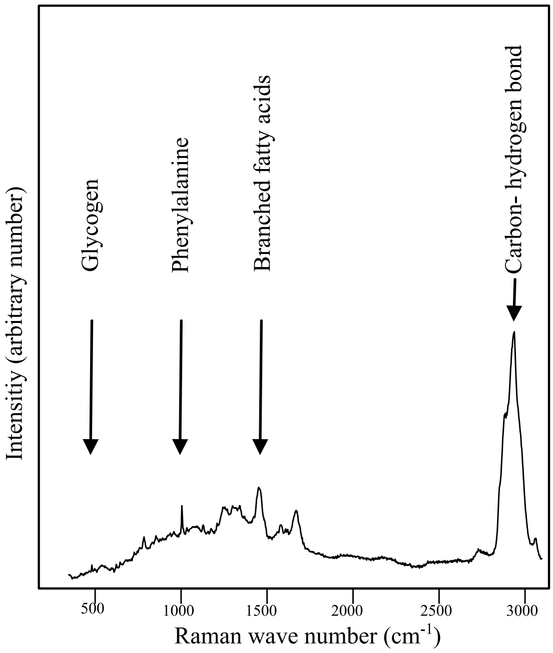

Figure 22: Representative spectra of a cell obtained from a ^{13}C-cellulose microcosm amended with inorganic N. Specific cell markers such as the Phe, glycogen, C-H bond peaks can be seen.

8.2.5.2 Microbial uptake of environmental amino acids hinders the application of ^{13}C-Phenylalanine Raman microspectroscopy to detect ^{13}C-enriched cells

As we could not identify a single ^{13}C-enriched cell by the characteristic shift of the Phe peak despite the fact that ^{13}C-enriched cells were detected by NanoSIMS, we hypothesized that microorganisms in our microcosms did not incorporate ^{13}C in amino acids but instead in other compounds. Potentially, they rather took up amino acids from soil than synthesizing them by using the C from the ^{13}C-cellulose, thus not being detectable through Raman microspectroscopy. We tested the strategy of Phe synthesis of soil microorganisms by providing them in different incubations with increasing concentrations of amino acids, while the concentration of glucose remained constant. Microorganisms incubated with ^{12}C-glucose and variable concentrations of ^{13}C-labeled amino acids show the Phe peak at 1004 cm^{-1} (corresponding to ^{12}C) at low ^{13}C-labeled amino acid concentrations (Figure 23A, C). The ^{13}C-Phe peak at 964 cm^{-1} could be detected in some cells at a concentration of 0.001 g/l. However, it was prevalently present at concentrations of 0.1 and 1 g/l, suggesting efficient uptake of ^{13}C-amino acids, in detail phenylalanine. This is also supported by a concentration dependent decrease of the ratio of the Raman intensities at 1004 cm^{-1} and 964 cm^{-1} (Figure 23C) and the co-clustering of spectra between 800 cm^{-1} and 1100 cm^{-1} from concentrations of 0.1 and 1 g/l revealed by multidimensional scaling (data not shown).

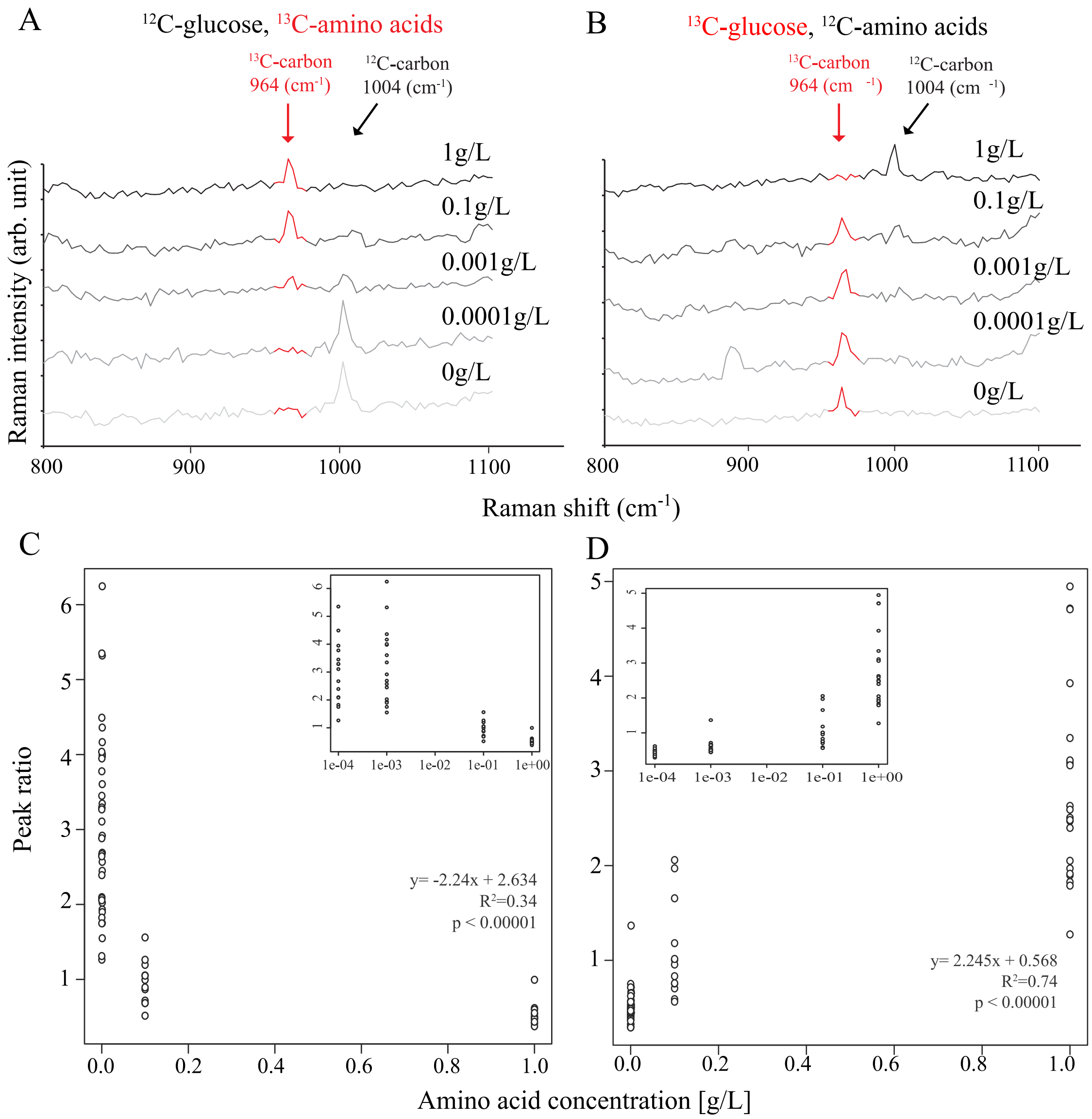

Figure 23: Representative spectra between 800 and 1100 cm^{-1} of cells grown in media containing ^{12}C-glucose and ^{13}C-labeled amino acids (A) or ^{13}C-glucose and ^{12}C-amino acids (B). C) and D) show the ratios of intensities at 1004 cm^{-1} and 964 cm^{-1} of incubations with ^{13}C-labeled amino acids (C) or ^{13}C-labeled glucose (D). In all incubations, glucose concentration is constant, while concentrations of ^{13}C-labeled amino acids vary.

The sister experiment using ^{13}C-labeled glucose and ^{12}C-amino acids depicts the same pattern. The Phe peak at 964 cm^{-1} (of ^{13}C-Phe) is most prevalent at lower amino acid concentrations (at which Phe was synthesized by ^{13}C-glucose) and shifts towards the ^{12}C-Phe derived peak at 1004 cm^{-1} at amino acid concentrations of 0.1 and 1 g/l. (Figure 23B, D). MDS shows that two major clusters are formed; one mostly represented by 0.1 and 1 g/l concentrations (data not shown).

8.2.5.3 D_2O as a general activity marker for soil microorganisms

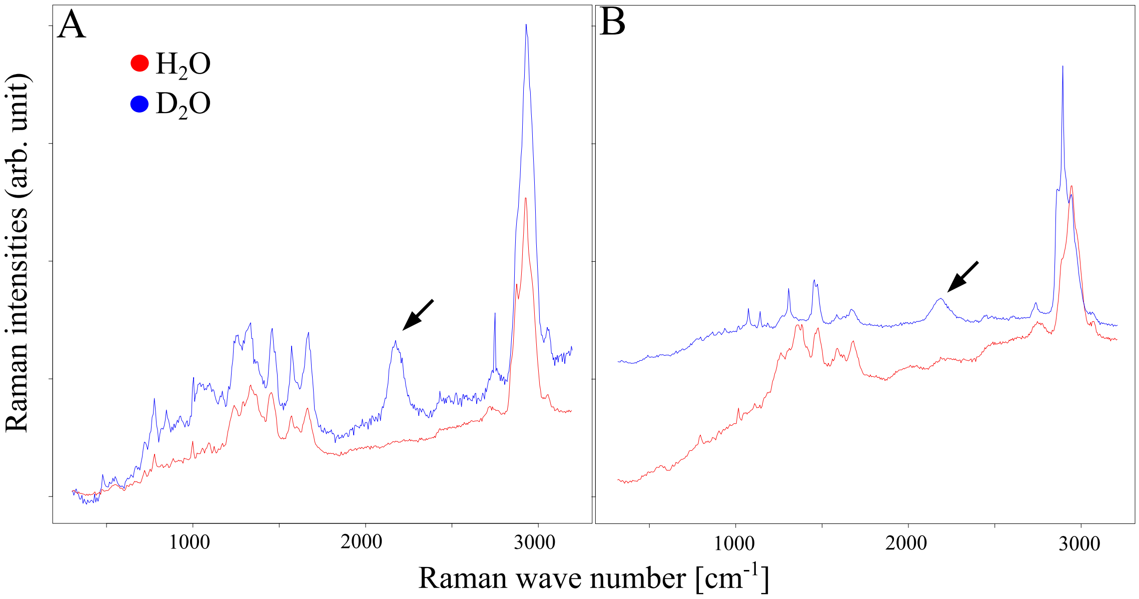

Figure 24: Unbaselined representative Raman spectra from enrichments of soil microorganism (A) and soil (B) incubated either with H_2O only (red) or in 50% D_2O (blue). Arrows highlight the C-D-related peak.

As shown in Figure 24A, after 48 hours of incubation cells from the enrichments of soil microorganisms grown on medium consisting of D_2O:H_2O (1:1, v/v) show the C-D related peak at 2150 cm^{-1}. This peak was detected in all of the measured cells. Cells derived from soils with approximately 50% moisture (D_2O:H_2O, 1:1, v/v) after 12 days of incubation mostly show spectra without this peak. However, it was possible to detect the peak in about 8% of the analyzed cells indicating 8% active cells under these conditions (Figure 24B). Interestingly, the Phe peak is not very prevalent in these samples.

9 Discussion

9.1 Cellulose degradation

We monitored degradation of ^{13}C-labeled cellulose in microcosms across different C and N amendments and two seasons by measuring enzymatic potential and ^{13}C- as well as general respiration over a time period of 25 days. PLFAs were extracted from summer soil to assess community shifts depending on incubation time or different background properties.

The natural spring community showed highest activities for cellobiohydrolase, arabinosidase and xylosidase, whereas the summer community showed highest potential concerning β-glucosidase (Table 3). Enzymatic activities are rather low in fall. It could be hypothesized that the spring community shows highest potential for complex C hydrolases due to new input of complex C- whereas the summer community shows higher β-glucosidase-activities due to a higher level of (partially) degraded components (Figure 4 and 5). The decreased activity levels in fall compared to summer could be due to temperature differences (Baldrian *et al.* 2013; Steinweg *et al.* 2013). However, previous studies do not show consistent results concerning activity-maxima or -minima of certain enzymes related to specific seasons (Andersson *et al.* 2004; Wittmann *et al.* 2004; Voříšková *et al.* 2014; Baldrian *et al.* 2013; Costa *et al.* 2013; Alster *et al.* 2013). This might be due to a variety of parameters influencing enzymatic potential (Baldrian *et al.* 2010; Wittmann *et al.* 2004) and the functional redundancy of cellulolytic microorganisms occupying different niches concerning these parameters.

The addition of inorganic N significantly increased cellulose degradation rates in summer and fall based on enzyme activities and ^{13}C respiration over time (Figure 6), and is also supported by higher yields of ^{13}C-enriched PLFAs, which were measured in summer microcosms. However, the equimolar addition of organic N did not seem to have a significant influence on enzyme activities (Figure 4 and 5), but it did increase ^{13}C mineralization, even though to a minor extent (Figure 6). This suggests that cellulose degradation is not only N limited, but its efficiency also is dependent on the quality of available N sources. Low C/N values have shown to increase cellulolytic activity in soil ecosystems (Kurka *et al.* 2000). By addition of casamino acids we also introduced additional C, leading to a less altered C/N ratio as compared to the inorganic N amendment. Increased $^{12}CO_2$ production in organic N amendments over time with and without cellulose as compared to the control and the inorganic N amended samples suggests that the organic N additions were also used as C sources (Figure 6).

Organic N had a higher influence than complex C on cellobiohydrolase, glucosidase and xylosidase activities in fall as compared to summer (Figure 4 and 5). Our sampling site has been shown to encompass lower levels of inorganic N (Kaiser *et al.* 2011) as well as amino acids (Hackl *et al.* 2005) in fall, suggesting a generally higher demand for N in this season. Addition of C sources only had a minor influence on (hemi-) cellulolytic activities, suggesting that cellulolytic microbial communities in summer as well as in fall are not limited in C sources (Figure 4 and 5). Addition of C sources led to an insignificant decrease of $^{13}CO_2$ respiration and a high increase of respired $^{12}CO_2$ (Figure 6). $^{12}CO_2$ respiration rates for C additions reveal that the added amount of C rather served as C-source, than significantly enhancing cellulose degradation. This is also supported by the fact that amendment with the readily oxidizable glucose led to highest $^{12}CO_2$ levels and lowest $^{13}CO_2$ levels. Incubations with non-crystalline cellulose and xylan had less influence in both directions but showed the same trend.

Fall microcosms clearly showed lower enzymatic activities in the first part of the incubation experiment as compared to the respective samples in summer (Figure 4 and 5). After 25 days, however, no significant differences were detectable anymore; in fact cellobiohydrolase-activity was even significantly higher than in summer. It is possible that the fall microbial community needed time to adapt to the significantly higher temperatures during incubation. However, only insignificant differences could be obtained concerning $^{12+13}C$ respiration rates.

Addition of ^{13}C-labeled cellulose increased SOC respired $^{12}CO_2$ 1.06 to 1.3 fold as compared to the respective controls (Figure 6, Supplementary Figure 3 and 4). This is probably due to a SOC-mineralization priming effect introduced by cellulose, which has been shown by Fontaine and colleagues (Fontaine *et al.* 2004). In this study it was further revealed that the increase of total soil respiration primed by cellulose was more prevalent in nutrient limited samples. This is also supported by a lower increase of total SOC-mineralization in our N amended microcosms. Independent from the amendments in summer we detected a strong decrease of enzymatic potential across all enzymes- at day 12 for cellobiohydrolases and at day 15 for glucosidases, arabinosidases and xylosidases respectively (Figure 4 and 5; Panels A and C). A similar pattern was observed in fall, however not that intense. Also PLFA yields of summer microcosms changed between days 12 and 25 across the different amendments (Figure 4 and 5; Panels B and D). This supports the hypothesis of two major phases in cellulose degradation, as shown by Hu & van Bruggen (1997).

The different additions did not only influence the efficiency of cellulose degradation, PLFA composition revealed different groups being selected depending on different additions. A significant 2-3 fold increase of PLFA biomass within the first 3 to 6 days of incubation suggests significant microbial growth in our microcosms (Figure 7A, Table 4). Influence of amendments on ^{13}C incorporation into PLFAs is comparable to $^{13}CO_2$ production. We obtained highest yields of PLFA derived ^{13}C in N amendments followed by the control and C additions (Figure 7B). Any markers, for bacteria as well as for fungi, showed highest enrichment levels in the N treatments. This supports enzyme and CO_2 data suggesting that N is a limiting factor for complex C degradation in soil. We did not observe significant changes in PLFA-community structure within a treatment across different time points, besides day 3 which will be discussed later. However, we observed that the addition of glucose led to a shift towards bacteria within the enriched community and the amendment with inorganic N towards fungi (Figure 9). The latter amendment showed clear fungal dominance after 6 days of incubation with a Bacteria/Fungi ratio below one. Organic N provoked a shift towards fungi in the second half of incubation.

Fungi are believed to prefer higher C/N ratios than bacteria - with overlaps (Strickland & Rousk 2010). This would suggest higher proportions of bacteria with elevated N and a larger proportion of fungi related to higher C concentrations - the exact opposite of what we found. However, stable isotope investigations and growth experiments have shown that readily oxidizable C sources (glucose, acetic acid) are more likely to be incorporated into bacteria than fungi (Rinnan & Bååth 2009; Koranda *et al.* 2014; Meidute *et al.* 2008). Even though we focus on the degradation of cellulose and subsequent uptake of cellulose derived C, we hypothesize that due to preferable utilization of the amended glucose, bacteria were more likely being primed for cellulose degradation in these microcosms.

Fungal communities show different responses to elevated N levels. Some studies show a decrease of fungal biomass (Denef *et al.* 2009; de Vries *et al.* 2006; de Vries *et al.* 2007; Frey *et al.* 2004), which follows the predicted trend of higher C/N ratios. However, also the triggering of fungi by elevated N was shown multiple times (Fontaine *et al.* 2011; Rousk & Bååth 2007; Meidute *et al.* 2008). Remarkably, Koranda and colleagues also found a significant increase of cellulolytic fungal biomass under elevated N conditions using soil from the same site (Koranda *et al.* 2014). Thus, it still is not fully known which mechanisms drive these community shifts as we deal with complex environments and complex communities within them.

The first time point (Day 3) shows a distinct ^{13}C-PLFA-composition across all treatments. This is suggested by co-clustering of most treatments (Control, Glucose, CMC/Xylan and organic N) and a distinct cluster of the inorganic N samples (Figure 10 and 11). The distinctive character of these PLFA compositions might rely on a preferential incorporation of ^{13}C that derives from more readily oxidizable contaminants in the cellulose by a certain population of microorganisms. Interestingly, we also see a high proportion of the general marker 16:00 after 3 days of incubation across all samples (Figure 8). It is the highest abundant marker in all treatments and shows a 3-4 fold higher abundance in the enriched community as compared to starting soil and the unenriched population of our microcosms. As abundance is highest in the Glucose and inorganic N amended samples it is unlikely that this is due to a prevalent fraction of either bacteria or fungi as these treatments clearly selected for either one of them. As this phenomenon is only detectable in the first time point and only in the enriched populations it also might be due to stress factors as changing environment and competition towards the labeled substrate. However, indices for this not being the case are (1) 16:00 has not been shown to be a marker related to stress factors (Frostegård *et al.* 2011), (2) the abundance shift of marker 16:00 can only be seen in the ^{13}C population, suggesting a reason linked to the substrate.

9.2 Development and testing of sample preparation strategies for single-cell analysis of soil microorganisms

Polycarbonate filters are standard in FISH applications of many environmental samples, when cells have to be concentrated as it is the case in aquatic samples or our Nycodenz cell fraction. However, when used for NanoSIMS measurements of cells enriched in ^{13}C they might lead to a dilution of the signal by emitting ^{12}C ions even though being gold-palladium sputter coated. Furthermore, they are very thin and flexible and thus difficult to handle during sample preparation. During handling they can be easily distorted, which leads to an uneven surface and to problems during analysis.

In search for possible alternatives, the first step was to determine the topography of various possible alternative filters under the SEM (Figure 12). This revealed that filters made of nylon as well as of cellulose-nitrate show pore sizes up to 5 times larger than indicated, increasing risk of losing cells during the filtering process. Furthermore nylon harbors a highly uneven topology, which potentially masks the filtered sample. Additionally, the filter material shows instability during the scanning process and is hygroscopic which leads to higher evacuation times. Using silver as filter-material would be ideal as it is naturally conductive and makes the sputtering process unnecessary. However, during general storage conditions these filters seem to oxidize easily (indicated by crystals in Figure 12A), which reduces conductivity. Aluminum-oxide filters seem to have the indicated pore size and do not show major irregularities in topography. Unfortunately, this filter material is highly fragile, making it inapplicable for combination with (CARD-) FISH. However, for applications that do not require FISH for the identification of target cells (e.g. investigations of cultures), these filters might be of interest, as they would not introduce atoms such as C or N during analysis. As aluminum-oxide is an isolating material, it will need extensive sputtering with gold-palladium to be applicable for NanoSIMS that requires conductivity. Therefore, testing of different gold-palladium layers on this filter material is still required to evaluate the necessary conducting coating thickness to overcome the problem of conductivity. For application where cells have to be identified by (CARD-)FISH prior to NanoSIMS analysis, polycarbonate filters still seem the best option for samples where cells have to be concentrated by filtration. To overcome the introduction of C atoms during analysis, we propose to use a thicker layer of gold-palladium coating. We successfully resolved the uneven surface introduced during handling by attaching the filter to a silicon wafer piece just before mounting on the NanoSIMS holder (Figure 19).

Investigations on the osmotic behavior of cells after fixation are rare and were mainly focused on cells or tissues of animals. Bone and Denton showed that Fish-tissue was still osmotically active after formaldehyde fixation, which was also confirmed by Paljarvi and colleagues investigating rat brain tissue (Bone & Denton 1971; Paljärvi *et al.* 1979). However, it is not clear to which extent these results are conferrable to bacteria or Archaea, due to different membrane-protein contents and the absence of cell walls in cells of mentioned cell-types.

Due to its osmotic strength 1x PBS is the standard washing buffer for a variety of cells; e.g. FISH (Amann *et al.* 1990). However, after drying of washed samples residual salt crystals can interfere with NanoSIMS or Raman microspectroscopy. In our experiment we tried to reduce the buffer concentration as far as possible without destroying the cell integrity. Interestingly, the results were contrary to what we expected. *E. coli* as well as *B. subtilis* cells appear most intact after water treatment (Figure 13). Increasing the buffer concentration led to a constant loss of cell integrity. After washing with 1 x PBS, cells appeared turgid and swollen, and could hardly be identified as cells. We hypothesize that this is due to different turgor pressures that cells experience when exposed to different buffer strengths. Due to the higher salt concentration inside the cells when cells are washed in water, water flows into the cell leading to a higher turgor pressure, which stabilizes the cells during drying. By increasing the buffer concentration, less water flows into the cells as the osmotic difference decreases, which leads to less stabilization through the turgor pressure during the drying process. 1x PBS washed cells that were DAPI stained (which introduces additional water-washing steps) show partially restored morphology (Figure 15). This can also be explained by increased turgor pressure when exposed to water, as the osmotically active components are still present in the cell.

Generally, the Gram-negative *E. coli* cells seemed to be more sensitive to the osmotic effects of the different buffer strengths than the Gram-positive *B. subtilis* cells. To investigate the influence of different fixation methods on the morphological integrity of cells, the experiment was repeated with PFA-fixed *B. subtilis* (as an example of “overfixed” cells) and EtOH-fixed *E. coli* cells (as an example of “underfixed” cells) washed with 1x PBS and water (Figure 14). “Overfixed” Gram-positive cells seem to show no severe morphology changes compared between the two washing solutions in contrast to “underfixed” Gram-negative cells that nearly loose cell integrity when washed with 1x PBS. This finding reflects the fixation principle of formaldehyde cross-links cell proteins, leading to a higher stability as compared to the denaturing effect of the ethanol fixation (Dapson 2007). However, the problem with formaldehyde as a fixative is that due to the mentioned effect Gram-positive cells have to be harshly permeabilized in order to be able to perform (CARD-)FISH afterwards (Schönhuber *et al.* 1997; Bidnenko *et al.* 1998). Thus, for this cell types ethanol fixation is the preferred fixation method (Roller *et al.* 1994).

To apply single cell methods such as NanoSIMS and Raman microspectroscopy, the investigated sample should encompass a high concentration of cells and should be as clean as possible. Previous applications of FISH or CARD-FISH on soil samples relied on dilution to reduce the influence of soil particles (Eickhorst & Tippkötter 2008). However, by dilution, the cell to particles ratio does not significantly change. To obtain a clean sample with a sufficient amount of cells, the cells have to be detached from the particles, separated from them and if necessary concentrated. In this thesis we tested the applicability of this strategy to investigate soil microorganisms through the single-cell methods NanoSIMS and Raman microspectroscopy. We were able to detach cells from particles of two different soils and physically remove them obtaining a rather clean sample. As indicated in Figure 16 and 18 (panels A and C), the soil particle load was significantly reduced after Nycodenz centrifugation, especially regarding larger particles that would make NanoSIMS analysis very complicated and tedious. SIMS analysis of cells in soil so far have not been combined with a cell extraction method prior to measurements (Cliff *et al.* 2002; Herrmann *et al.* 2007). However, extracting and concentrating cells from a soil sample reduces the possibility of soil particles interfering with the measurements and also makes it possible to analyze multiple cells in a single run. The analysis of a high number of cells (or as high as technically possible) is particularly important when analyzing environmental microbial populations, in which activity will most likely vary greatly (e.g. shown for diazotrophic populations in Lechene *et al.*, 2007 and Woebken *et al*., 2012). We have shown that our soil sample preparation protocol is compatible with NanoSIMS measurements (Figure 20 and 21), enabling now the examination of single-cell activities in target microbial populations in soil samples.

Raman spectroscopy has been used to detect the microbial uptake and incorporation of different ^{13}C-labeled C sources (Huang *et al.* 2004; Huang *et al.* 2007; Huang and Ferguson, *et al.* 2009; Li *et al.* 2012). Using our developed soil sample preparation method to recover soil microorganisms, we were able to obtain single cells that can be measured with Raman microspectroscopy (Figure 22). We wanted to apply this protocol to detect ^{13}C-enriched microbial cells from the cellulose-degradation experiments in spring 2013 (described under 7.3) using the characteristic ^{13}C- Phe-peak at 964 cm^{-1}. Given a detection limit of approximately 10 atom% for ^{13}C with Raman microspectroscopy (Huang *et al.* 2007), we were optimistic to detect enriched cells as NanoSIMS measurements revealed enrichment levels from 11 to 55 atom%. Surprisingly, we could not detect a single cell with the ^{13}C-Phe peak at 964 cm^{-1} across 200 measured cells of the same samples used for NanoSIMS measurements. The most likely reason for this finding seems that Phe was rather taken up from the environment than newly synthesized through ^{13}C-labeled C sources by the microorganisms. In order to test this hypothesis we removed cells from their natural soil matrix and incubated them aerobically with a constant concentration of ^{12}C or ^{13}C glucose and varying levels of background amino acids, ^{13}C- or ^{12}C-labeled, respectively. In both experiments the community strategy shifted from synthesis to uptake of amino acids between concentrations of 0.001g/l and 0.1 g/l (7.35 µM and 735.3 µM based on the average molar mass of amino acids) (Figure 23). This transition range is most likely due to measurement of different organisms with different efficiency in the uptake of amino acids. Hackl and colleagues estimated the amino acid concentration at our sampling site (Hackl *et al.* 2005). With variations from 0.0058 g/l (42 µM) in spring to 0.0011 g/l (11.03 µM) in fall it seems that the amino acid concentration was high enough to enable amino acid uptake thus suppressing Phe synthesis from ^{13}C labeled cellulose. This appears to be a general issue in soil systems, as amino acid concentrations can – depending on the type of soil, season and vegetation – reach values of up to 158 µM (alpine dry meadow soil) and 416 µM (pine wood soil) (Kielland 1995; Raab *et al.* 1999; Hackl *et al.* 2005). As the ^{13}C-Phe related Raman peak relies on the fact that Phe has to be synthesized de novo to be detectable, and to overcome the above-mentioned issues, one could instead try to detect ^{13}C incorporation into other compounds (Huang *et al.* 2004; Li *et al.* 2012). However many of these compounds – e.g. pigments – are not prevalent across different organisms, which makes it less applicable for environmental samples.

Water is the primary hydrogen source for lipid biosynthesis (Valentine *et al.* 2004; Wegener *et al.* 2012); thus, deuteriated water (D_2O) should be a very suitable substrate to generally detect active cells due to the incorporation of deuterium into cellular biomass. Deuteriated water can be considered the least community-altering stable isotope substrate in activity studies compared to ^{13}C- or ^{15}N-conatining substrates, as the latter can often be used as nutrient source by certain microorganisms thereby altering the nutrient regime in stable isotope incubations. Heavy isotope-labeled H_2O (in these cases $H_2{}^{18}O$) has previously been used to differentiate between active and inactive members of the microbial community and to identify bacteria that respond quickly to rewetting (Schwartz 2007; Aanderud & Lennon 2011).

It was recently shown that the C-D peak of lipids can be relatively easily detected by Raman microspectroscopy, thus enabling the identification of active cells by D_2O incubations followed by Raman microspectroscopy. We have shown that all soil microorganisms enriched in media consisting of 50% D_2O show the characteristic C-D peak (at 2150 cm^{-1}), indicating actively growing cells (Figure 24A). In contrast, only about 10% of the cells that were analyzed from soil samples incubated in 50% D_2O showed the specific peak after 12 days of incubation, indicating that only a small proportion of soil microorganisms were active. Due to the low number of measured cells (n= 40), this estimation might be biased, however, we successfully show the proof-of-concept by measuring general activity of soil microorganisms through deuterium incorporation and detection of the C-D related peak by Raman microspectroscopy. As Raman can be used to identify these organisms quickly and in a non destructive manner, this leaves open possible downstream applications like incubation experiments or single cell genomics (Huang, Ward, *et al.* 2009), which could also be applied to more complex substrates labeled with deuterium.

9.3 Conclusion and Outlook

Cellulose degradation is a very energy and N demanding process. A variety of enzymes are necessary to make this macromolecule accessible for microorganisms and to break the crystalline structure down to a unit that can be taken up by cells and utilized as a C source. We have shown that the addition of N sources, especially inorganic N primed cellulose degradation significantly, as demonstrated with enzyme assays, respiration rates and also ^{13}C-labeled PLFAs. Furthermore, inorganic N leads to a clear community shift towards fungi during incubation, whereas glucose provoked a shift towards bacteria, indicating the different niches of these microbial groups. Thus, we have identified edaphic compounds that (1) influence the efficiency of cellulose degradation as shown by $^{13}CO_2$ measurements and enzyme assays and (2) lead to a shift of the microbial community as shown by ^{13}C-PLFA analysis.

As a next step we will perform ^{13}C-DNA-SIP to reveal the active microbial groups in greater detail. ^{12}C-DNA and ^{13}C-DNA of our microcosms will be separated by ultracentrifugation, unenriched and enriched DNA will be used to generate libraries of bacterial 16S rRNA and fungal ITS genes to investigate the cellulolytic communities on a finer scale across different amendments and time. Furthermore, it would be interesting to investigate cellulose degradation across different seasons in more detail. It has been shown that bacterial and fungal soil communities change depending on the season (Lipson & Schmidt 2004; Voříšková *et al.* 2014). Also, the complex C quality and soil properties change with differing seasons. This suggests that the quality of cellulose degradation changes across different seasons due to different condition, limiting factors and therefore different active groups.

Single-cell methods require a clean sample for analysis with a high concentration of cells. To achieve these requirements for soil samples, cells have to be detached from soil particles, separated and if necessary concentrated. Using the protocol optimized in this thesis, we were able to investigate ^{13}C- and ^{15}N-enriched cells by NanoSIMS, making it a possible tool for further application in soil samples. The protocol can also be used to prepare cells from soil samples for Raman microspectroscopy. However, the characteristic ^{13}C-Phe peak for the detection of ^{13}C-incorporation in cellular biomass is less applicable in soil, as it relies on the de novo synthesis of phenylalanine from ^{13}C-labeled C compounds. Our experiments have shown that if Phe is present in the environment it is preferably taken up instead of being newly synthesized. In these cases, other Raman peaks might have to be used instead of the Phe peak to allow detection of ^{13}C-enriched cells by Raman microspectroscopy. We could detect incorporation of deuterium from D_2O into lipids from soil microorganisms using Raman microspectroscopy, indicating that D_2O incubations in combination with Raman microspectroscopy might serve as a suitable non-destructive setup to investigate the active proportion of soil microorganisms. This is still one of many unsolved questions in soil microbial ecology.

We have shown that it is possible to prepare a cell fraction from soil samples that is suitable for the investigation by NanoSIMS (and Raman microspectroscopy). We plan to use this approach for further investigations of celluloytic microorganisms. Based on our data on cellulolytic activity at Klausen-Leopoldsdorf and the expected sequence information from the ^{13}C-DNA-SIP experiments, we will apply the CARD-FISH-NanoSIMS approach to chosen treatments (such as inorganic N addition and glucose addition in comparison to no addition controls) to obtain more detailed information on the single-cell activity of certain targeted cellulolytic groups over the investigated time course, under the different treatments and potentially at different seasons.

10 References

Aanderud, Z.T. & Lennon, J.T., 2011. Validation of heavy-water stable isotope probing for the characterization of rapidly responding soil bacteria. *Applied and environmental microbiology*, 77(13), pp.4589–96.

Alberto Agnelli, Judith Ascher, Giuseppe Corti, Maria Teresa Ceccherini, Paolo Nannipieri, G.P., 2004. Distribution of microbial communities in a forest soil profile investigated by microbial biomass, soil respiration and DGGE of total and extracellular DNA. *Soil Biology and Biochemistry,* 36(5), pp.859–868..

Alster, C.J. *et al.*, 2013. Microbial enzymatic responses to drought and to nitrogen addition in a southern California grassland. *Soil Biology and Biochemistry*, 64, pp.68–79.

Amann, R.I., Krumholz, L. & Stahl, D. a, 1990. Fluorescent-oligonucleotide probing of whole cells for determinative, phylogenetic, and environmental studies in microbiology. *Journal of bacteriology*, 172(2), pp.762–70.

Andersson, M., Kjøller, A. & Struwe, S., 2004. Microbial enzyme activities in leaf litter, humus and mineral soil layers of European forests. *Soil Biology and Biochemistry*, 36(10), pp.1527–1537.

Bailey, V.L. *et al.*, 2013. Linking microbial community structure to β-glucosidic function in soil aggregates. *The ISME journal*, 7(10), pp.2044–53.

Bajpai, P.K., 2009. Xylanases. In *ENCYCLOPEDIA of Microbiology, Third edition*. pp. 600 – 612.

Baldrian, P. *et al.*, 2010. Distribution of microbial biomass and activity of extracellular enzymes in a hardwood forest soil reflect soil moisture content. *Applied Soil Ecology*, 46(2), pp.177–182.

Baldrian, P. *et al.*, 2013. Responses of the extracellular enzyme activities in hardwood forest to soil temperature and seasonality and the potential effects of climate change. *Soil Biology and Biochemistry*, 56, pp.60–68.

Baldrian, P. & Valášková, V., 2008. Degradation of cellulose by basidiomycetous fungi. *FEMS Microbiology Reviews*, 32(3), pp.501–521.

Bastias, B.A. *et al.*, 2009. Influence of repeated prescribed burning on incorporation of 13C from cellulose by forest soil fungi as determined by RNA stable isotope probing. *Soil Biology and Biochemistry,* 41(3), pp.467–472.

Batjes, N.H., 1996. Total carbon and nitrogen in the soils of the world. *Eur. J. Soil Sci.,* 47, pp.151–163.

Beguin, P., 1990. Molecular Biology of Cellulose Degradation. *Annu. Rev. Microbiol.*, 44(1), pp.219–248.

Behrens, S. *et al.*, 2008. Linking Microbial Phylogeny to Metabolic Activity at the Single-Cell Level by Using Enhanced Element Labeling-Catalyzed Reporter Deposition Fluorescence In Situ Hybridization (EL-FISH) and NanoSIMS. *Appl. Environ. Microbiol.*, 74(10), pp.3143–3150.

Bergner, G. *et al.*, 2011. Quantitative detection of C-deuterated drugs by CARS microscopy and Raman microspectroscopy. *The Analyst*, 136(18), pp.3686–93.

Bernard, L. *et al.*, 2007. Dynamics and identification of soil microbial populations actively assimilating carbon from ^{13}C-labeled wheat residue as estimated by DNA- and RNA-SIP techniques. *Environ Microbiol*, 9(3), pp.752–764.

David Berry, Esther Mader, Dagmar Woebken, Yun Wang, Di Zhu, Tae Kwon Lee, Marton Palatinszky, Arno Schintlmeister, Markus Schmid, Naama Shterzer, Itzhak Mizrahi, Isabella Rauch, Thomas Decker, Thomas Bocklitz, Jürgen Popp, Christopher, M. Gibson, Patrick W. Fowler, Wei E. Huang, Michael Wagner. Heavy water (D_2O) incorporation as a universally applicable activity marker for microbial communities with single cell resolution. submitted

Bidnenko, E. *et al.*, 1998. Estimation of the State of the Bacterial Cell Wall by Fluorescent In Situ Hybridization Estimation of the State of the Bacterial Cell Wall by Fluorescent In Situ Hybridization. *Applied and Environmental Microbiology*, 64(8), pp.3059–3062.

Boer, W. De *et al.*, 2005. Living in a fungal world: impact of fungi on soil bacterial niche development. *FEMS microbiology reviews*, 29(4), pp.795–811.

Bone, Q. & Denton, E.J., 1971. THE OSMOTIC EFFECTS OF ELECTRON MICROSCOPE FIXATIVES. *The Journal of Cell Biology*, 49, pp.571–581.

Boschker, H.T.S., Nold, S.C. & Wellsbury, P., 1998. Direct linking of microbial populations to specific biogeochemical processes by ^{13}C-labelling og biomarkers. *Nature*, 392, pp.801–805.

Boxer, S.G., Kraft, M.L. & Weber, P.K., 2009. Advances in imaging secondary ion mass spectrometry for biological samples. *Annual review of biophysics*, 38, pp.53–74.

Brady, N.C. & Weil, R.R., 1974. *The nature and properties of soils* Eighth edi. N. C. Brady & R. R. Weil, eds., Upper Saddle River, New Jersey: Prentice Hall.

Buckley, D.H. *et al.*, 2007. Stable isotope probing with 15N achieved by disentangling the effects of genome G+C content and isotope enrichment on DNA density. *Appl. Environ. Microbiol.*, 73(10), pp.3189–95.

Cadisch, G. *et al.*, 2005. Technical considerations for the use of 15N-DNA stable-isotope probing for functional microbial activity in soils. *Rapid communications in mass spectrometry : RCM*, 19(11), pp.1424–8.

Ciais, P., C. Sabine, G. Bala, L. Bopp, V. Brovkin, J. Canadell, A. Chhabra, R. DeFries, J. Galloway, M. Heimann, C. Jones, C. Le Quéré, R.B. Myneni, S.P. and P.T., 2013. *2013: Carbon and Other Biogeochemical Cycles. In: Climate Change 2013: The Physical Science Basis. Contribution of Working Group I to the Fifth Assessment Report of the Intergovernmental Panel on Climate Change*,

Cliff, J.B. *et al.*, 2002. Exploration of Inorganic C and N Assimilation by Soil Microbes with Time-of-Flight Secondary Ion Mass Spectrometry Exploration of Inorganic C and N Assimilation by Soil Microbes with Time-of-Flight Secondary Ion Mass Spectrometry †. *Applied and Environmental Microbiology*, 68(8), pp.4067–4073.

Costa, D., Freitas, H. & Sousa, J.P., 2013. Influence of seasons and land-use practices on soil microbial activity and metabolic diversity in the "Montado ecosystem." *European Journal of Soil Biology*, 59, pp.22–30.

Dapson, R.W., 2007. Macromolecular changes caused by formalin fixation and antigen retrieval. *Biotechnic & histochemistry*, 82(3), pp.133–40.

Dekas, A.E. & Orphan, V.J., 2011. Identification of diazotrophic microorganisms in marine sediment via fluorescence in situ hybridization coupled to nanoscale secondary ion mass spectrometry (FISH-NanoSIMS). *Methods Enzymol.*, 486, pp.281–305.

Dekas, A.E., Poretsky, R.S. & Orphan, V.J., 2009. Deep-sea archaea fix and share nitrogen in methane-consuming microbial consortia. *Science*.

DeLong, E., Whickham, G. & Pace, N., 1989. Phylogenetic stains: ribosomal RNA-based probes for the identification of single cells. *Science*, 243(4896), pp.1360–1363.

Denef, K. *et al.*, 2009. Microbial community composition and rhizodeposit-carbon assimilation in differently managed temperate grassland soils. *Soil Biology and Biochemistry*, 41(1), pp.144–153.

Deutscher, J., Francke, C. & Postma, P.W., 2006. How phosphotransferase system-related protein phosphorylation regulates carbohydrate metabolism in bacteria. *Microbiology and molecular biology reviews : MMBR*, 70(4), pp.939–1031.

Doi, R.H. & Kosugi, A., 2004. Cellulosomes: plant-cell-wall-degrading enzyme complexes. *Nature reviews. Microbiology*, 2(7), pp.541–51.

Dumont, M.G. & Murrell, J.C., 2005. Stable isotope probing - linking microbial identity to function. *Nat Rev Micro*, 3, pp.499–504.

Eichorst, S. A *et al.*, 2013. Community dynamics of cellulose-adapted thermophilic bacterial consortia. *Environmental microbiology*, 15(9), pp.2573–87. Available at: http://www.ncbi.nlm.nih.gov/pubmed/23763762 [Accessed December 8, 2013].

Eichorst, S. A. & Kuske, C.R., 2012. Identification of cellulose-responsive bacterial and fungal communities in geographically and edaphically different soils by using stable isotope probing. *Applied and environmental microbiology*, 78(7), pp.2316–27.

Eichorst, S.A. & Woebken, D., 2014. Investigation of Microorganisms at the Single-cell Level using Raman Microspectroscopy and High-resolution Secondary Ion Mass Spectrometry. In *Applications of Molecular Microbiological Methods*. pp. 203–2011.

Eickhorst, T. & Tippkötter, R., 2008. Detection of microorganisms in undisturbed soil by combining fluorescence in situ hybridization (FISH) and micropedological methods. *Soil Biology and Biochemistry*, 40(6), pp.1284–1293.

Fontaine, S. *et al.*, 2004. Carbon input to soil may decrease soil carbon content. *Ecology Letters*, 7(4), pp.314–320.

Fontaine, S. *et al.*, 2011. Fungi mediate long term sequestration of carbon and nitrogen in soil through their priming effect. *Soil Biology and Biochemistry*, 43(1), pp.86–96.

Fontaine, S.A.M. & Abbadie, L., 2003. The priming effect of organic matter: a question of microbial competition. *Soil Biology and Biochemistry*, 35, pp.837–843.

Frey, S.D. *et al.*, 2004. Chronic nitrogen enrichment affects the structure and function of the soil microbial community in temperate hardwood and pine forests. *Forest Ecology and Management*, 196(1), pp.159–171.

Frostegård, Å. *et al.*, 2011. Use and misuse of PLFA measurements in soils. *Soil Biology and Biochemistry*, 43(8), pp.1621–1625.

Frostegård, Å., Tunlid, A. & Baath, E., 1991. Microbial biomass measured as total lipid phosphate in soils of different organic content. *Journal of Microbiological Methods*, 14, pp.151–163.

Fuchslueger, L. *et al.*, 2014. Experimental drought reduces the transfer of recently fixed plant carbon to soil microbes and alters the bacterial community composition in a mountain meadow. *The New phytologist*, 201(3), pp.916–27.

Gans, J., Wolinsky, M. & Dunbar, J., 2005. Computational improvements reveal great bacterial diversity and high metal toxicity in soil. *Science*, 309(5739), pp.1387–1390.

Hackl, E. *et al.*, 2005. Composition of the microbial communities in the mineral soil under different types of natural forest. *Soil Biology and Biochemistry*, 37(4), pp.661–671.

Hadley, W., 2009. *ggplot2: elegant graphics for data anlysis*, Springer New York. Available at: http://had.co.nz/ggplot2/book.

Halliwell, G., 1965. Catalytic Decomposition of Cellulose Under Biological Conditions. *The Biochemical journal*, 95, pp.35–40.

Halm, H. *et al.*, 2009. Co-occurrence of denitrification and nitrogen fixation in a meromictic lake, Lake Cadagno (Switzerland). *Environmental Microbiology*, 11(8), pp.1945–1958.

Handelsman, J.M.R.R.S.F.B.J.C. *et al.*, 1998. Molecular biological access to the chemistry of unknown soil microbes: a new frontier for natural products. *Chemistry & Biology*, 5, pp.245–249.

Herrmann, A.M. *et al.*, 2007. A novel method for the study of the biophysical interface in soils using nano-scale secondary ion mass spectrometry. *Rapid Communications in Mass Spectrometry*, 21(1), pp.29–34.

Hu, S. & van Bruggen AHC, 1997. Microbial Dynamics Associated with Multiphasic Decomposition of ^{14}C-Labeled Cellulose in Soil. *Microbial ecology*, 33(2), pp.134–43.

Huang, W.E. *et al.*, 2004. Raman microscopic analysis of single microbial cells. *Analytical chemistry*, 76(15), pp.4452–4458.

Huang, W.E. *et al.*, 2007. Raman-FISH: combining stable-isotope Raman spectroscopy and fluorescence in situ hybridization for the single cell analysis of identity and function. *Environmental Microbiology*, 9(8), pp.1878–1889.

Huang, W.E., Ferguson, A., *et al.*, 2009. Resolving genetic functions within microbial populations: in situ analyses using rRNA and mRNA stable isotope probing coupled with single-cell raman-fluorescence in situ hybridization. *Applied and environmental microbiology*, 75(1), pp.234–41.

Huang, W.E., Ward, A.D. & Whiteley, A.S., 2009. Raman tweezers sorting of single microbial cells. *Environmental Microbiology Reports*, 1(1), pp.44–49.

Hugenholtz, P., 2002. Exploring prokaryotic diversity in the genomic era. *Genome Biology*, 3(2), pp.reviews0003.1–reviews0003.8.

Kaiser, C. *et al.*, 2010. Belowground carbon allocation by trees drives seasonal patterns of extracellular enzyme activities by altering microbial community composition in a beech forest soil. *The New phytologist*, 187(3), pp.843–58.

Kaiser, C. *et al.*, 2011. Plants control the seasonal dynamics of microbial N cycling in a beech forest soil by belowground C allocation. *Ecology*, 92(5), pp.1036–51.

Kielland, K., 1995. Landscape patterns of free amino acids in arctic tundra soils. *Biogeochemistry*, 31(2), pp.85–98.

Koranda, M. *et al.*, 2014. Fungal and bacterial utilization of organic substrates depends on substrate complexity and N availability. *FEMS microbiology ecology*, 87(1), pp.142–52.

Koranda, M. *et al.*, 2013. Seasonal variation in functional properties of microbial communities in beech forest soil. *Soil biology & biochemistry*, 60(100), pp.95–104.

Kubiske, M.E. *et al.*, 1997. Populus tremuloides photosynthesis and crown architecture in response to elevated CO2 and soil N availability. *Oecologia*, 110(3), pp.328–336. Available at: http://link.springer.com/10.1007/PL00008813.

Kurka, A. *et al.*, 2000. Decomposition of cellulose strips in relation to climate , litterfall nitrogen , phosphorus and C / N ratio in natural boreal forests. *Plant and Soil*, 219, pp.91–101.

Kuzyakov, Y., Friedel, J.K. & Stahr, K., 2000. Review of mechanisms and quantification of priming effects. *Soil Biology & Biochemistry*, 32, pp.1485–1498.

Lal, R., 2004. Soil carbon sequestration to mitigate climate change. *Geoderma*, 123(1-2), pp.1–22.

Lechene, C. *et al.*, 2006. of Biology BioMed Central High-resolution quantitative imaging of mammalian and bacterial cells using stable isotope mass spectrometry. *Journal of Biology*, 5(6), p.20.

Lee, C.G. *et al.*, 2011. Bacterial populations assimilating carbon from 13C-labeled plant residue in soil: Analysis by a DNA-SIP approach. *Soil Biology and Biochemistry*, 43(4), pp.814–822.

Lehmann, J., Kinyangi, J. & Solomon, D., 2007. Organic matter stabilization in soil microaggregates: implications from spatial heterogeneity of organic carbon contents and carbon forms. *Biogeochemistry*, 85(1), pp.45–57.

Li, M. *et al.*, 2012. Rapid resonance Raman microspectroscopy to probe carbon dioxide fixation by single cells in microbial communities. *The ISME journal*, 6(4), pp.875–85.

Lipson, D.A. & Schmidt, S.K., 2004. Seasonal Changes in an Alpine Soil Bacterial Community in the Colorado Rocky Mountains Seasonal Changes in an Alpine Soil Bacterial Community in the Colorado Rocky Mountains. *Applied and Environmental Microbiology*, 70(5), pp.2867 – 2879.

Van Manen, H.-J., Lenferink, A. & Otto, C., 2008. Noninvasive imaging of protein metabolic labeling in single human cells using stable isotopes and Raman microscopy. *Analytical chemistry*, 80(24), pp.9576–82.

Marx, M., Wood, M. & Jarvis, S.C., 2001. A microplate fluorimetric assay for the study of enzyme diversity in soils. , 33.

Masle, J., 2000. The effects of elevated CO(2) concentrations on cell division rates, growth patterns, and blade anatomy in young wheat plants are modulated by factors related to leaf position, vernalization, and genotype. *Plant physiology*, 122(4), pp.1399–415.

Matthäus, C. *et al.*, 2009. New Ways of Imaging Uptake and Intracellular Fate of Liposomal Drug Carrier Systems inside Individual Cells, Based on Raman Microscopy. *Molecular Pharmacology*, 5(2), pp.287–293.

Matthysse, A.G. & Holmes, K. V, 1981. Elaboration of Cellulose Fibrils by Agrobacterium tumefaciens During Attachment to Carrot Cells.

McLean, E.O., 1982. Soil pH and lime requirements. In *Methods of soil analysis. Part 2- Chemical and microbiological properties (2nd edition)*. pp. 199 – 223.

Meidute, S., Demoling, F. & Bååth, E., 2008. Antagonistic and synergistic effects of fungal and bacterial growth in soil after adding different carbon and nitrogen sources. *Soil Biology and Biochemistry*, 40(9), pp.2334–2343.

Moran, M.A., 2009. Metatranscriptomics: Eavesdropping on Complex Microbial Communities. *Microbe*, 4(7), pp.329–335.

Mummey, D.W.H.J.S. *et al.*, 2006. Spatial stratification of soil bacterial populations in aggregates of diverse soils. *Microbial ecology*, 51(3), pp.404–11.

Musat, N. *et al.*, 2008. A single-cell view on the ecophysiology of anaerobic phototrophic bacteria. *Proceedings of the National Academy of Sciences*, 105(46), pp.17861–17866.

Nobles, D.R., Romanovicz, D.K. & Brown, R.M., 2001. Cellulose in Cyanobacteria . Origin of Vascular Plant Cellulose Synthase ?

Oksanen, J. *et al.*, 2013. vegan: Community Ecology Package. R package version 2.0-10.

Paljärvi, L., Garcia, J. & Kalimo, H., 1979. The efficiency of aldehyde fixation for electron microscopy: stabilization of rat brain tissue. *The Histochemical Journal*, 11, pp.267–276.

Puppels, G.J. *et al.*, 1990. Studying single living cells and chromosomes by confocal Raman microspectroscopy. *Nature*, 347(6290), pp.301–303.

R Development Core Team, 2008. A language and environment for statistical computing. Available at: www.R-project.org.

R.H. Marchessault, J.. H., 1957. Experimental Evaluation of the Lateral-Order Distribution in Cellulose. *Textile Research Journal*, 01(27(1)), pp.30 – 41.

Raab, T.K., Lipson, D.A. & Monson, R.K., 1999. Soil Amino Acid Utilization among Species of the Cyperaceae : Plant and Soil Processes. *Ecology*, 80(7), pp.2408–2419.

Radajewski, S. *et al.*, 2000. Stable-isotope probing as a tool in microbial ecology. *Nature*, 403(6770), pp.646–649.

Radajewski, S., Mc Donald, I.R. & Murrel, J.C., 2003. Stable-isotope probing of nucleic acids: a window to the function of uncultured microorganisms. *Current Opinion in Biotechnology*, 14(3), pp.296–302.

Raman, C.V. & Krishnan, K.S., 1928. A new type of Secondary Radiation. *Nature*, 121, pp.501–502.

Rinnan, R. & Bååth, E., 2009. Differential utilization of carbon substrates by bacteria and fungi in tundra soil. *Applied and environmental microbiology*, 75(11), pp.3611–20.

Roesch, L.F.W. *et al.*, 2007. Pyrosequencing enumerates and contrasts soil microbial diversity. *ISME J*, 1(4), pp.283–290.

Roller, C. *et al.*, 1994. In situ probing of Gram-positive bacteria with high DNA G+C content using 23S rRNA-targeted oligonucleotides. *Microbiology*, (140), pp.2849–2858.

Rousk, J. & Bååth, E., 2007. Fungal and bacterial growth in soil with plant materials of different C/N ratios. *FEMS microbiology ecology*, 62(3), pp.258–67.

Saiya-Cork, K.., Sinsabaugh, R.. & Zak, D.., 2002. The effects of long term nitrogen deposition on extracellular enzyme activity in an Acer saccharum forest soil. *Soil Biology and Biochemistry*, 34(9), pp.1309–1315.

Schloss, P.D. & Handelsman, J., 2006. Toward a census of bacteria in soil. *PLoS computational biology*, 2(7), p.e92.

Schlösser, a & Schrempf, H., 1996. A lipid-anchored binding protein is a component of an ATP-dependent cellobiose/cellotriose-transport system from the cellulose degrader Streptomyces reticuli. *European journal of biochemistry / FEBS*, 242(2), pp.332–8.

Schmidt, O., 2006. *Wood and tree fungi*, Berlin, Germany: Springer-Verlag.

Schneider, T. *et al.*, 2012. Who is who in litter decomposition? Metaproteomics reveals major microbial players and their biogeochemical functions. *ISME J*.

Schönhuber, W. *et al.*, 1997. Improved sensitivity of whole-cell hybridization by the combination of horseradish peroxidase-labeled oligonucleotides and tyramide signal amplification . Improved Sensitivity of Whole-Cell Hybridization by the Combination of Horseradish Peroxidase-Labele. *Applied and Environmental Microbiology*, 63, pp.3268–3273.

Schuster, K.C., Urlaub, E. & Gapes, J.R., 2000. Single-cell analysis of bacteria by Raman microscopy: spectral information on the chemical composition of cells and on the heterogeneity in a culture. *Journal of Microbiological Methods*, 42(1), pp.29–38.

Schwartz, E., 2007. Characterization of growing microorganisms in soil by stable isotope probing with H218O. *Applied and environmental microbiology*, 73(8), pp.2541–6.

Seifert, J. *et al.*, 2012. PROTEIN-BASED STABLE ISOTOPE PROBING (PROTEIN-SIP) IN FUNCTIONAL METAPROTEOMICS. *Mass Spectrometry Reviews*, 31, pp.683–697.

Sexstone, A.J. *et al.*, 1985. Direct measurement of oxygen profiles and denitrification rates in soil aggregates. *Soil Sci Soc Am J*, 49, pp.645–651.

Six, J. *et al.*, 2004. A history of research on the link between (micro)aggregates, soil biota, and soil organic matter dynamics. *Soil and Tillage Research*, 79(1), pp.7–31.

Snajdr, J. *et al.*, 2011. Transformation of Quercus petraea litter: successive changes in litter chemistry are reflected in differential enzyme activity and changes in the microbial community composition. *FEMS microbiology ecology*, 75(2), pp.291–303.

Šnajdr, J. *et al.*, 2008. Spatial variability of enzyme activities and microbial biomass in the upper layers of Quercus petraea forest soil. *Soil Biology and Biochemistry*, 40(9), pp.2068–2075.

Steinweg, J.M. *et al.*, 2013. Activation energy of extracellular enzymes in soils from different biomes. *PloS one*, 8(3), p.e59943.

Stevenson, B.S. *et al.*, 2004. New strategies for cultivation and detection of previously uncultured microbes. *Appl. Environ. Microbiol.*, 70(8), pp.4748–4755.

Strickland, M.S. & Rousk, J., 2010. Considering fungal:bacterial dominance in soils – Methods, controls, and ecosystem implications. *Soil Biology and Biochemistry*, 42(9), pp.1385–1395.

Štursová, M. *et al.*, 2012. Cellulose utilization in forest litter and soil: identification of bacterial and fungal decomposers. *FEMS Microbiology Ecology*, 80(3), pp.735–746.

Swift, M.J., Heal, O.W. & Anderson, J.M., 1979. *Decomposition in terrestrial ecosystems,* Oxford, United Kingdom: Blackwell Scientific Publications, Oxford, United Kingdom.

Taubert, M. *et al.*, 2012. Protein-SIP enables time-resolved analysis of the carbon flux in a sulfate-reducing, benzene-degrading microbial consortium. *The ISME journal*, 6(12), pp.2291–301.

Taylor, J.. *et al.*, 2002. Comparison of microbial numbers and enzymatic activities in surface soils and subsoils using various techniques. *Soil Biology and Biochemistry*, 34(3), pp.387–401.

Tonegawa, A. *et al.*, 2002. Deuterium NMR and Raman Spectroscopic Studies on Conformational Behavior of Lipophilic Chains in the C 12 E 3 / Decane / Water System. *Verlag der Zeitschrift für Naturforschung, Tübingen*, 57 a, pp.320–326.

Uhlík, O. *et al.*, 2009. DNA-based stable isotope probing: a link between community structure and function. *The Science of the total environment*, 407(12), pp.3611–9.

Valentine, D.L. *et al.*, 2004. Hydrogen isotope fractionation during H_2 / CO_2 acetogenesis : hydrogen utilization efficiency and the origin of lipid-bound hydrogen. *Geobiology*, 2, pp.179–188.

Velicer, G.J., 2003. Social strife in the microbial world. *Trends in Microbiology*, 11(7), pp.330–337.

Venables, W.N. & Ripley, B.D., 2002. *Modern Applied Statistics with S* Fourth., New York: Springer.

Vogel, C. *et al.*, 2014. Submicron structures provide preferential spots for carbon and nitrogen sequestration in soils. *Nature communications*, 5, p.2947.

Voříšková, J. *et al.*, 2014. Seasonal dynamics of fungal communities in a temperate oak forest soil. *The New phytologist*, 201(1), pp.269–78.

Voroney, P., 2007. The Soil Habitat. In *Soil Microbiology, Ecology and Biochemistry*. pp. 25 – 49.

De Vries, F.T. *et al.*, 2007. Fungal biomass in pastures increases with age and reduced N input. *Soil Biology and Biochemistry*, 39(7), pp.1620–1630.

De Vries, F.T. *et al.*, 2006. Fungal/bacterial ratios in grasslands with contrasting nitrogen management. *Soil Biology and Biochemistry*, 38(8), pp.2092–2103.

Wagner, M., 2009. Single-cell ecophysiology of microbes as revealed by raman microspectroscopy or secondary ion mass spectrometry imaging. *Annu. Rev. Microbiol.*, 63(1), pp.411–429.

Waldrop, M.P., Zak, D.R. & Sinsabaugh, R.L., 2004. Microbial community response to nitrogen deposition in northern forest ecosystems. *Soil Biology and Biochemistry*, 36(9), pp.1443–1451.

Wegener, G. *et al.*, 2012. Assessing sub-seafloor microbial activity by combined stable isotope probing with deuterated water and 13C-bicarbonate. *Environmental microbiology*, 14(6), pp.1517–27.

Wei, L. *et al.*, 2013. Vibrational imaging of newly synthesized proteins in live cells by stimulated Raman scattering microscopy. *Proceedings of the National Academy of Sciences*, 110, pp.11226–11231.

Whitman, W.B., Coleman, D.C. & Wiebe, W.J., 1998. Prokaryotes: the unseen majority. *Proc. Natl. Acad. Sci.*, 95, pp.6578–6583.

Wilmes, P. & Bond, P.L., 2006. Metaproteomics: studying functional gene expression in microbial ecosystems. *Trends in microbiology*, 14(2), pp.92–7.

Wittmann, C. *et al.*, 2004. Areal activities and stratification of hydrolytic enzymes involved in the biochemical cycles of carbon, nitrogen, sulphur and phosphorus in podsolized boreal forest soils. *Soil Biology and Biochemistry*, 36(3), pp.425–433.

Woebken, D. *et al.*, 2012. Identification of a novel cyanobacterial group as active diazotrophs in a coastal microbial mat using NanoSIMS analysis. *The ISME journal*, 6(7), pp.1427–39.

Woebken D, Burow L, Behnam F, Mayali X, Schintlmeister A, Fleming E, Prufert-Bebout L, Singer S, López Cortés A, Hoehler T, Pett-Ridge J, Spormann A, Wagner M, Weber P, Bebout B. 2014. Revisiting N2 fixation in Guerrero Negro intertidal microbial mats with a functional single-cell approach. *ISME J.* , in press

Wong, K.K.Y., Tan, L.U.L. & Saddler, J.N., 1988. Multiplicity of β-1,4-xylanase in microorganisms: functions and applications. *Microbiol. Rev.*, 52(3), pp.305–317.

Wyman, C.E. *et al.*, 2005. Hydrolysis of Cellulose and Hemicellulose. In *Polysaccharides Structural Diversity and Functional Versatility*.

Xie, G. *et al.*, 2007. Genome Sequence of the Cellulolytic Gliding Bacterium \emph{Cytophaga hutchinsonii}. *Appl. Environ. Microbiol.*, 73(11), pp.3536–3546.

El Zahar Haichar, F. *et al.*, 2007. Identification of cellulolytic bacteria in soil by stable isotope probing. *Environmental microbiology*, 9(3), pp.625–34.

Zak, D., Pregitzer, K. & Curtis, P., 2000. Atmospheric CO2, soil-N availability, and allocation of biomass and nitrogen by Populus tremuloides. *Ecological …*, 10(1), pp.34–46.

Zausig, J., Stepniewski, W. & Horn, R., 1993. Oxygen concentration and redox potential gradients in unsaturated model soil aggregates. *Soil Science Society of America {…}*.

Zogaj, X. *et al.*, 2001. The multicellular morphotypes of Salmonella typhimurium and Escherichia coli produce cellulose as the second component of the extracellular matrix. *Molecular microbiology*, 39(6), pp.1452–63.

11 Appendix

11.1 Supplementary figures

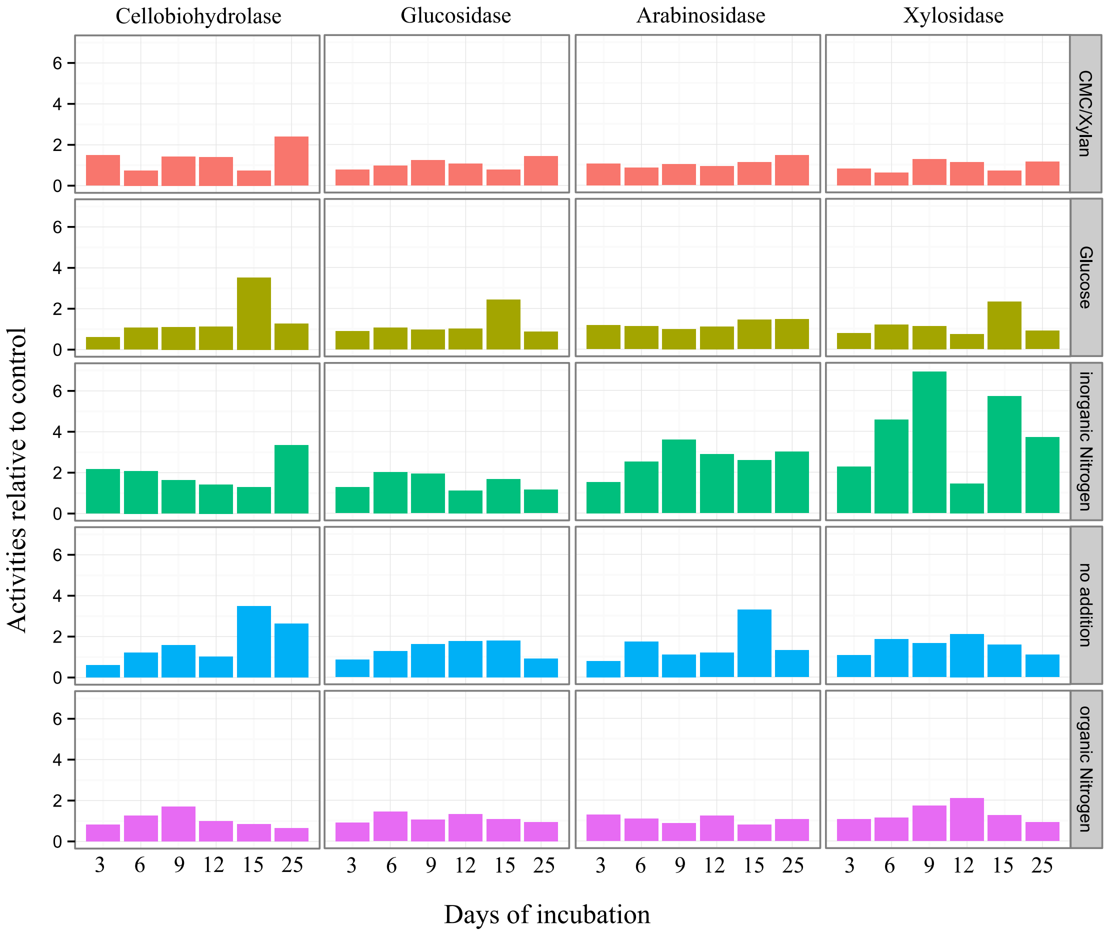

Supplementary Figure 1: Relative enzyme activities of summer microcosms. Calculated as the ratio of activities from cellulose amended samples to respective controls without cellulose.

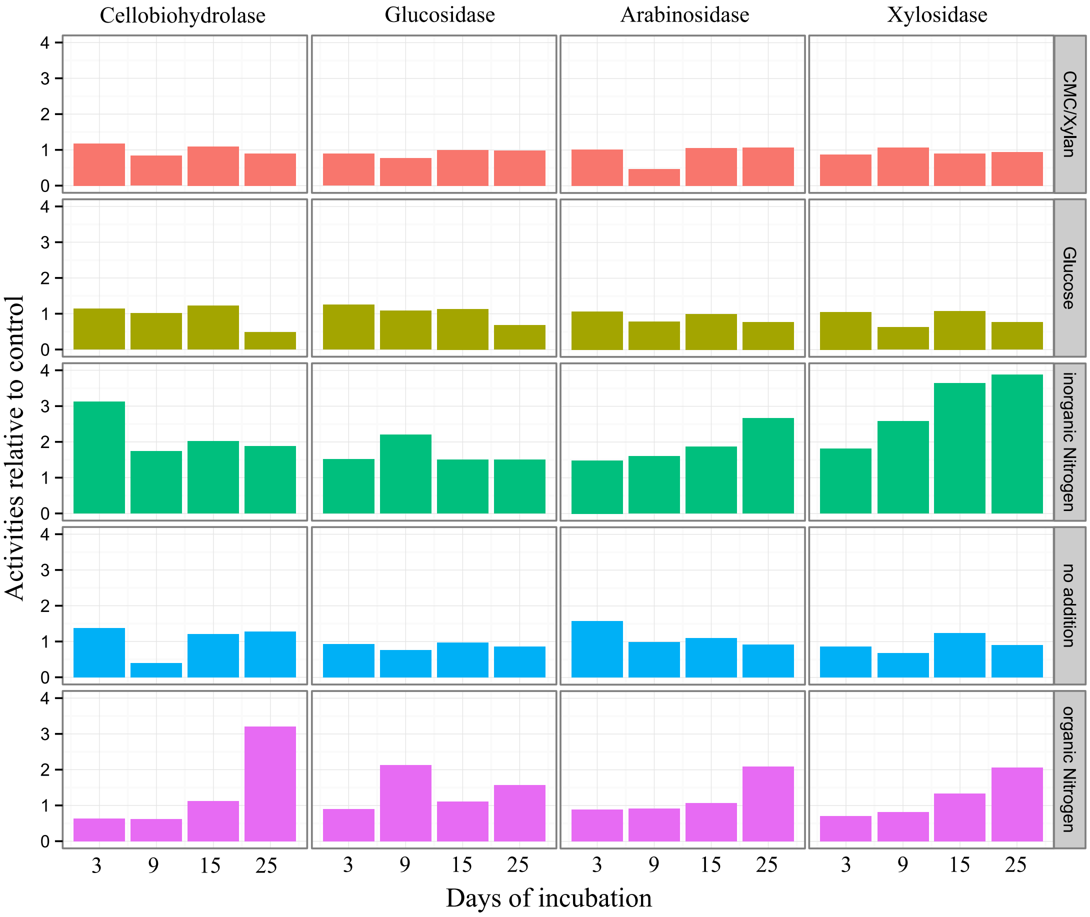

Supplementary Figure 2: Relative enzyme activities of fall microcosms. Calculated as the ratio of activities from ^{13}C-Cellulose amended samples to respective controls without cellulose

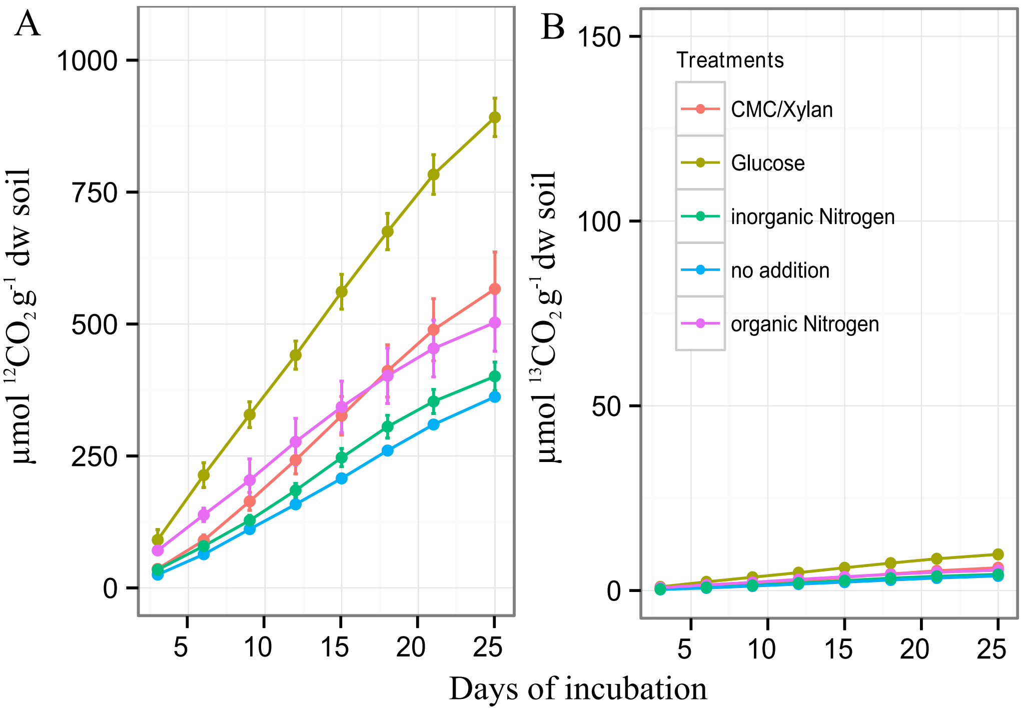

Supplementary Figure 3: $^{12}CO_2$ (A) and $^{13}CO_2$ (B) evolution from control microcosms without ^{13}C labeled cellulose in summer.

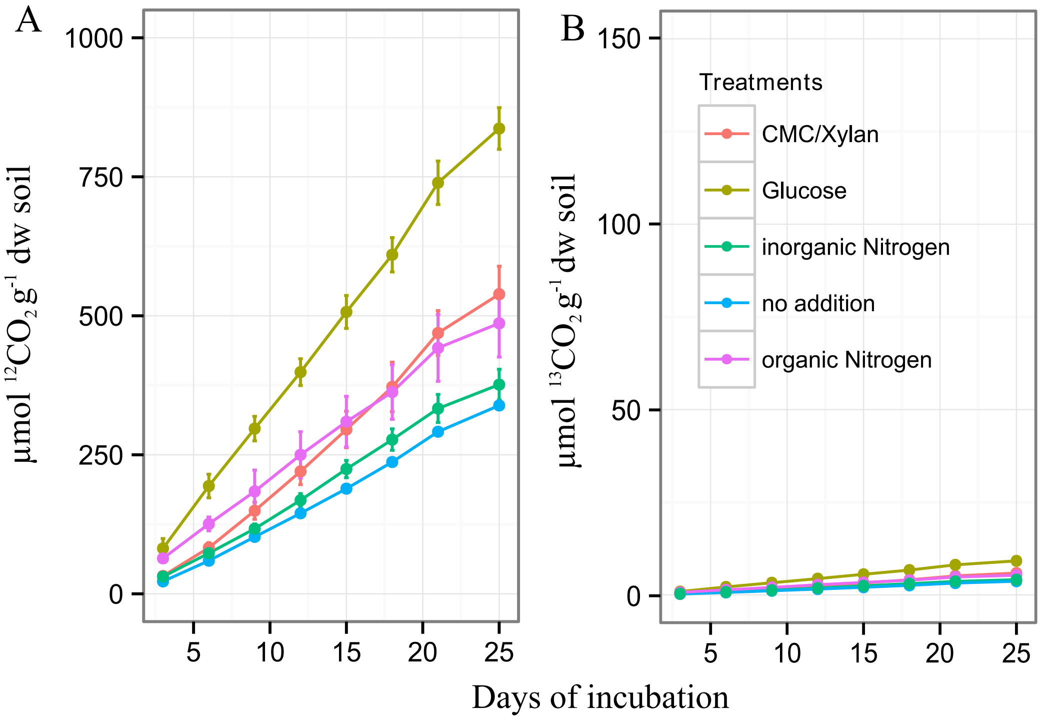

Supplementary Figure 4: $^{12}CO_2$ (A) and $^{13}CO_2$ (B) evolution from control microcosms without ^{13}C labeled cellulose in fall.

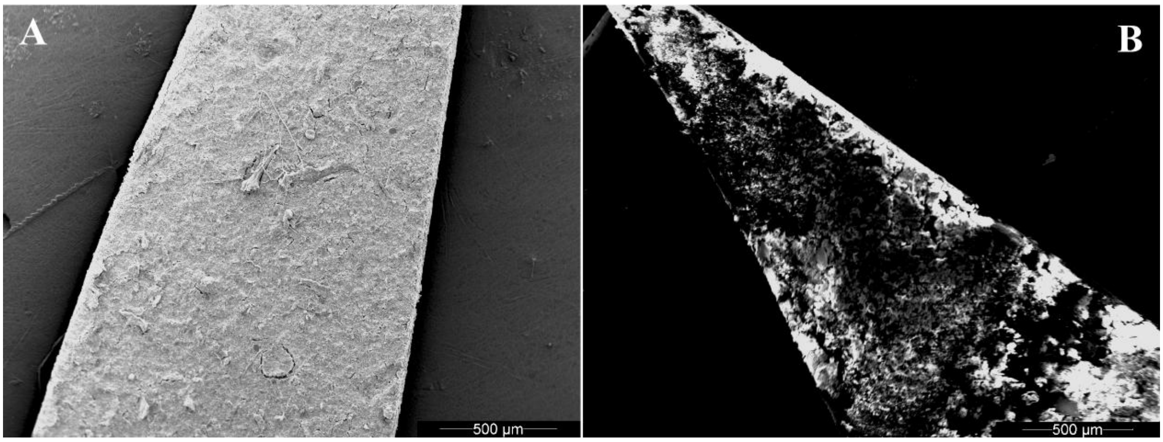

Supplementary Figure 5: SEM of undiluted soil samples from A) KLD, and B) Neustift filtered onto 0.2 µm polycarbonate filter.

11.2 Recipes

11.2.1 10 x PBS:

Dissolve 80 g NaCl, 2 g KCl, 14.4 g Na_2HPO_4 (Roth) and 2.4 g KH_2PO_4 (Roth) per liter sterile water. Adjust pH to 7.4 with 1 M HCl. Dilute 1:10 for 1 x PBS

11.2.2 Sodium-acetate- Buffer:

Dissolve 13.6 g Sodium acetate trihydrate (Sigma Aldrich) per liter sterile water. Adjust pH to 5.5 with glacial acetic acid (Roth).

11.2.3 Citric acid buffer:

Dissolve 31.52 g Citric acid (Riedel-de Haën, Seelze, Germany) per liter sterile water. Adjust pH to 4.0 with NaOH (liquid, 50 %.).

11.2.4 Vitamin Basal salt medium

VSB medium at a pH of 6.5 was prepared as described by Stevenson and colleagues (Stevenson *et al.* 2004).

The medium consisted of 1 x basal medium I, SL-10 trace element solution (1 ml/liter), Vitamin mixture (1ml/liter), Vitamin B12 (1 ml/liter) and was buffered to a pH of 6.5 with MES-buffer (final concentration: 10 mM).

The medium was prepared for the Amino acid incubation of soil enrichments (7.5.1.2.1) and was prepared with 50% D_2O for the activity studies (7.5.1.2.2)

Basal Medium I:

Component	Final concentration in medium
NaCl	17mM
$MgCl_2$•$6H_2O$	3.1mM
$CaCl_2$•2H2O	1.0mM
NH_4Cl	4.7mM
KH_2PO_4	1.5mM
KCl	6.7mM
Na_2SO_4	2mM

SL-10 Trace Metals:

Component	per liter medium
HCl	10 ml
$FeCl_2 \cdot 4H_2O$	1.5 g
$CoCl_2 \cdot 6H_2O$	190 mg
$MnCl_2 \cdot 4H_2O$	100 mg
$ZnCl_2$	70 mg
H_3BO_3	6 mg
$Na_2MoO_4 \cdot 2H_2O$	36 mg
$NiCl_2 \cdot 6H_2O$	24 mg
$CuCl_2 \cdot 2H_2O$	2 mg

Vitamin mixture:

Following engridents were dissolved in 100ml Sodium-phosphate buffer (10 mM, pH= 7.1):

Component	Per 100 ml
4-aminobenzoic acid	4 mg
D (+)-biotin	1 mg
Nicotinic acid	10 mg
Calcium D (+)-pantothenate	5 mg
Pyridoxine dihydrochloride	15 mg

12 Lebenslauf

Florian Strasser
Lebenslauf

Persönliche Daten

Name	Florian Strasser
Geburtsdatum/Ort	21.06.1988/Linz, Österreich
Nationalität/Staatsbürgerschaft	Österreich
Adresse	Universität Wien Division of Microbial Ecology (DoME) Althanstr. 14 A-1090 Wien
E-Mail	strasser@microbial-ecology.net
Aktuelle Position	Master Student

Schulausbildung

1994 – 1998	Volksschule Asten
1998 – 2006	Europagymnasium Auhof, Linz
2007 – 2011	Bachelor studies Biology (Microbiology and Genetics)

Berufserfahrung

2013- jetzt	**Master Student**, “Molecular microbiology and immunology”. NanoSIMS group, Division of Microbial Ecology, University of Vienna, Austria. Group Leader: Dagmar Woebken.
2010-2011	Internship in Blineder Bau AG, 4210 Gallneukirchen
2007- 2011	Internships as cleaning staff in Riepl Architektur, 4020 Linz
2006- 2007	Zivildienst, Bezirksseniorenheim Engerwitzdorf, 4209 Engerwitzdorf

Kenntnisse	Molekularbiologie, Bioinformatik, Mikroskopie, Biogeochemie, analytische Chemie,
Fremdsprachen	Deutsch und Englisch (flieβend in Wort und Schrift)
Referenzen	auf Anforderung